MODULATION OF SEROTONIN TRANSPORTER FUNCTION AND PHARMACOLOGY BY SUBUNIT INTERACTIONS AND AN ENDOGENOUS REGULATORY FACTOR

By

I. Scott Ramsey

Dissertation
Submitted to the Faculty of the
Graduate School of Vanderbilt University
in partial fulfillment of the requirements
for the degree of

DOCTOR OF PHILOSOPHY
in
Pharmacology

December, 2001
Nashville, Tennessee

Approved
Prof. Louis J. DeFelice – Thesis Advisor
Prof. Randy D. Blakely – Committee Chair
Prof. Lee E. Limbird
Prof. David M. Lovinger
Prof. Kevin Strange

ACKNOWLEDGEMENTS

This work was generously supported by a Predoctoral National Research Service Award (MH12303) and Training Grant in Pharmacology (GM07628) from the National Institutes of Health.

I would like to extend special thanks to Lou DeFelice for his generous mentorship and wholehearted support of the learning process during my tenure as a graduate student in his laboratory. Lou's dedication to maintaining an intellectual environment that is unencumbered by the accretions of dogmatic principle represents all that is good about the scientific method. He has inspired me to hold tight on the rugged path to true discovery.

Special thanks are also due to Randy Blakely for his liberal intellectual and practical support of this research project. Randy's unbridled enthusiasm for science and his penchant for prolific idea generation have enormously aided the development of this thesis project.

I would also like to acknowledge the significant contribution of the members of the thesis committee, Lee Limbird, David Lovinger, and Kevin Strange, for providing the direction and focus, critical insight, and freedom to experiment that have made this thesis project the bracing adventure that is has been.

My gratitude is extended to members of the Department of Pharmacology who, in various ways, have supported (and endured) my residence in training at Vanderbilt. I'd particularly like to acknowledge Ron Emeson, Karen Gieg, Pamela Harrell, and Elaine Sanders-Bush.

To Ellen Carter in the Office of Biomedical Research Education and Training, thank you for helping me to make the right choice.

My thanks would not be complete without a special thanks to those who have extended their kind friendship: Erika Adkins, April Bragg, Dawn Borromeo, JP Johnson, John Partridge, George Patterson, Dan Prudhomme, and Craig Tucker. Fond memories of Nashville and environs are rooted in our good times.

To my family, and particularly Mary Lou and Dave, my deepest thanks for your unwavering support, unconditional love, and thorough inculcation into the joys of life and the liberty of learning.

And to my dear love Lara, with whom I share daily bread, epiphanic exuberation, and everything in between, thank you for your sincere love and support. The journey to *l'inconnu* is impossible without you.

TABLE OF CONTENTS

LIST OF TABLES

LIST OF FIGURES

CHAPTER I

INTRODUCTION

Background

Serotonin (5-HT) is a neuromodulator that is involved in a variety of behaviors, including mood, sleep, pain, appetite, aggression, and sexual behavior [1-3]. 5-HT is synthesized by a subset of neurons in the central nervous system that have cell bodies located in the dorsal raphe nucleus. These serotonergic neurons project widely throughout the brain and spinal cord to secrete 5-HT from axon terminals and varicosities[4-6]. Released 5-HT binds to at least fifteen distinct G-protein-coupled receptors (GPCRs, e.g. 5-HT_{1A}, 5-HT_7) and one ionotropic receptor (5-HT_3) to exert its effects on neuronal excitability [3,5,6]. Serotonin GPCRs are localized both pre- and post-synaptically and mediate a multitude of neuronal functions including inhibition of transmitter release by coupling to voltage-gated and inwardly rectifying K^+ channels and modulation of post-synaptic excitability stimulation of intracellular signaling cascades through activation of adenylyl cyclase and phospholipase Cβ [3].

5-HT may be cleared by diffusion, enzymatic degradation, or the action of a Na^+- and Cl^--dependent plasma membrane serotonin transporter [7,8]. Among these mechanisms the latter is dominant, as evidenced by the effects of transport blockers on serotonergic signaling and neurotransmission [9-11]. In some brain regions, 5-HT diffuses to sites distant from its release; serotonergic neurotransmission is therefore not bounded by temporal and spatial constraints of a synaptic architecture that are characteristic of fast glutamatergic and GABA-ergic synapses [12]. Dopamine, and perhaps other biogenic amines, is released from dendrites by the dopamine transporter (DAT) operating in reverse [13], in contrast to the accepted model of transmitter release by secretion from synaptic vesicles. The activity of neurotransmitter transporters is therefore central to shaping responses at target metabotoropic receptors [12,14].

Antidepressants and serotonin-selective reuptake inhibitors (SSRIs) block SERT activity and increase extracellular 5-HT concentrations [6,11,15-17]. These drugs are useful for the treatment of human disease (depression, obsessive-compulsive disorder, bulimia and eating disorders, anxiety and panic disorders, postanoxic intention myoclonus, alcoholism, and premenstrual dysphoric disorder) [18-22]. Although transporter inhibition is the proximal event in antidepressant action, the clinical benefit of antidepressant medications requires weeks of continuous dosing, indicating that their mechanism of action involves events downstream from acute transporter blockade [6,23]. Long-term effects of SSRI treatment may be due to changes in intrinsic properties of SERT structure, function, or regulation. Thus, understanding SERT function and pharmacology remains a primary goal in the search to develop of novel treatments for diseases associated with serotonergic dysfunction.

SERT is also a receptor for psychostimulant drugs with abuse potential such as 3,4-methylenedeoxymethamphetamine (ecstasy, MDMA), d-amphetamine (AMPH), and cocaine [24-29]. In contrast to the antidepressants and cocaine, which are non-transported SERT ligands, psychostimulant drugs serve as alternative substrates that compete with 5-HT for transport [28,30-36]. Cocaine also blocks DAT to cause a prominent hyperlocomotory response [29,37-39]. However, cocaine exerts non-locomotor behavioral effects even in mice lacking functional DAT [40], indicating that inhibition of 5-HT transport also plays a role in its mechanism of action [41-43].

SERT function is well-studied in platelet vesicle and brain synaptosomal preparations. 5-HT transport requires extracellular Na^+ and to a lesser extent Cl^-, is stimulated by intracellular K^+ or H^+, and depends on 5-HT concentration with apparent Michaelis-Menten type kinetics [44-49]. The effect of Na^+, K^+–ATPase inhibitors (i.e. oubain) and ATP depletion on 5-HT transport is indirect, since these treatments deplete the ion gradients (primarily Na^+) that are required for 5-HT accumulation [17,45,50]. A classical model of 5-HT transport postulates ion:substrate coupling due to fixed stoichiometric transport of 5-HT and other ions. Depending on predicted stoichiometry, classical models result in the net movement of zero or 1 elementary

charge (*e*) into the cell per 5-HT molecule [45,48,49,51]. Classical transport models therefore predict little or no current to be generated during the transport process.

Electrophysiological studies in a native preparation suggest that the classical model does fully describe the properties of the 5-HT transport system *in situ*. In identified serotonergic neurons of the leech *Hirudo*, 5-HT induces a current that is a) Na^+- and voltage-dependent, b) rapidly activated in response to stimulation of presynaptic 5-HT release, c) correlated with presynaptic 5-HT uptake, and d) inhibited by SERT-selective antidepressants [52]. The 5-HT-induced current in *Hirudo* is therefore attributed to an as yet unidentified leech SERT and suggests that SERTs may generate substantial ion currents concomitant with 5-HT transport in other systems. These findings reinforce the notion that neurotransmitter transporters play a centrally important role in serotonergic neurotransmission because of their ability to modulate synaptic physiology both electrically and chemically.

Identification, cloning, and expression of transporter genes has enabled the identification of amino acid residues that are important for transporter structure and function. cDNAs encoding a mammalian neurotransmitter transporters were first identified for the rat γ-aminobutyric acid transporter 1 (rGAT1) and human (-)-norepinephrine transporter (hNET) [53,54]. Mammalian rat (rSERT) and human (hSERT) serotonin transporters subsequently identified by homology to GAT and NET sequences [27,55-57], helped to define the GAT/NET family of neurotransmitter transporters. GAT/NET family cDNA sequences encode carriers for neurotransmitters, solutes, amino acids, as well as orphan transporters with no known function [11,15,58-68]. Hydropathy analyses of primary amino acid sequences predict that GAT/NET transporters share a predicted topology containing 12 putative α-helical transmembrane domains (TMDs) that are joined by loop regions of unknown structure; amino- and carboxy-termini are intracellular in these models (Fig. 1) [53-55,69].

Heterologous expression of transporter cDNAs enables identification of amino acid residues that are important for tertiary and quaternary structure, ligand recognition, and transport mechanisms. Transfection of cDNA encoding SERT into

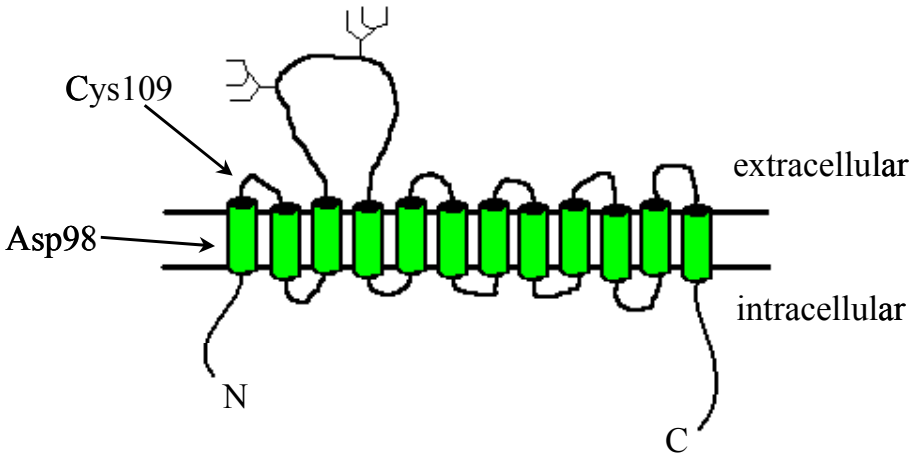

Figure 1. Predicted transmembrane topology for mammalian SERTs.
Shaded cylinders represent twelve putative transmembrane-spanning segments (TMDs); glycosylation sites in the large extracellular loop 2 are indicated by branched structures. Relative positions of mutations (D98G, C109A) utilized in this study are indicated by arrows.

mammalian cells is sufficient to impart 5-HT transport activity that recapitulates many of the hallmark properties seen in brain and platelet preparations: potent activation by 5-HT, Na^+- and Cl^--dependence, and cocaine and antidepressant sensitivity [27,45,55,57]. Rat (rSERT) and human (hSERT) serotonin transporters share 92% overall amino acid sequence identity; of the divergent residues, half are localized to the putative intracellular tail regions and only 14 substitutions are located within predicted TMD helices [27,55-57].

rSERT and hSERT exhibit similar dependencies for 5-HT and ions and relatively subtle differences in inhibitory potency for antidepressants and psychostimulants, suggesting that transmembrane regions are likely to be integral ligand recognition [70-73]. Ligand binding is similarly localized to discrete TMD regions in related catecholamine transporters [74-76]. Mutation of the few TMD residues that are divergent in otherwise conserved SERT sequences has proven fruitful for identifying of substrate and inhibitor

binding sites. Single residue switches confer differences in antidepressant potency between hSERT and rSERT [70] and hSERT and dSERT [72].

Residues implicated in 5-HT translocation and gating have also been identified. For example, an aspartate in putative TMD1 that is conserved among biogenic amine transporters is required for transporter function: when rSERT (Asp98) or hNET (Asp75) are mutated, transport activity is severely compromised or ablated [77]. The loss in transport activity is not paralleled by commensurate decreases in plasma membrane localization, indicating that the mutation interferes with ligand recognition and catalytic activity [77]. Application of an alternative substrate (gramine) rescues the effect of the Asp98 to Glu mutation in rSERT, arguing that TMD1 directly contacts 5-HT [77]. A role for TMD1 in substrate recognition is also supported by a recent mutagenesis screen [78]. Cysteine mutagenesis and MTS reagent reactivity studies and single-channel biophysical investigation of SERT currents also implicate TMDs 3 and 7 in 5-HT recognition and transporter gating [79-82].

In general, transport studies of cloned SERTs are consistent with the a classical model possessing fixed ion:substrate stoichiometry [27,55,57,83-85]. SERT pharmacology measured in brain and platelet preparations exhibits subtle but potentially important differences to that seen transfected mammalian cells. Although 5-HT potency ranges from 50 nM to 1 μM in various different preparations, K_M values tend to be significantly lower in brain synaptosomal preparations than in transfected cells or vesicles [86-90].

Heterologous expression permits investigation of transporter function using voltage clamp to control membrane voltage and is therefore inherently suited to the study of electrically active proteins such as transporters and ion channels that bind and catalyze the transmembrane flux of charged ionic and molecular substrates. Indirect approaches for estimating ion:substrate stoichiometry (i.e. ion substitution experiments or by addition of ionophores to alter plasma membrane ion gradients) yield variable conclusions for the magnitude of SERT-associated charge movement [17,44,45,47-49,51,84,91,92]. Biophysical studies of GAT/NET transporters have been largely confined to intact host cell membranes, raising the possibility that studies in cells versus vesicles and

synaptosomes may come to different conclusions regarding ion:substrate stoichiometry and transporter-associated currents.

Experimentally, the function of expressed GAT/NET transporters deviates from the classical model's expectation of fixed ion:substrate stoichiometry, viz., for each neurotransmitter molecule transported, tens to hundreds of elementary charges (*e*) move through the transporter. Large (- 30 pA to –50 pA at –120 mV) 5-HT-induced and antidepressant-sensitive currents are recorded in HEK-293 cells expressing hSERT [87]. hNET and rGAT1 generate similar sized currents in transfected cells [93,94]. Large SERT currents are also seen in *Xenopus laevis* oocytes [95-98]. Transport and current exhibit similarities in ion, substrate, and inhibitor sensitivities, suggesting that ligand recognition and activation mechanisms for substrate-induced currents and substrate transport functionally linked [77,87,93,98,99].

In addition to substrate-induced current, GAT/NET transporters generate a constitutive current (also termed leak current or slippage) in addition to both capacitive and resistive non-steady-state currents [94-98,100]. Transporter-mediated ion channel activity, evidenced by single-channel currents or current fluctuations attributable to channel noise, is reported for rGAT1, hNET, and rSERT [82,101,102], suggesting that large macroscopic transporter currents are generated by ion channel activity [103-105]. Channel-like conductances may therefore represent a conserved mechanism among members of the GAT/NET gene family that explains currents in excess of predictions based on fixed stoichiometry [98,103-105].

However, large transporter-associated currents and channel-like activity are not universally observed. Currents consistent with classical transporter models are reported for rGAT1 [106-108] and rPROT [109]. In the face of conserved sequence in the *GAT/NET* family that would suggest similar structure and function, the apparent discrepancies in the literature regarding ion fluxes in excess of transmitter flux are puzzling. Variable stoichiometry and excess current may therefore depend on as yet unidentified factors. Heterologous expression systems that are commonly used to study transporter function could yield disparate results if they fail to fully reconstitute

interactions between expressed transporters and other proteins or cellular factors that alter transporter function.

Indeed, GAT/NET transporters are known to associate with proteins that alter their function and subcellular distribution[110-112]. For SERT, changes in 5-HT transport, 5-HT-induced current, and plasma membrane transporter density are associated with protein kinase C (PKC) activation, SERT phosphorylation, and ligand occupancy [87,113-116]. GAT/NET transporters form regulated complexes with Protein phosphatase 2A (PP2A) and Syntaxin 1A [111]. The PDZ-containing protein PICK-1 associates with catecholamine transporters and governs their distribution in neurons [112]. PKC and syntaxin 1A both interact with rGAT1 to control transporter trafficking and intrinsic activation by substrate [110,117,118]. Associated proteins in heteromeric transporter complexes are therefore appropriately situated to regulate other aspects of GAT/NET transporter function. Allosteric interactions between subunits of an oligomeric SERT complex [119] and between binding sites for different SERT ligands [120] may provide additional means for functional modulation of transporter activity [121-123]. The extent to which neurotransmitter transporters function as channels versus transporters may therefore depend on a variety of factors that interdependently affect transporter function.

The multi-subunit structural paradigm is well established for voltage- and ligand-gated ion channels [124-131]. Channel activity in GAT/NET transporters suggests that that they may also form a multisubunit structure. Although the functional relevance of oligomerization for neurotransmitter transporter physiology remains unknown, evidence from a variety of experimental approaches supports the idea that GAT/NET transporters form functional oligomeric protein complexes.

1) Epitope-tagged SERTs are co-immunoprecipitated from transiently transfected HeLa cells, indicating that SERTs form an SDS-stable oligomer [119]. Furthermore, co-expression of MTSEA-sensitive or -insensitive mutants exhibit alters the degree of MTSEA inhibition, indicating that interactions between individual SERT proteins residing on the plasma membrane can modulate transporter function [119].

2) Fluorescent resonance energy transfer (FRET) is observed in HEK-293 and HeLa cells transiently expressing SERT-GFP fusion proteins [132]. SERT proteins are therefore constitutively localized in close physical proximity [132]. SERT- GFP fluorescence elutes with large molecular weight fractions (320 - 800 kDa), suggesting that SERT is part of a large complex or SERT oligomer [132].

3) SERT proteins can be chemically cross-linked, indicating that they lie in close proximity, as would be expected for an oligomeric protein structure [133].

4) 5-HT transport is susceptible to trans-dominant inhibition when mSERT is co-expressed with transport-incompetent transmembrane deletion mutants in COS-1 cells [134]. Expression of concatenated mSERT cDNAs leads to transport properties (V_{max}, K_M) that are unchanged for the dimeric construct whereas the tetramer exhibits a 90% decrease in V_{max} (no change in K_M) and the trimer is inactive [134].

5) Partially purified SERT binding activity from human placenta tracks with a protein of ~300 kDa [135], about 4 times larger than the 68 kDa expected from the deduced amino acid sequence of mammalian SERT cDNA clones [27,55,57]. Other studies have arrived at either similarly large estimates [136,137] or sizes expected for a SERT monomer [138,139] depending on the purification strategy and tissue source used.

6) Radiation-induced loss of radioligand binding to hDAT indicates a target size of dimeric (~140 kDa, [140]) or tetrameric size (~280 kDa, [141]).

7) Discrete immunoreactive bands of ~200 kDa in size are seen in Western blots from rat platelets and HeLa cells transiently expressing rSERT [142]. One possible explanation is that rSERT exists as an oligomer in the plasma membrane and SDS-resistant oligomers result from membrane solubilization.

8) 5-HT and SERT inhibitors slow the dissociation rate of previously bound [^{3}H]-imipramine and [143-146], consistent with allosteric interactions between multiple SERT binding sites. Furthermore, [^{3}H]-imipramine binding exhibits distinct affinity states, [122,147,148] that could be due to inter-subunit interactions in a SERT oligomer.

Despite nearly 30 years of study, the availability of an arsenal of selective and clinically effective pharmacological agents, and molecular cloning of transporter

cDNAs, many fundamental aspects of neurotransmitter transporter biology remain unclear at the molecular level. For example, what mechanisms govern variable ion:substrate stoichiometry in GAT/NET transporters? Do interactions between subunits of an oligomeric SERT protein complex affect 5-HT transport or 5-HT-induced current under physiological conditions? What are the functional ramifications of transporter oligomerization? This dissertation addresses these questions in detail. Our results contradict expectations based on simple models of transporter function and lead us to conclude that SERT function is described by cooperative interactions between subunits of the SERT oligomer and another cellular factor. We present a novel integrated model of SERT structure and function to describe our findings. These conclusions may lead to the development of novel therapies for the treatment of diseases where SERT dysfunction or dysregulation is implicated.

Research Design

Our primary goal is to determine whether subunits of the oligomeric SERT complex exhibit functional cooperativity. We have designed our experiments to measure intrinsic properties of SERT function. By utilizing functional assays in intact membranes of living cells, we minimize the possibility that artifacts inherent to purely biochemical approaches influence our conclusions. Our approach utilizes two different heterologous expression systems to express recombinant SERT protein. We exploit functional differences between wild-type SERT and previously reported SERT mutants in co-expression studies to assay for functional interactions. We also deliberately alter SERT expression level by varying the quantity of cDNA in transfections or cRNA in oocyte injections.

In order to test for SERT functional cooperativity, we employ the following logical arguments:

1) For SERTs that function independently, we predict that functional properties in co-expression studies are predicted by the sum of individual responses determined from individual expression.

2) Simple models of transporter function based on independent function allow us to generate expectations for functional properties in heterologous expression studies.

3) Ratiometric measurements of SERT activity allow us to identify SERT properties that are independent of expression level.

In our design, the null hypothesis is that the data conform to the expectations of a simple model based on independent behavior. Deviation from the null hypothesis suggests functional complexity that may be result from allosteric cooperativity. The presence of novel phenotypes in response to co-expression or varying expression level thus argues strongly for the presence of allosteric interactions between different SERT functional units or between SERT and other factors.

The primary limitation in our approach therefore lies in the quality of the primary data: if properties of *wt* and mutant SERTs are not significantly different when measured individually, we will not be able to discriminate differences from our

predictions following co-expression. A strength of the experimental design is the use of multiple different approaches to test for functional cooperativity. By focusing our efforts on SERT properties that exhibit obviously different phenotypes, we mitigate against the possibility of making erroneous conclusions from spurious data.

CHAPTER II

METHODS

CHO-K1 Cells

Molecular Biology. The rat SERT cDNA in the pcDNA3 vector was used as the template for site-directed mutagenesis to create rSERT C109A using the Quick Change Mutagenesis kit (Stratagene) and the following synthetic oligonucleotide primers (Vanderbilt Molecular Biology Core Facility):

sense: 5'-CGGTTTCCTTACATAGCCTACCAGAATGGCGGA-3'

antisense: 3'-GCCAAAGGAATGTATCGGATGGTCTTACCGCCG-5'

Three independent C109A mutant clones were subjected to analytical digestion and automated DNA sequence analysis (Prism 310, ABI Instruments) for confirmation, and two clones were selected for expression in mammalian cells. No difference between the two independent clones is seen in functional assays. cDNAs encoding the human serotonin transporter (hSERT), rat serotonin transporter (rSERT), rSERT D98G point mutant (D98G), human (-)-norepinephrine transporter (hNET), rat brain-specific proline transporter (rPROT), frog (-)-epinephrine transporter (fET), and rat GABA transporter 1 (rGAT1) in pcDNA3 vector were generously provided by R. D. Blakely (Vanderbilt University Medical Center). The "flip" splice variant of the AMPA-type ionotropic glutamate receptor D (GluR4-flip) in pRK-5 was kindly provided by S. Sikes (D. Lovinger laboratory, Vanderbilt University Medical Center). CD8 cDNA was provided by J. P. Johnson (P. Bennett laboratory, Vanderbilt University Medical Center). HA-tagged alpha 2A adrenergic receptor (HA-α_{2A}R) cDNA in pcDNA3 was supplied by C. Tan (L. Limbird laboratory, Vanderbilt University Medical Center). pEGFP-N1 is from Clontech.

Plasmids containing wild-type or mutant cDNAs are prepared using standard methods. XL1-Blue or DH5α strains of E. Coli are grown in LB or NZY medium under carbenicillin (50 mg/ml) or kanamycin (100 mg/ml, pEGFP-N1 only) selection.

Plasmid DNA is isolated from bacterial lysates using QiaSpin Mini or QiaFilter Maxi columns (Qiagen). All DNA preparations are subjected to restriction digest to confirm plasmid integrity and spectrophotometry at 260 nm and 280 nm to determine DNA concentration and purity. DNA is stored at –20°C and diluted in sterile water to appropriate concentrations on the day of transfection.

Transient transfection of CHO-K1 cells. CHO-K1 cells (American Type Culture Collection) are grown in culture with Ham's F-12 culture medium (Life Technologies) supplemented with 10% FBS (Hyclone Laboratories) and 10 Units/ml Penicillin-Streptomycin (Life Technologies) and seeded at a density of ~$1x10^4$ cells/well in 48-well tissue culture plates 24 hours prior to transfection. The culture medium is removed and replaced with serum-free medium (Opti-MEM, Life Technologies, 0.5 ml/well) immediately prior to transfection. Lipofectamine (Life Technologies) is mixed with cDNA (diluted in Opti-MEM according to manufacturer's directions) such that each well receives a total of 1µl Lipofectamine and 400 ng total cDNA. F-12 medium containing serum (0.5 ml/well) is added 6-10 hr. after initiation of transfection, and cells are allowed to grow for another 12 hr. before being used for transport assays.

Expression of marker proteins. Transfected CHO-K1 cells are lifted from wells by trypsinization (2 min. at 24°C, 0.05% trypsin, 0.5 mM EDTA, Life Technologies), centrifuged (500 x g, 5 min.), and resuspended in Na-KRH. CD8 expression is assayed by incubating cell suspensions (2 ml) with anti-CD8 beads (5 µl Dynabeads M-450 CD8, Dynal Biotech) with gentle agitation (5 min., 24°C). Cells suspensions are aliquoted onto glass coverslips and allowed to adhere (10 min., 24°C), then gently washed with Na-KRH to remove unbound beads. Cells are visually scored for adherent beads under 20X magnification on an inverted microscope). EGFP expression is performed similarly, except bead incubation is omitted and cells are assayed for green fluorescence using mercury vapor illumination and a FITC filter cube (EM-2, Olympus).

[^{3}H]-5-HT transport. Wells containing transiently transfected CHO-K1 cells are washed with 2 x 0.5 ml Krebs-Ringer's-HEPES (KRH) buffer (120 mM NaCl, 1.3 mM KCl, 2.2 mM $CaCl_2$, 1.2 mM $MgSO_4$, 1.2 mM KH_2PO_4, 10 mM HEPES, 10 mM glucose, 100 µM

pargyline, and 100 μM ascorbic acid, pH 7.4 at 24°C). Cells are washed 2 times with KRH (0.5 ml/well) to remove growth medium and KRH is replaced (180 μl/well). Cells are preincubated in KRH (10 min. at 24°C) containing indicated drugs. In Na^+-substitution experiments, NaCl is isotonically replaced by choline-Cl, N-methyl-D-glucamine-Cl (NMDG), or LiCl to make choline-KRH, NMDG-KRH, or Li-KRH, respectively. Assays are initiated by addition of [^{3}H]-5HT (Amersham, 25 nM final concentration) and incubated for 2-16 min., as indicated, at 24°C. Assays are terminated by rapid aspiration of the medium followed by 3 x 0.5 ml washes with ice-cold KRH. Following aspiration of the final wash, 1% SDS (200 μl/well) is added to each well and the cells solubilized by orbital shaking (0.5-1 hr.). Cell extracts are added to scintillation vials containing 3.5 ml Ecoscint H (National Diagnostics) and incorporated [^{3}H] radioactivity is counted by liquid scintillation spectrometry and automatically converted to [^{3}H]-DPM (1600 TS, Beckman Instruments). Nonspecific 5HT transport is defined with citalopram (10 μM) or substitution of Na-KRH with NMDG-KRH as indicated. Data represent mean ± SEM from 3 replicate wells unless otherwise indicated.

[^{3}H]-GABA transport. Cells are assayed for GABA transport exactly as for 5-HT transport except that [3H]-GABA (New England Nuclear, 25 nM final concentration) was added to wells containing cells.

Inhibition by MTS reagents. Cell are washed with Li-KRH (2 x 0.5 ml) and preincubated in Li-KRH (180 μl/well) for 10 min, 24°C. MTSET (25 mM) or MTSEA (0.25 mM) is freshly diluted in Li-KRH to 10X final concentration and immediately added to reaction wells (20 μl/well) containing Li-KRH (180 μl/well). The reaction is terminated at the indicated time by addition of excess Na-KRH (0.5 ml/well) followed by rapid aspiration and replacement with fresh Na-KRH (0.5 ml/well). Control cells are washed with Li-KRH and incubated for 15 min. in the absence of MTSEA (0.25 mM) or MTSET (2.5 mM). Preincubation in Li-KRH alone does not affect subsequent 5-HT transport measurements in Na-KRH (data not shown).

Xenopus laevis oocytes

Molecular biology. Plasmid vectors containing cDNA inserts downstream of a T7 promoter sequence are used for production of RNA for oocyte injection. cDNA encoding the human serotonin transporter in pOTV vector (hSERT) was a kind gift of M. Sonders, Vollum Institute). rSERT and D98G (in pBS II SK$^-$, Stratagene) were generously provided by R. Blakely (Vanderbilt University Medical Center). cDNA templates are linearized by Not I digestion. ZH4IR was a gift of F. Bezanilla (UCLA). Linear cDNA is precipitated by addition of 2 volumes 100% ethanol and 0.5 volumes 3M sodium acetate, pH 5.2 and overnight incubation at –20^{o}C. *In vitro* transcribed RNA (cRNA) is produced according to manufacturer's instruction (T7 mMessage mMachine, Ambion) and precipitated by the LiCl method. After precipitation, cRNA is diluted to 1.0 mg/ml with sterile water and stored at –80°C until use. Human serotonin transporter cDNA in pOTV vector (hSERT) was a gift of Mark Sonders (Vollum Institute).

cRNA injection. Oocytes are isolated as described previously [95] and incubated in frog Ringer's (96 mM NaCl, 2 mM KCl, 4 mM $MgCl_2$, 0.6 mM $CaCl_2$, 5 mM HEPES, 100 μM pargyline, and 100 μM ascorbic acid, pH 7.6 at 24°C, 195-205 mOsm). cRNA is diluted with sterile water to appropriate concentrations and stored on ice on the day of injection. Oocytes are injected (Nanoject, Drummond Scientific) with 41.4 nl cRNA solution and incubated in culture medium (frog Ringer's supplemented 5% dialyzed horse serum (Hyclone Laboratories), 100 μg/ml streptomycin, 50 μg/ml tetracycline, 550 μg/ml sodium pyruvate (Sigma) for 2-18 days at either 18^{o}C or 24^{o}C, as indicated. Due to time-, temperature-, and oocyte batch-dependent variability in SERT expression profiles (see Figs, 9, 10), we routinely compare measurements functional measurements between different oocytes from the same batch. Experiments are repeated at least twice in separate oocyte batches to confirm the reproducibility of our findings.

[^{3}H]-5-HT transport. Oocytes are washed once in 10 ml frog Ringer's and preincubated in 180 μl/well frog Ringer's (10 min. at 24°C) with or without added inhibitors. Assays are initiated by addition of [^{3}H]-5-HT (12-30 nM final concentration) in a volume of 200

or 500 µl and are allowed to proceed for the indicated time at 24°C. For 5HT concentration-dependent kinetic studies, [^{3}H]-5-HT (30 nM) is supplemented with non-radiolabeled 5-HT to the indicated final concentration. In competition studies, 5-HT and AMPH are added 3 min. prior and cocaine and paroxetine are added 10 min. prior to initiation of the assay. Reactions are terminated by 3 x 2 ml washes in ice-cold frog Ringer's and incorporated [^{3}H] radioactivity is determined as described. The final wash is aspirated and incorporated [^{3}H] radioactivity is determined as described. Non-specific [^{3}H]-5-HT accumulation is defined in non-injected oocytes and is not significantly different from that measured in the presence of 10 µM citalopram or 10 µM cocaine (data not shown). Data represent mean ± SEM from at least 3 replicate oocytes unless otherwise indicated.

Two-electrode voltage clamp. Oocytes are impaled with glass microelectrodes (A-M systems) containing 3M KCl (1-3 MΩ resistance) and whole-cell two-microelectrode voltage clamp (TEVC) is achieved using a Geneclamp 500 amplifier (Axon Instruments, Foster City, CA. A Digidata 1200 A/D converter (Axon) interfaced to a PC computer running Clampex 7 software (Axon) is used to control membrane voltage and for data acquisition. Resting membrane potentials are between -20 mV and -60 mV, depending on cRNA injected and incubation conditions. Oocytes are voltage clamped at –80 mV and holding currents are between -10 nA and –90 nA. In order to discriminate 5-HT-induced current from current carried by 5-HT itself (labeled $I_{5\text{-}HT}$ in [95]), we employ the following nomenclature for the current induced by 5-HT: $I_{(5\text{-}HT)} = [I_{(10\ \mu M\ 5\text{-}HT)}] - [I_{(Control)}]$. $I_{(5\text{-}HT)}$ is elicited by superfusion of frog Ringer's (~2 ml/min) containing 5-HT (0.32 - 32 µM) at pH 7.6 or pH 5.0, 24°C, as indicated. For some experiments conducted at pH 5.0, methanesulfonate (5 mM) is included in the Ringer's solution; H^+ potentiation of $I_{(5\text{-}HT)}$ was not different under these conditions. Data were low-pass filtered at 0.5 kHz and digitized at 1 kHz; baseline currents are subtracted offline and digitally sampled at 10 Hz for graphical presentation. For voltage ramps, oocytes are clamped at –40 mV, and subjected to the indicated voltage protocol in the absence and presence of 5-HT (10 µM).

Data are low-pass filtered at 1-2 kHz and digitized at 2-5 kHz, offline subtracted, and digitally sampled at 100 Hz for presentation using Origin 5.0 (Microcal).

Charge/transport ratio (ρ). Voltage-clamped oocytes are superfused with Ringer's containing 5-HT (3.2 μM) and [^{3}H]-5-HT (30 nM) for 1 or 2 min at 24°C. Oocytes are washed and incorporated [^{3}H] radioactivity is determined as described. $Q_{5\text{-HT}}$ is calculated assuming a valence of +1*e* for 5-HT. Currents are baseline-subtracted and integrated offline (Origin) to determine total net charge movement ($Q_{(5\text{-HT})}$) and ρ is calculated for each oocyte from the quotient of $Q_{5\text{-HT}}$ and $Q_{(5\text{-HT})}$ (Eqn. 2) Specific 5-HT transport and charge movements are defined by subtracting responses in non-injected oocytes of the same batch from those in SERT cRNA-injected oocytes.

Western Blotting. An equal number of oocytes from each cRNA injection (typically 20-30) are washed with ice-cold frog Ringer's and incubated with 1.0 mg/ml EZ-Link Sulfo-NHS-biotin (Pierce) in with ice-cold frog Ringer's with gentle agitation for 60 min. Oocytes are incubated for 60 min. in ice-cold frog Ringer's containing 100 mM glycine, washed twice, and stored at –80°C until further use (< 1 month). After thawing on ice, oocytes are solubilized as previously described [149] with minor modifications. Briefly, oocytes are incubated with lysis buffer (150 mM NaCl, 10 mM Tris-HCl, pH 7.4 @ 24°C, 1 mM EDTA, 1% Triton X-100, 1 μg/ml aprotionin, 1 μg/ml leupeptin, 1 μM pepstatin and 250 μM phenylmethylsulfonyl fluoride, 20 μl/oocyte) for 10 min on ice. Extracts are triturated with a pipette until smooth, allowed to sit for 15 min. on ice, and centrifuged (15,000 x g, 15 min.) to pellet insoluble yolk material. The supernatant is removed and an aliquot saved for determination of total protein using the BCA Reagent (Pierce). Immunopure Immobilized Streptavidin beads (Pierce) are washed by centrifugation with lysis buffer (3 x 0.5 ml) and the final bead pellet resuspended to ~ 2X bead volume with lysis buffer. Oocyte extracts are incubated with 50 μl streptavidin bead slurry for 60 min., 24°C with rocking, then centrifuged for 10 min. at 15,000 x g, 4°C. The supernatant (intracellular fraction) is saved and the pellet (surface fraction) washed twice with 1 ml ice-cold lysis buffer. Streptavidin beads are incubated with 40 μl 4X loading buffer (62.5 mM Tris-HCl, pH 7.0, 10% glycerol, 2% SDS, 0.05% 2-

mercaptoethanol) for 30 min. at 24°C to elute biotinylated proteins and the entire sample is loaded in a single lane for SDS-PAGE in 10% acrylamide slab gels. For intracellular fractions, we load 25 μg /lane total protein (5% of the total extract). Proteins are transferred to Immobilion-P membranes (Millipore) overnight (4°C) and washed three times with PBS-T (phosphate-buffered saline, 0.1% Tween-20, 0.5 g/ml nonfat dry milk powder) for 15 min, 24°C. Blots were incubated for 60 min. at 24°C with anti-hSERT mouse monoclonal antibody ST51-2 (MAb Technologies) diluted 1:2,000 in PBS-T, then washed three times with PBS-T (15 min.) before incubation with a peroxidase-conjugated AffiniPure Goat anti-mouse antibody (Jackson ImmunoReasearch) diluted 1:20,000 in PBS-T for 60 min. at 24°C. Immunoreactive proteins are detected using the Renaissance Western Blot Chemiluminescence Reagent Plus (NEN Life Science Products) and Hyperfilm XL (AmershamPharmacia) per manufacturer's instructions. Exposed film is scanned (Duoscan T1200, Agfa) and quantified using Quantity One densitometry software (Bio-Rad).

Chapter III

Results

Heterologous expression of mammalian SERTs in an immortalized cell line

The Chinese hamster ovary cell line (CHO-K1) is devoid of endogenous 5-HT transport activity, making it a suitable host for heterologous expression of recombinant serotonin transporter (SERT). Although parental CHO-K1 cells accumulate 5-HT at a low rate (Na-KRH, 2.1 ± 0.1 fmol/min./well, data not shown), this activity is independent of Na^+ (NMDG-KRH, 2.1 ± 0.1 fmol/min./well, data not shown) and insensitive to blockade by addition of the antidepressant SSRI citalopram (Na-KRH + 10 μM CIT, 1.9 ± 0.2 fmol/min./well, data not shown). We therefore define specific 5-HT transport ($\Phi_{5\text{-HT}}$) in CHO-K1 cells as that which is blocked by addition of 10 μM CIT or substitution of Na^+ with $NMDG^+$.

Transfection of rSERT cDNA (in pcDNA3 vector) in CHO-K1 cells results in robust $\Phi_{5\text{-HT}}$ above background (Fig. 2). Cells transfected with rSERT cDNA alone (200 ng/well) generate a 21-fold increase in $\Phi_{5\text{-HT}}$ over background. When the amount of rSERT (200 ng/well) and Lipofectamine (1 μl/well) are held constant but the amount of empty pcDNA3 vector increases, we observe a biphasic increase in $\Phi_{5\text{-HT}}$ with a peak (58-fold over CIT) at 200 ng added pcDNA3 (Fig. 2). Further increases in pcDNA3 inhibit $\Phi_{5\text{-HT}}$ (2-fold increase over CIT with 800 ng/well added pcDNA3, Fig. 2). In subsequent studies, the total amount of cDNA transfected is therefore kept constant (400 ng/well).

The magnitude of $\Phi_{5\text{-HT}}$ also depends on the amount of cDNA transfected. $\Phi_{5\text{-HT}}$ increases hyperbolically with increasing rSERT cDNA in the transfection (Fig. 3). In a representative experiment, maximal $\Phi_{5\text{-HT}}$ is achieved at ~100 ng rSERT and the data are well fit to the Hill equation (Fig. 3, $\Phi_{5\text{-HTmax}}$ = 30.5 ± 1.3 fmol/min./well, $EC_{50\ cDNA}$ = 19.3 ± 3.7 ng/well, n_H = 1.1 ± 0.5). cDNA potency for $\Phi_{5\text{-HT}}$ is relatively constant across different cells and rSERT cDNA plasmid preparations ($EC_{50\ cDNA}$ = 28.2 ± 5.0 ng/well,

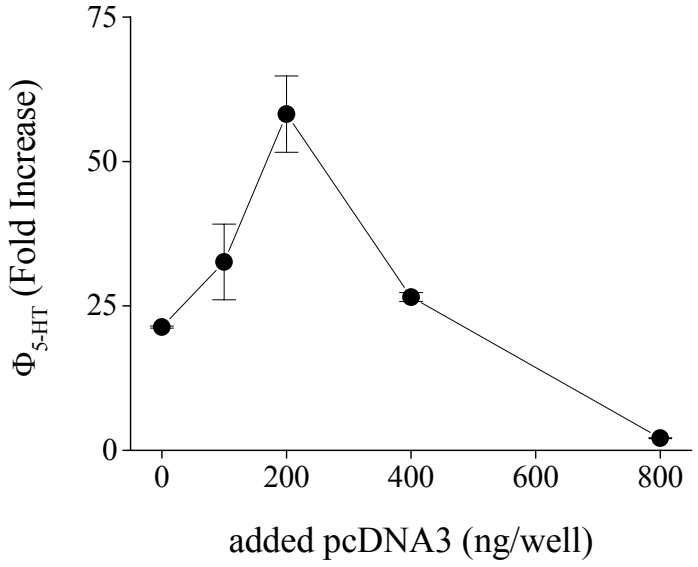

Figure 2. $\Phi_{5\text{-HT}}$ depends on the amount of cDNA transfected.
CHO-K1 cells are transfected with 200 ng rSERT (in pcDNA3 vector) and indicated amounts of empty pcDNA3. $\Phi_{5\text{-HT}}$ is measured during 10 min. incubations (24°C). Data are expressed as the fold increase in $\Phi_{5\text{-HT}}$ above that observed in the presence of citalopram (30 μM). Data represent mean ± SEM from n = 3 wells/condition from a single representative experiment. $\Phi_{5\text{-HT}}$ (rSERT, 200 ng/well alone) in this experiments is 12.8 ± 0.5 fmol/min./well. In the presence of CIT, 5-HT accumulation (0.6 ± 0.1 fmol/min./well) is not different from non-transfected cells (data not shown).

mean ± SEM, n = 3 separate experiments with different batches of cells and cDNA, data not shown).

MTSEA and MTSET inhibit SERT-mediated $\Phi_{5\text{-HT}}$ primarily by covalent modification of cysteine 109 (Cys109) [150]. In order to verify that the membrane-impermeant reagent MTSET inhibits $\Phi_{5\text{-HT}}$ by reacting with Cys109 under our experimental conditions, we constructed a single point mutation in rSERT, Cys109 to alanine (C109A). Physiological Na^+ concentrations (120 - 140 mM) protect rSERT from MTSET inhibition [150] and replacement of Na^+ with Li^+ facilitates MTS-dependent inactivation [149]. We incubate transfected cells in Li-KRH for varying times to inactivate

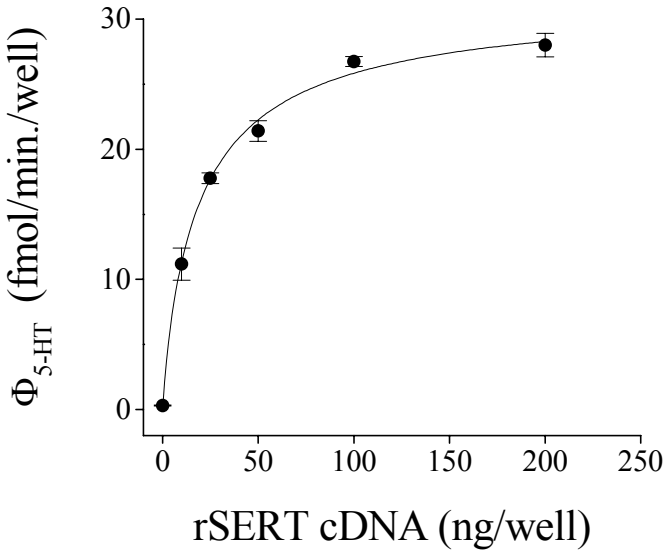

Figure 3. $\Phi_{5\text{-HT}}$ depends on quantity of rSERT cDNA in transfected CHO-K1 cells.
CHO-K1 cells are transfected in culture wells with the indicated quantity of rSERT cDNA. Empty pcDNA3 vector is added to achieve a total of 400 ng/well. Data represent means ± SEM from n = 3 wells/condition in a representative experiment. Solid line represents a fit to the Hill equation ($\Phi_{5\text{-HTmax}}$ = 30.15 ± 1.3 fmol/min./well, $EC_{50\ cDNA}$ = 19.3 ± 3.7 ng/well, n_H = 1.1 ± 0.5).

SERT, and then thoroughly wash cells with Na-KRH prior to measuring the remaining $\Phi_{5\text{-HT}}$ under standard assay conditions (Na-KRH).

In a representative experiment, rSERT and C109A express equivalent levels of $\Phi_{5\text{-HT}}$ (25 ng/well rSERT, 24.7 ± 1.7 fmol/min./well; 25 ng/well C109A, 17.3 ± 0.1 fmol/min./well). Our results independently verify that the Cys109 to Ala mutation does not dramatically alter SERT activity or plasma membrane localization [150,151]. Co-transfection of rSERT + C109A leads to an increase in $\Phi_{5\text{-HT}}$ (rSERT 25 ng/well + C109A 25 ng/well: 30.4 ± 1.1 fmol/min./well, data not shown). The fractional increase in $\Phi_{5\text{-HT}}$ in resulting from addition of C109A is consistent with the increase in $\Phi_{5\text{-HT}}$ that is

observed when the quantity of rSERT cDNA is increased from 25 ng to 50 ng (Fig. 3, 17.7 fmol/min./well to 22.2 fmol/min./well, respectively).

As expected [150], rSERT and C109A are differentially sensitive to inhibition of $\Phi_{5\text{-}HT}$ by MTS reagents. In a representative experiment, preincubation (10 min., Li-KRH) with MTSET (2.5 mM) or MTSEA (0.25 mM) inhibits $\Phi_{5\text{-}HT}$ 87.6% or 87.8%, respectively, in cells transfected with rSERT alone (data not shown). In cells transfected with C109A alone, inhibition by MTSEA and MTSET is 21.2% and 8.0%, respectively ($p < 0.001$ vs.

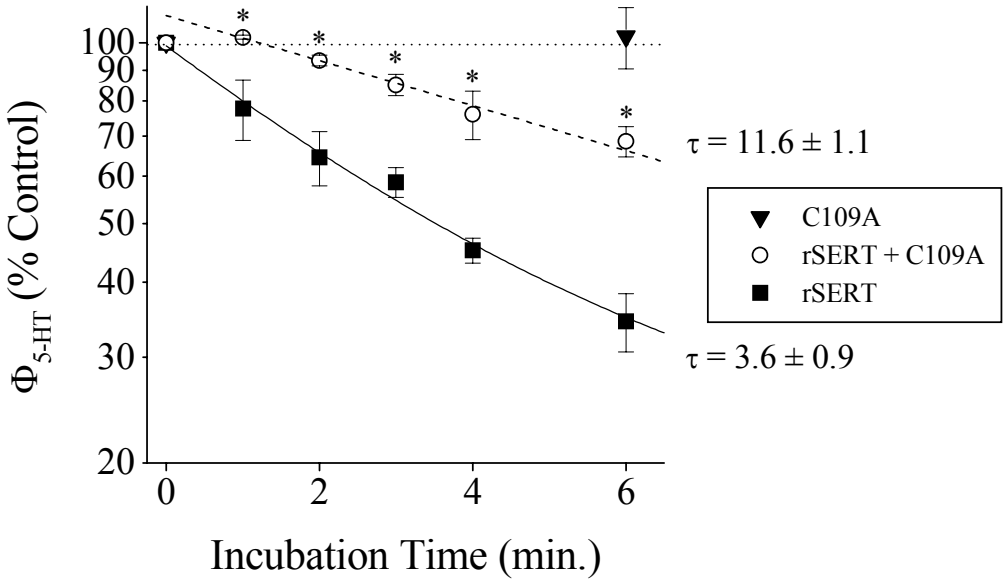

Figure 4. Interactions between rSERT and C109A alter the timecourse for MTSET inhibition of $\Phi_{5\text{-}HT}$.
CHO-K1 cells are transfected with 25 ng rSERT alone (filled squares, solid line), 25 ng rSERT + 125 ng C109A (open squares, dashed line), or 125 ng C109A alone (filled triangles) and incubated for the indicated time in Li-KRH + MTSET (2.5 mM) prior to $\Phi_{5\text{-}HT}$ assays (15 min., 24°C). Data are expressed as a percentage of $\Phi_{5\text{-}HT}$ in cells incubated (Li-KRH, 15 min., 24°C) in the absence of MTSET. Data represent means ± SEM from n = 3 separate experiments. * indicates $p < 0.05$ vs. rSERT alone. Lines represent fits to a single exponential decay function with indicated time constant (τ) ± 95% C. I.

rSERT, Student's non-paired t-test, data not shown).

Fig. 4 shows the results of an experiment designed to test whether co-transfection of rSERT and C109A exhibit functional interactions. MTSET incubation decreases rSERT-mediated $\Phi_{5\text{-}HT}$ in a time-dependent fashion (Fig. 4). For MTSET incubations between 1 min. and 6 min., fractional inhibition of $\Phi_{5\text{-}HT}$ is lower in cells transfected with rSERT, 25ng/well + C109A, 25ng/well than in cells transfected with rSERT alone, 25 ng/well (Fig. 4, $p < 0.05$, Student's non-paired t-test). The data are well fit to an exponential decay function with a single time constant (Fig. 4, rSERT, 25ng/well, $\tau = 3.7 \pm 0.9$ min.). C109A alone is unaffected by MTSET over this incubation time, but in cells co-expressing rSERT + C109A, the timecourse for inhibition of $\Phi_{5\text{-}HT}$ is slowed and the data between 2 min. and 6 min. MTSET incubation are fit to an exponential (Fig. 4, rSERT, 25ng/well + C109A, 25 ng/well, $\tau = 11.2 \pm 1.1$ min.). Although we fit the portion rSERT + C109A timecourse where $\Phi_{5\text{-}HT}$ decreases to a single exponential, the data exhibit complex behavior at early MTSET incubation times (c.f. 1 min. MTSET incubation, where $\Phi_{5\text{-}HT}$ is not different form control). Importantly, the MTSET timecourse is clearly different in co-transfected cells, indicating that MTSET sensitivity is altered by interactions between rSERT and C109A. We see similar results when rSERT and rSERT + C109A are incubated with MTSEA (0.25 mM, data not shown). Since the expectation for independence predicts that rSERT confers MTS sensitivity even when co-expressed with C109A, our findings violate the null hypothesis.

Although rSERT interacts with C109A to alter sensitivity to synthetic MTS reagents, it is of interest to know whether SERT function is sensitive to inter-subunit interactions under physiological conditions. Mutation of Asp98 renders SERT inactive (D98G) or seriously compromised (D98E) for $\Phi_{5\text{-}HT}$ [77]. If SERTs interact, then D98G might alter $\Phi_{5\text{-}HT}$ when co-expressed with rSERT. Under our experimental conditions, transfection of D98G (350 ng/well) generates small but detectable $\Phi_{5\text{-}HT}$ (Fig. 5, $\Phi_{5\text{-}HT} = 1.2 \pm 0.1$ fmol/min./well; 7.5% of rSERT control, 50 ng/well). Increasing the quantity of D98G in cells co-transfected with a constant amount of rSERT (50 ng/well) causes $\Phi_{5\text{-}HT}$

to decrease (Fig. 5). Although no effect is seen when the ratio of D98G to rSERT cDNA is 2:1 or below, D98G significantly inhibits $\Phi_{5\text{-HT}}$ at cDNA ratios of 4:1 and 7:1 (Fig. 5, $\Phi_{5\text{-HT}}$ = 48.2 % of control and 40.8 % of control, respectively).

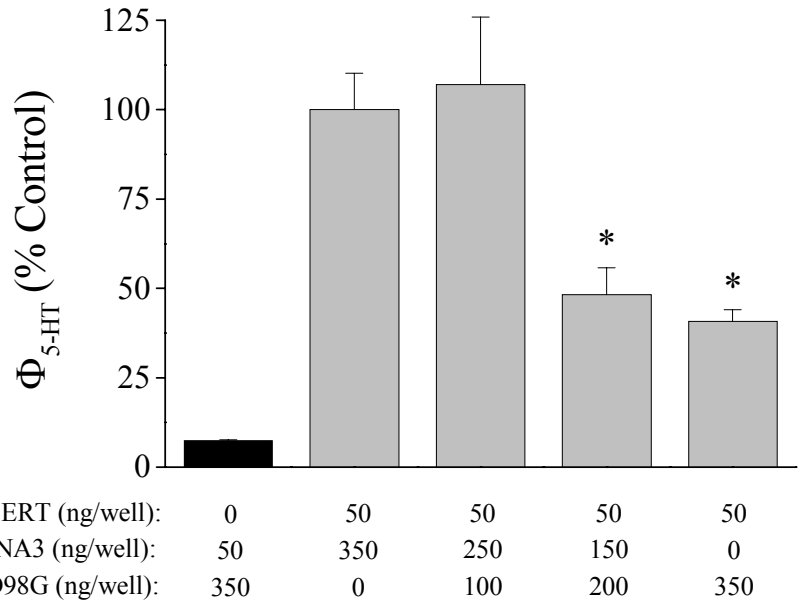

Figure 5. D98G inhibits $\Phi_{5\text{-HT}}$ when co-transfected with rSERT.
CHO-K1 cells are transfected with the indicated cDNAs and $\Phi_{5\text{-HT}}$ is measured in 15 min. assays. Data are expressed as the percentage of $\Phi_{5\text{-HT}}$ relative to cells transfected with 50 ng rSERT + 350 ng pcDNA3. Data represent means ± SEM from n = 3 wells/condition. $\Phi_{5\text{-HT}}$ for D98G alone is 1.7 ± 0.2 fmol/min./well in this experiment. * indicates $p < 0.05$ vs. 50 ng/well rSERT + 350 ng/well pcDNA3.

Na^+ potency can be determined by isotonic replacement of Na^+ with Li^+, $choline^+$, or $NMDG^+$ in the KRH buffer. Fits of the data to the Hill equation establish the half-maximal effective Na^+ concentration ($EC_{50\ Na}$). In preliminary experiments in human embryonic kidney 293 (HEK-293) cells stably expressing hSERT (HEK-hSERT), we find that apparent Na^+ potency depends on the substituting cation. Although Na^+ potency is highest in Li-KRH (Hill fit: $EC_{50\ Na}$ = 8.0 ± 1.8 mM, n_H = 1.6 ± 0.8, data not

shown), residual $\Phi_{5\text{-}HT}$ (~15% of that in Na-KRH) is consistently observed in Li-KRH. Li^+ has other effects on SERT [95,96,149] and is therefore not an inert Na^+ substitute. The large organic cations choline$^+$ and NMDG$^+$ are commonly used Na^+ substitutes. We observe that Na^+ potency is much higher in the latter (Hill fits: choline-KRH, $EC_{50\ Na}$ = 82.6 ± 8.2 mM, n_H = 1.5 ± 0.8; NMDG-KRH, $EC_{50\ Na}$ = 16.8 ± 5.2 mM, n_H = 1.5 ± 0.6, data not shown), suggesting that choline$^+$ is also not an inert Na^+ substitute for SERT. We therefore substitute Na-KRH with NMDG-KRH to determine Na^+ potency in subsequent experiments.

In addition to reduced $\Phi_{5\text{-}HT}$ (~40% of rSERT), D98E displays decreased Na^+ potency for $\Phi_{5\text{-}HT}$ (estimated $EC_{50\ Na}$ > 100 mM) [77]. These results suggest that D98G, which generates even less $\Phi_{5\text{-}HT}$ than rSERT or D98E but similar levels of surface protein expression [77], is further compromised in terms of Na^+ recognition. In CHO-K1 cells, D98G mediates Na^+-dependent $\Phi_{5\text{-}HT}$, but Na^+ potency is dramatically reduced relative to rSERT ($EC_{50\ Na}$ = 68.5 ± 3.1 mM, n_H = 1.9 ± 0.2, data not shown). Consistent with the idea that a nearby tyrosine in TMD1 is required for high affinity CIT recognition [72], Na^+-dependent D98G-mediated $\Phi_{5\text{-}HT}$ is insensitive to inhibition by CIT (10 μM), perhaps due to a substantial decrease in CIT affinity for D98G. Na^+ potency in rSERT-transfected CHO-K1 cells (Fig. 6A & Table 1, $EC_{50\ Na}$ = 13.8 ± 2.2 mM, n_H = 2.0 ± 0.2, mean ± SD from n = 12 separate experiments) is similar to that seen in other studies [17,77,84]. D98G (350 ng/well) decreases $\Phi_{5\text{-}HT}$ an average of 58% (n = 3 experiments, Fig. 5 and data not shown) when co-transfected with rSERT (50 ng/well) and causes Na^+ potency to decrease significantly (Fig. 6A & Table 1, $EC_{50\ Na}$ = 21.8 ± 3.6 mM, n_H = 1.9 ± 0.4, mean ± SD from n = 3 separate experiments; $p < 0.001$ vs. rSERT, Student's non-paired t-test). Fig. 6A shows the Na^+-dependence of $\Phi_{5\text{-}HT}$ for rSERT (50 ng/well) and rSERT + D98G (50 ng/well + 350 ng/well, respectively) normalized to their respective maxima, which emphasizes the large decrease in Na^+ potency (56.5% vs. rSERT alone) seen with D98G co-transfection.

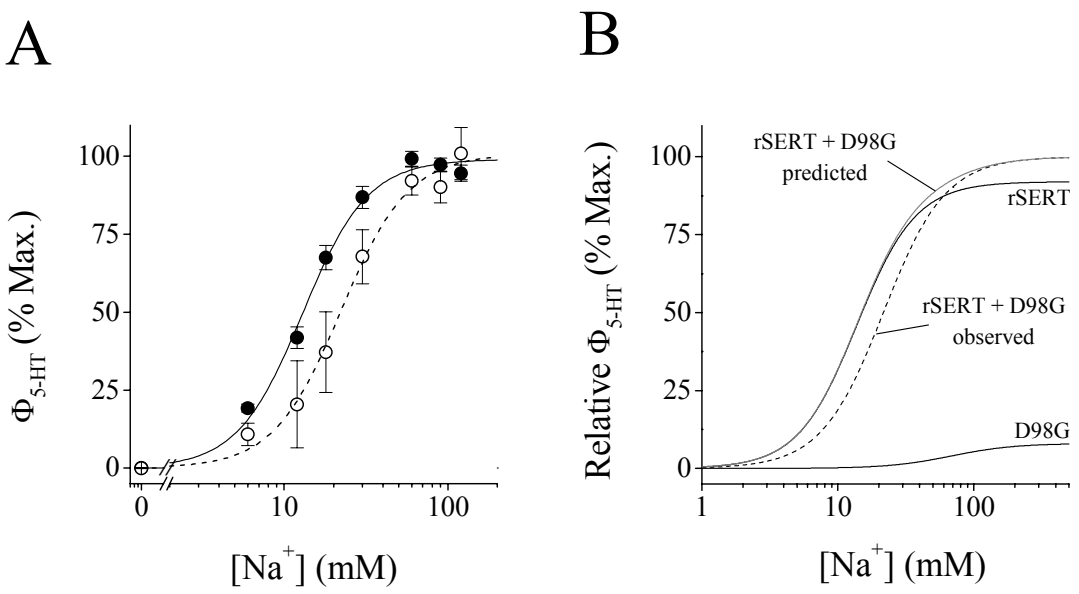

Figure 6. D98G decreases Na+ potency when co-transfected with rSERT.
A, CHO-K1 ells are transfected with 50 ng rSERT (filled circles, solid line) or 50 ng rSERT + 350 ng rSERT D98G (open squares, dashed line). Data are expressed as a percentage of maximal $\Phi_{5\text{-HT}}$ for each transfection condition. Data represent means ± SEM from n = 12 (rSERT) or n = 3 (rSERT + D98G) separate experiments. Lines represent fits to the Hill equation (rSERT, $EC_{50\ Na}$ = 13.8 ± 2.2 mM, n_H = 2.0 ± 0.2; rSERT + D98G, $EC_{50\ Na}$ = 21.6 ± 6.1mM, n_H = 1.9 ± 0.4; mean S.D. from n = 12 or n = 3 experiments; Student's non-paired t-test, $p < 0.001$). **B**, Model showing Hill fits to actual data for rSERT (upper black line, relative $\Phi_{5\text{-HT}}$ = 92%, $EC_{50\ Na}$ = 13.8 mM, n_H = 2.0) , D98G (lower black line, relative $\Phi_{5\text{-HT}}$ = 8%, $EC_{50\ Na}$ = 68.5 mM, n_H = 1.9), and rSERT + D98G (rSERT + D98G observed, dashed line, $\Phi_{5\text{-HT}}$ = 100%, $EC_{50\ Na}$ = 21.6 mM, n_H = 1.9), and the sum of the Hill functions for rSERT and D98G (rSERT + D98G expected, gray line, $\Phi_{5\text{-HT}}$ = 100%, $EC_{50\ Na}$ = 14.9 mM).

For SERTs operating according to a simple classical transporter model, $EC_{50\ Na}$ is an intrinsic property of each transporter. For independent rSERT and D98G function, Na^+ potency in cells expressing rSERT + D98G should be described by the sum of Hill functions that describe their respective Na^+–dependence when expressed individually. We model independence in cells expressing rSERT + D98G to generate the expected $EC_{50\ Na}$ in cells transfected with rSERT + D98G in Fig. 6B. The relative contributions of rSERT and D98G to the sum are derived from individual expression data (rSERT, relative $\Phi_{5\text{-HTmax}}$ = 92%, $EC_{50\ Na}$ = 13.8 mM; D98G, relative $\Phi_{5\text{-HTmax}}$ = 8%, $EC_{50\ Na}$ = 68.5

mM). For the sum of Hill equations for rSERT and D98G (Fig. 6B, rSERT + D98G, $\Phi_{5\text{-}HTmax}$ = 100%, $EC_{50\ Na}$ = 14.9 mM) $EC_{50\ Na}$ increases 8% from rSERT alone.

Since rSERT + D98G transfection decreases $\Phi_{5\text{-}HT}$ ~60% relative to rSERT alone (Figs. 5, 6), we also model independent rSERT and D98G Na^+ potencies under conditions where we increase the fractional contribution of D98G to the Hill sum (rSERT, $\Phi_{5\text{-}HTmax}$ = 80%, $EC_{50\ Na}$ = 13.8 mM; D98G, $\Phi_{5\text{-}HTmax}$ = 20%, $EC_{50\ Na}$ = 68.5 mM). When D98G mediates 20% of the total $\Phi_{5\text{-}HT}$, $EC_{50\ Na}$ increases 24% (rSERT + D98G, $\Phi_{5\text{-}HTmax}$ = 1.0, $EC_{50\ Na}$ = 17.1 mM, data not shown) compared to rSERT alone. Experimentally, D98G causes Na^+ potency to decrease 57%, 2.4-fold more than the adjusted model predicts. The observed data is not predicted by models of independent rSERT and D98G function, and we therefore conclude that SERTs function cooperatively when assayed for Na^+–dependent $\Phi_{5\text{-}HT}$.

An alternative explanation for the data in Fig. 6 is that $EC_{50\ Na}$ is sensitive to the absolute level of $\Phi_{5\text{-}HT}$. We therefore measure Na^+ potency in cells transfected with varying amounts of rSERT cDNA (10 – 50 ng/well). When the magnitude of $\Phi_{5\text{-}HT}$ is manipulated by changing the amount of rSERT cDNA transfected to mimic the decrease in $\Phi_{5\text{-}HT}$ caused by D98G co-transfection, we observe no significant shift in Na^+ potency (Fig. 7). In a representative experiment, 5-HT transport is 65% smaller at 10 ng/well ($\Phi_{5\text{-}HT}$ = 3.4 fmol/min./well) than at 50 ng/well ($\Phi_{5\text{-}HT}$ = 9.6 fmol/min./well). However, Na^+ potency is invariant over this cDNA range (10 ng/well, $EC_{50\ Na}$ = 13.0 ± 2.0 mM; 10 ng/well, $EC_{50\ Na}$ = 12.9 ± 0.7 mM). Fig. 7 shows the results from two such experiments and an exponential fit to the data. The 95% confidence limits of the fit, weighted by the error associated with the individual data points, indicate that at low $\Phi_{5\text{-}HT}$, $EC_{50\ Na}$ is clearly differentiated from the experimental value observed when rSERT and D98G are co-transfected (Fig. 6, $EC_{50\ Na}$ = 21.6 mM). Thus, simply decreasing $\Phi_{5\text{-}HT}$ is insufficient to shift $EC_{50\ Na}$. At high SERT expression, $EC_{50\ Na}$ tends to increase slightly (Fig. 7).

Because hSERT and rGAT1 interact in FRET assays [132], GAT/NET transporters are believed to form hetero-oligomers. In CHO-K1 cells, co-transfection of rSERT with

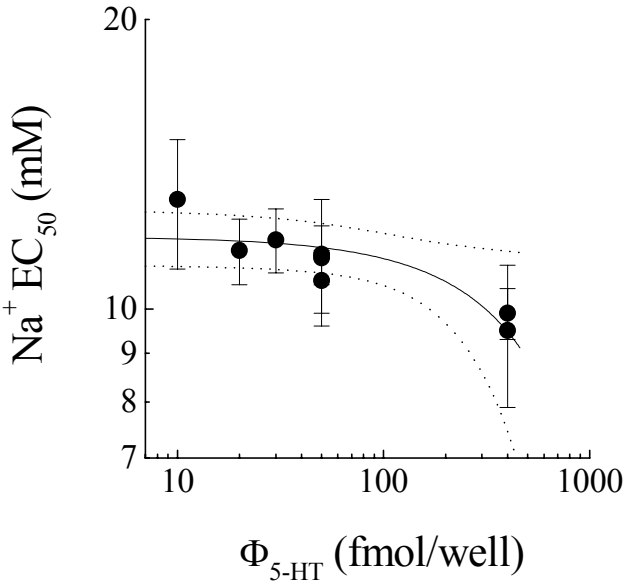

Figure 7. Na^+ potency is independent of the magnitude of $\Phi_{5\text{-HT}}$.
CHO-K1 cells are transfected with 10, 20, 30, 50, or 400 ng rSERT and assayed for Na^+-dependent $\Phi_{5\text{-HT}}$ in 15 min. assays as described. Data represent $EC_{50\ Na}$ ± 95% C.I. of Hill fits to data from n = 4 – 6 oocytes in two separate experiments. Solid line represents an exponential fit to the data and dotted lines represent 95% C.I. of the fit.

other GAT/NET transporters decreases $\Phi_{5\text{-HT}}$, although the absolute level of inhibition is variable (data not shown). Fig. 8 shows the sensitivity of rSERT-mediated $\Phi_{5\text{-HT}}$ to co-transfection with rGAT1. Relative to cells transfected with rSERT alone (rSERT 25 ng/well, $\Phi_{5\text{-HT}}$ = 7.9 ± 0.6 fmol/min./well), addition of rGAT1 cDNA (rSERT 25ng/well + rGAT1 125 ng/well, $\Phi_{5\text{-HT}}$ = 1.4 ± 0.1 fmol/min./well) decreases $\Phi_{5\text{-HT}}$ by 82%. rGAT1 (125ng/well) alone does not transport 5-HT above background levels defined by NMDG-KRH (data not shown). The effect of rGAT1 on rSERT-mediated $\Phi_{5\text{-HT}}$ is not reciprocal. Consistent with previous observations that GAT1-mediated Φ_{GABA} is more rapid than $\Phi_{5\text{-HT}}$ in SERT [11,105,106], we find that rGAT1 alone (25 ng/well) accumulates

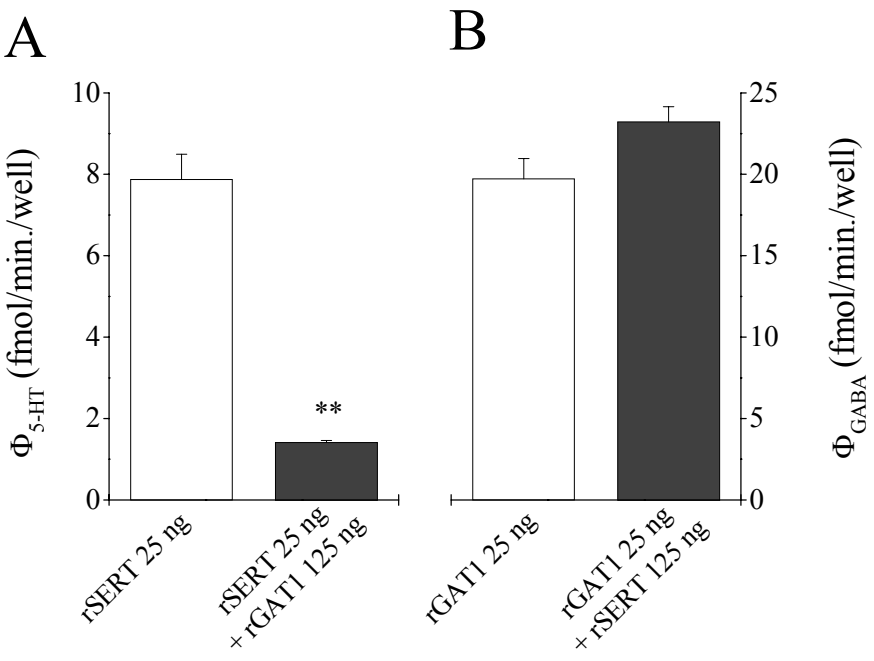

Figure 8. rSERT and rGAT1 are differentially sensitive to co-expression.
CHO-K1 cells are transfected with **A**, 25 ng rSERT alone (open bar) or 25 ng rSERT + 125 ng rGAT1 (shaded bar); or **B**, 25 ng rGAT1 alone (open bar) or 25 ng rGAT1 + 125 ng rSERT (shaded bar). Non-specific transport is defined in NMDG-KRH. Data represent means ± SEM from n = 3 well/condition in a representative experiment.

GABA (Φ_{GABA} = 19.7 ± 1.3 fmol/min./well) faster than rSERT transports 5-HT in CHO-K1 cells. However, Φ_{GABA} is unaffected by co-transfection of a 5-fold excess of rSERT (25 ng rGAT1 + 125 ng rSERT, Φ_{GABA} = 23.2 ± 0.9 fmol/min./well). Na^+ potency for Φ_{GABA} is also unchanged by rSERT co-expression (rGAT1, $EC_{50\ Na}$ = 51.2 ± 6.4 mM; rGAT1 + rSERT, $EC_{50\ Na}$ = 58.4 ± 10.5 mM, data not shown).

In contrast to rGAT1, hSERT does not interact with the dopamine D2 receptor (D_2R) in FRET assays, suggesting GAT/NET family specificity for transporter oligomerization [132]. In order to test specificity in CHO-K1 cells, we co-transfect a number of different cDNAs with rSERT. Co-transfection of cDNAs encoding hNET,

fET, rPROT, HA-tagged alpha 2A adrenergic receptor (HA-α_{2A}R), and an AMPA-type ionotropic glutamate receptor (GluR4) all inhibit rSERT-mediated $\Phi_{5\text{-HT}}$ under our experimental conditions. rGAT1 consistently inhibits $\Phi_{5\text{-HT}}$ more effectively than GluR4, but their effects on Na^+ potency are equivalent (Table 1). Table 1 summarizes results from selected rSERT co-transfections. In general, co-transfection of rSERT with cDNAs encoding polytopic integral membrane proteins decreases $\Phi_{5\text{-HT}}$.

Not all co-transfection conditions lead to inhibition of $\Phi_{5\text{-HT}}$. Under similar conditions, increasing the amount pcDNA3 (Fig. 2) or rSERT itself (Fig. 3) actually enhances $\Phi_{5\text{-HT}}$. In addition, co-transfection of the single-TMD T-cell co-receptor (CD8) or and the cytosolic green fluorescent protein (EGFP-N1) does not affect $\Phi_{5\text{-HT}}$ (Table 1), and similar results are seen when EGFP is co-transfected (50 ng/well rSERT + 350 ng/well partner cDNA, data not shown). In order to determine whether CD8 and EGFP are expressed in CHO-K1 cells, we visually assay transfected cells for CD8 and GFP expression. Cells co-transfected with CD8 (rSERT, 50 ng/well + CD8, 350 ng/well) bind anti-CD8 beads (data not shown). Non-transfected cells bind few if any anti-CD8 beads, indicating that CD8 is expressed with rSERT under our conditions. Cells co-transfected with EGFP-N1 (rSERT, 50 ng/well + EGFP, 350 ng/well) exhibit characteristic green fluorescence (data not shown), indicating that EGFP is also expressed with rSERT. The failure of CD8 and EGFP to alter $\Phi_{5\text{-HT}}$ is therefore not due to lack of protein expression.

In both HEK-hSERT cells and transiently transfected CHO-K1 cells, we observe Hill slopes in the range of 1.5 to 2.0 (data not shown, Fig. 6A, Table 1). Hill fits in excess of 1.0 indicate positive cooperativity in the Na^+-dependent activation of $\Phi_{5\text{-HT}}$. Ion some studies, Hill slope values are interpreted to directly report the number of ions co-transported with 5-HT are therefore used to calculate ion:substrate stoichiometry [17,103,152,153]. However, the exact role of Na^+ in the mechanism of 5-HT transport remains unclear, and we can identify no *a priori* reason why the Hill slope should necessarily reflect Na^+:5-HT co-transport. We therefore regard Hill slope to report intrinsically cooperative behavior in SERT function and assign no particular mechanistic meaning to

its value. Indeed, different studies variously report that $\Phi_{5\text{-HT}}$ depends either hyperbolically or sigmoidally on Na^+ concentration [48,49,92],. suggesting that differences in experimental protocols may contribute to variations in Hill slope. Nonetheless, Hill slopes for Na^+ at rSERT are relatively constant at ~ 2.0 in our studies, regardless of transfection conditions.

Table 1. $\Phi_{5\text{-HT}}$ **and** Na^+ **potency are sensitive to rSERT co-transfection.**
CHO-K1 cells are transfected with the indicated cDNA. Empty pcDNA3 vector is added to achieve a total of 400 ng/well. Data represent means ± SEM from the indicated number of experiments. * Indicates statistical significance by Student's unpaired t-test: $p < 0.05$ vs. 50 ng rSERT alone.

cDNA transfection	EC_{50Na} (mM)	*5HT Transport* (% of rSERT)	*Hill slope* (n_H)	*experiments* (n)
rSERT 50 ng	13.8 ± 2.2	100	2.04 ± 0.23	12
rSERT 50 ng **+ D98G** 350 ng	21.8 ± 3.6 *	41.8 ± 13.1 *	1.85 ± 0.38	3
rSERT 50 ng **+ CD8** 350 ng	11.0 ± 0.8	85.1 ± 15.1	2.71 ± 0.15	4
rSERT 50 ng **+ rGAT1** 350 ng	18.4 ± 2.1 *	9.0 ± 1.7 *	2.08 ± 0.24	4
rSERT 50 ng **+ GluR4-flip** 350 ng	19.7 ± 2.4 *	30.1 ± 3.0 *	2.39 ± 0.57	4
rSERT 10 ng	16.6	37.8 *	1.91	2

Heterologous expression of mammalian SERTs in <u>Xenopus</u> <u>laevis</u> oocytes

Following cRNA injection, oocytes may be maintained in culture (18°C) for 14-16 days with modest attrition rates (~50%, data not shown). Oocyte survival is assayed by visual identification of intact vitelline sheath and plasma membrane with no evidence of cytoplasmic leakage. Exogenous infection of oocytes in culture is kept to a minimum by addition of antibiotics to the culture medium and by the use of sterile transfer pipettes for handling oocytes, but survival is highly variable depending on unknown factors that vary between oocyte batches. The survival of oocytes at room temperature

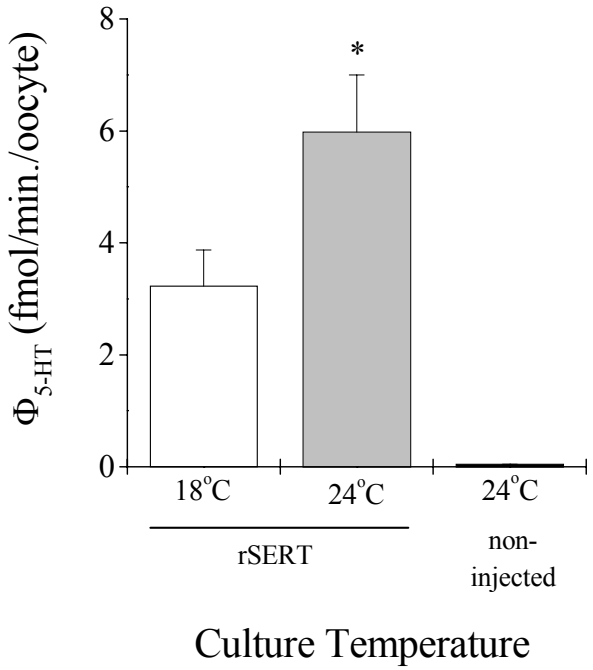

Figure 9. Increasing culture temperature stimulates expression of $\Phi_{5\text{-HT}}$ in *Xenopus laevis* oocytes.
Oocytes are injected with 42 ng rSERT cRNA and cultured for 3 days at the indicated temperature. $\Phi_{5\text{-HT}}$ is measured in 30 min. assays (24°C). Data represent means ± SEM from n = 5 oocytes/condition in a single representative experiment. * $p < 0.05$ vs. 18°C.

(24°C) is greatly diminished, especially after 3 days in culture (< 25% remaining, data not shown). However, Fig. 9 shows that 24°C culture (total $\Phi_{5\text{-HT}}$ = 6.0 ± 1.0 fmol/min./oocyte) stimulates expression of $\Phi_{5\text{-HT}}$ ~2-fold over 18°C culture (total $\Phi_{5\text{-HT}}$ = 3.2 ± 0.6 fmol/min./oocyte). Under the same conditions, non-injected oocytes do not accumulate appreciable levels of [^{3}H]-5HT (Fig. 9, non-injected total $\Phi_{5\text{-HT}}$ = 0.043 ± 0.003 fmol/min./oocyte).

$\Phi_{5\text{-HT}}$ is also sensitive to culture time and the species of cRNA injected. Fig. 10 shows that expression of $\Phi_{5\text{-HT}}$ develops more rapidly in oocytes injected with hSERT than rSERT cRNA. The timecourse for hSERT is biphasic, with a peak at ~48 hr.

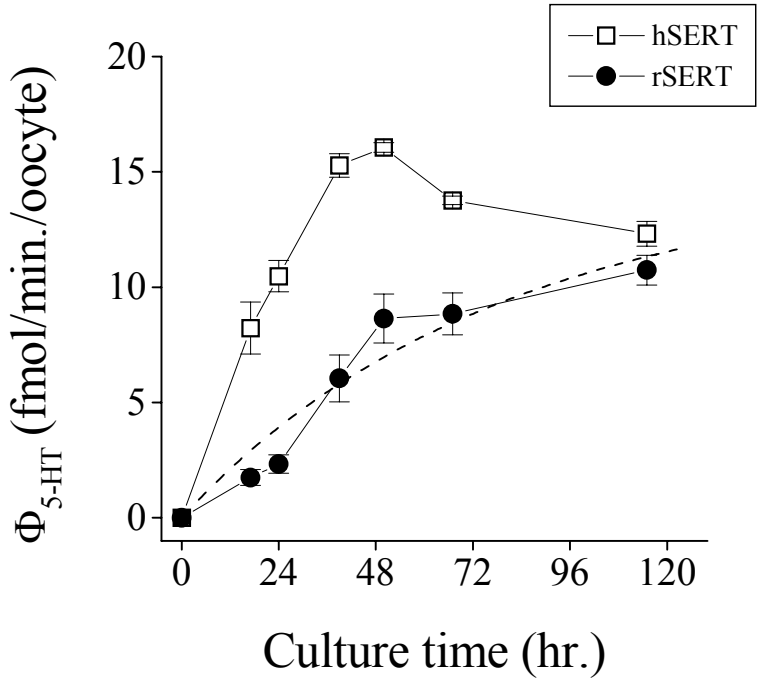

Figure 10. Expression of $\Phi_{5\text{-HT}}$ develops more rapidly for hSERT than for rSERT. Oocytes are injected with 21 ng cRNA encoding either hSERT (open squares) or rSERT (filled circles) on and cultured for the indicated time (24°C). $\Phi_{5\text{-HT}}$ is measured in 30 min. assays. Data represent means ± SEM from n = 3 - 6 oocytes/condition in a single representative experiment. Dashed line represents a fit to a single exponential function (A = 12.5 ± 3.4 fmol/min./oocyte, τ = 68.9 ± 32.3/hr.).

Although $\Phi_{5\text{-}HT}$ decreases somewhat between 48 hr. and 70 hr., it is relatively stable over longer culture times (Fig. 10). In contrast, $\Phi_{5\text{-}HT}$ mediated by rSERT continues to rise over the culture time tested (118 hr.). The rSERT timecourse is fit to a monophasic exponential function (Fig. 10, τ = 69/hr.). The exact timecourse for expression of $\Phi_{5\text{-}HT}$ varies between different batches of oocytes, but trends observed in Figs. 9 and 10 are consistent across oocyte batches. hSERT generates more $\Phi_{5\text{-}HT}$ than rSERT at short culture times due to its more rapid onset. rSERT-mediated $\Phi_{5\text{-}HT}$ continues to increase over the culture times tested (at both 24°C and 18°C), and both clones reach a similar steady-state $\Phi_{5\text{-}HT}$ at long culture times. We perform subsequent experiments with both hSERT and rSERT under varying experimental conditions. For hSERT, $\Phi_{5\text{-}HT}$ and $I_{(5\text{-}HT)}$ are measured in oocytes incubated for 4 days or less at 24°C in all experiments; in some experiments (Figs. 14, 16), rSERT-injected oocytes are cultured for up to 16 days (at 18°C) to achieve higher expression prior to performing functional assays for $\Phi_{5\text{-}HT}$ and $I_{(5\text{-}HT)}$.

The effect of increasing culture time on hSERT-mediated function is shown in Fig. 11. $\Phi_{5\text{-}HT}$ assays are conducted in the presence of low substrate concentration (30 nM [^{3}H]-5-HT) over short incubation time (2.5 min. @ 24°C). Fig. 11A shows that $\Phi_{5\text{-}HT}$ increases sigmoidally with respect to the amount of hSERT cRNA injected: the data are well fit to the Hill equation (day 2, $\Phi_{5\text{-}HTmax}$ = 1.5 ± 0.1 fmol/min./oocyte, $EC_{50\ cRNA}$ = 0.8 ± 0.1 ng/oocyte, n_H = 1.3; day 4, $\Phi_{5\text{-}HTmax}$ = 2.6 ± 0.1 fmol/min./oocyte, $EC_{50\ cRNA}$ = 2.5 ± 0.1 ng/oocyte, n_H = 1.3). A plot of the normalized data (Fig. 11B) emphasizes the 3-fold decrease in cRNA potency for $\Phi_{5\text{-}HT}$ in oocytes cultured for 2 additional days. Increasing the amount of cRNA injected also leads to a sigmoid increase in $I_{(5\text{-}HT)}$, but cRNA potency does not change from day 2 to day 4 (Fig. 11C, D). Fits to the Hill equation demonstrate that cRNA potency for $I_{(5\text{-}HT)}$ on day 2 is similar to that seen for on day 4 (Fig. 11C, day 2, $I_{5\text{-}HTmax}$ = -28.7 ± 0.5 nA, $EC_{50\ cRNA}$ = 1.5 ± 0.1 ng/oocyte, n_H = 1.4 ± 0.1; day 4, $I_{5\text{-}HTmax}$ = -35.3 ± 0.5 nA, $EC_{50\ cRNA}$ = 1.1 ± 0.1 ng/oocyte, n_H = 1.3 ± 0.1). Thus, cRNA potency for $I_{(5\text{-}HT)}$ and $\Phi_{5\text{-}HT}$ is differentially sensitive to culture time.

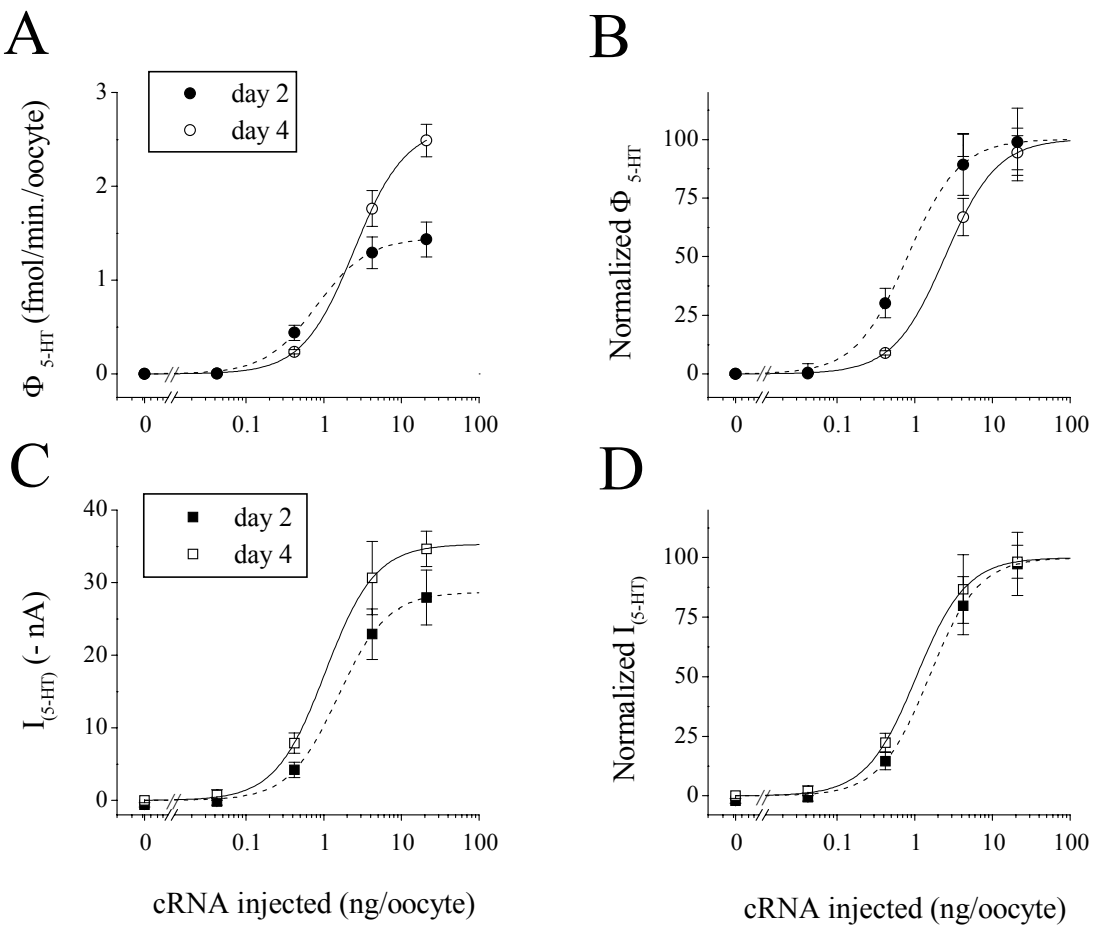

Figure 11. Increasing culture time decreases cRNA potency for $\Phi_{5\text{-HT}}$ but not $I_{5\text{-HT}}$.
Oocytes are injected with hSERT cRNA and cultured for 2 days (filled symbols, dashed lines) or 4 days (open symbols, solid lines) at 24°C. **A,** $\Phi_{5\text{-HT}}$ measured in 2.5 min. assays. **B**, $\Phi_{5\text{-HT}}$ normalized to the fitted maximum from **A**. Lines represent fits to the Hill equation (day 2, $\Phi_{5\text{-HTmax}}$ = 1.5 ± 0.1 fmol/min./oocyte, $EC_{50\ cRNA}$ = 0.8 ± 0.1 ng/oocyte, n_H = 1.3; day 4, $\Phi_{5\text{-HTmax}}$ = 2.6 ± 0.1 fmol/min./oocyte, $EC_{50\ cRNA}$ = 2.5 ± 0.1 ng/oocyte, n_H = 1.3). **C**, $I_{5\text{-HT}}$ measured at –80 mV (note inverted axis). **D**, $I_{5\text{-HT}}$ normalized to the fitted maximum from **C**. Data represent means ± SEM from n = 4 – 6 oocytes/condition in a single representative experiment. Lines represent fits to the Hill equation (day 2, $I_{5\text{-HTmax}}$ = -28.7 ± 0.5 nA, $EC_{50\ cRNA}$ = 1.5 ± 0.1 ng/oocyte, n_H = 1.4 ± 0.1; day 4, $I_{5\text{-HTmax}}$ = -35.3 ± 0.5 nA, $EC_{50\ cRNA}$ = 1.1 ± 0.1 ng/oocyte, n_H = 1.3 ± 0.1).

In order to correlate hSERT function with surface expression, we treat cRNA-injected oocytes with a membrane-impermeant biotinylating reagent (Sulfo-NHS-biotin), solubilize oocytes, and isolate plasma membrane proteins with streptavidin

beads. Following SDS-PAGE, we visualize hSERT protein using a monoclonal anti-SERT antibody (ST 51-2). Fig. 12 shows a representative Western blot from hSERT cRNA-injected oocytes. hSERT immunoreactivity is absent in non-injected oocytes (lane 1, 2), indicating that ST 51-2 detects authentic hSERT protein. In lanes loaded with

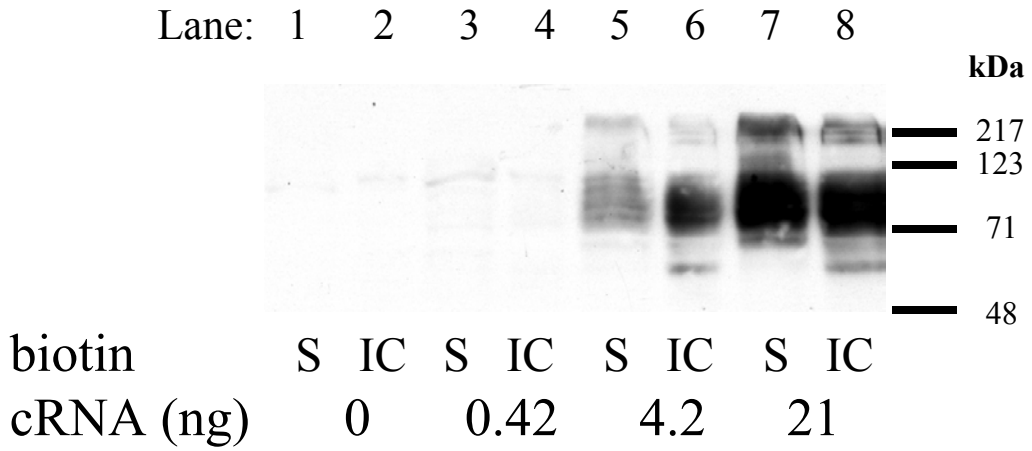

Figure 12. Surface hSERT expression depends on the amount of cRNA injected.
Oocytes are injected with SERT cRNA (0.41 to 41.4 ng/oocyte) and cultured for 2 days (24°C). A representative Western blot showing hSERT protein in biotinylated (S, surface) or non-biotinylated (IC, intracellular) fractions is shown. Lanes represent protein from 20 oocytes/condition. Equal protein is loaded in each lane.

protein from cRNA-injected oocytes, several forms of hSERT are detected: a small (~60 kDa) band that is present only in the intracellular fraction, a broad band (70-100 kDa) that is typical of mature hSERT [142], and a larger (~220 kDa) band in both surface and intracellular fractions that may represent an SDS-resistant SERT protein complex (Fig. 12). Band densities in biotinylated surface (S) and non-biotinylated intracellular (IC) fractions are comparable (Fig. 12, lanes 5, 6 and 7, 8) despite loading of IC lanes with 5% of the total extract and S lanes with the biotinylated bead eluate. Surface SERT therefore represents no more than 5% of the total SERT protein in the oocyte.

We also measure SERT function in the same batches of oocytes used for Western

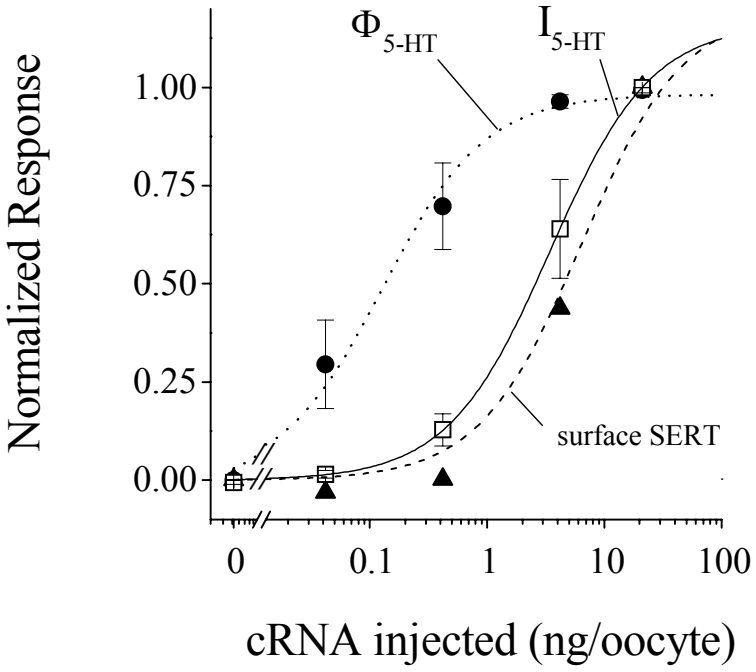

Figure 13. $\Phi_{5\text{-HT}}$ and $I_{5\text{-HT}}$ are differentially sensitive to hSERT expression level.
Oocytes are injected with SERT cRNA (0.41 to 41.4 ng/oocyte) and cultured for 2 days (24°C) $\Phi_{5\text{-HT}}$ (filled circles, dotted line) is measured in 2.5 min. (n = 3) or 30 min. (n = 2) assays. $I_{(5\text{-HT})}$ (open squares, solid line) is measured at -80 mV, pH 7.6. Surface SERT (filled triangles, dashed line) is measured by densitometry of mature surface SERT bands in Western blots. Data are expressed as a fraction of the indicated response in oocytes injected with 21 ng cRNA. Data represent means ± SEM (where shown) from n = 5 ($\Phi_{5\text{-HT}}$), 4 ($I_{(5\text{-HT})}$), or 2 (surface SERT) separate experiments. Lines represent fits to the Hill equation ($_{\text{-HT}}$, $EC_{50\ cRNA}$ = 0.13 ± 0.03 ng/oocyte; $I_{(5\text{-HT})}$, $EC_{50\ cRNA}$ = 3.42 ± 0.86 ng/oocyte; surface SERT, $EC_{50\ cRNA}$ = 6.36 ± 0.81 ng/oocyte; n_H = 1.0 for all fits).

blotting. The relative densities of the mature surface hSERT (70-100 kDa) bands from two different oocyte batches are averaged and plotted against the amount of cRNA in Fig. 13. Hill fits to the data show that the cRNA-dependence of surface SERT, $\Phi_{5\text{-HT}}$, and $I_{(5\text{-HT})}$ are not equal. As observed previously (Fig. 11), the cRNA-dependence of $I_{(5\text{-HT})}$ is shifted rightward with respect to $\Phi_{5\text{-HT}}$ (2 day culture, 24°C). At cRNA levels where $\Phi_{5\text{-HT}}$ approaches saturation (e.g. 1.5 ng/oocyte), $I_{(5\text{-HT})}$ is still rising and represents only 35% of the current measured after injection of 21 ng/oocyte.

Surprisingly, the cRNA dependence of cell surface hSERT protein is similar to $I_{(5\text{-}HT)}$ and quantitatively different from $\Phi_{5\text{-}HT}$ (Fig. 13, $\Phi_{5\text{-}HT}$, $EC_{50\ cRNA}$ = 0.13 ± 0.03 ng/oocyte; $I_{(5\text{-}HT)}$, $EC_{50\ cRNA}$ = 3.42 ± 0.86 ng/oocyte; surface SERT, $EC_{50\ cRNA}$ = 6.36 ± 0.81 ng/oocyte; n_H = 1.0 for all fits). SERT protein correlates linearly with $I_{(5\text{-}HT)}$ (R^2 = 0.90), but not $\Phi_{5\text{-}HT}$, indicating that plasma membrane expression of SERT is selectively reported by $I_{(5\text{-}HT)}$.

A similar difference in cRNA potency is seen for rSERT in oocytes cultured for

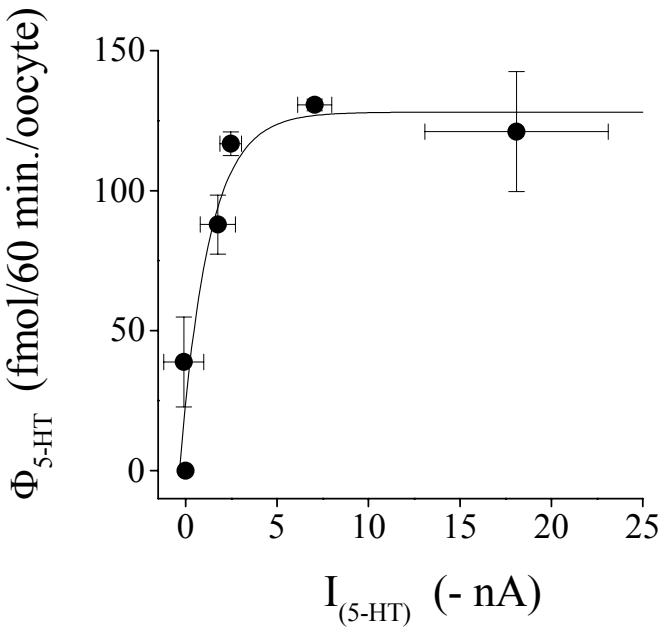

Figure 14. Increasing SERT expression reveals a functional conversion from $\Phi_{5\text{-}HT}$ mode to $I_{5\text{-}HT}$ mode.
Oocytes are injected with increasing amounts of rSERT cRNA and cultured for 14-16 days (18°C). $\Phi_{5\text{-}HT}$ is measured in 60 min. assays (12 nM [^{3}H]-5-HT) and $I_{5\text{-}HT}$ is at –80 mV, pH 7.6. Data represent means± SEM from n = 4 - 6 oocytes/condition in a single representative experiment. The solid line represents a fit to the exponential function $y = a - bc^x$, where a = 127.9 ± 15.3, b = 104.2 ± 20.9 and c = 0.53 ± 0.17. Prior to being plotted parametrically, data are fit to the Hill equation ($\Phi_{5\text{-}HTmax}$ = 126.0 ± 3.1 fmol 5HT/60 min./oocyte, $EC_{50\ cRNA}$ = 0.59 ± 0.02 ng/oocyte, n_H = 2.4 ± 0.2; $I_{(5\text{-}HT)max}$ = -40.0 ± 4.4 nA, $EC_{50\ cRNA}$ = 20.0 ± 4.8 ng/oocyte, n_H = 1.0 ± 0.2).

14-16 days at 18°C to maximize expression (Fig. 14). In order to determine whether accumulation of significant 5-HT inside the oocyte affects the cRNA dependence of $\Phi_{5\text{-}HT}$ and $I_{(5\text{-}HT)}$, we also increase incubation time for $\Phi_{5\text{-}HT}$ assays to 60 min. Even under conditions of high SERT expression and increased absolute 5-HT accumulation (~125 fmol/oocyte), rSERT cRNA exhibits differential potency for $\Phi_{5\text{-}HT}$ and $I_{(5\text{-}HT)}$. As for hSERT, increasing rSERT cRNA leads to sigmoidal rises in $\Phi_{5\text{-}HT}$ and $I_{(5\text{-}HT)}$ that are evident when the data are plotted as in Fig. 13 (not shown). At 4.1 ng/oocyte rSERT cRNA, $\Phi_{5\text{-}HT}$ has reached a plateau, but $I_{(5\text{-}HT)}$ increases 3.8-fold between 4.1 ng and 41.4 ng/oocyte cRNA (-7.1 ± 0.9 nA and -27.4 ± 2.6 nA, respectively, Fig. 14 data). Fig. 14 shows a parametric plot the data to emphasize the relationship between $\Phi_{5\text{-}HT}$ and $I_{(5\text{-}HT)}$. In the low cRNA range (≤ 1 ng/oocyte), increases in cRNA lead predominantly to more $\Phi_{5\text{-}HT}$. An inflection point is reached at 2-5 ng/oocyte; above 2 ng/oocyte, increasing cRNA generates primarily additional $I_{(5\text{-}HT)}$ (Fig. 14). A simple model of SERT function predicts that the slope of the parametric plot will be independent of the number of SERT proteins (N, Eqn. 3), and thus reflects only intrinsic properties of SERT function (i, p_o, ν, q). However, the slope of the line fit to the data is not constant (Fig. 14), suggesting that cooperative interactions govern the relative magnitudes of $\Phi_{5\text{-}HT}$ and $I_{(5\text{-}HT)}$.

Fig. 15 shows a current trace from a representative oocyte injected with rSERT cRNA (14 ng). $I_{(5\text{-}HT)}$ is elicited first at pH 7.6, and subsequently at pH 5.0. After establishing a stable baseline current (defined as zero current by offline leak subtraction), the oocyte is superfused with 5-HT (3.2 μM) long enough to determine steady-state 5-HT-induced current amplitude (Fig. 15, $I_{(5\text{-}HT)\ pH\ 7.6}$), then returned to control solution. Superfusion of frog Ringer's, pH 5.0, elicits a steady-state constitutive inward leak current (Fig. 15, $I_{H^+\ leak}$) in both non-injected and cRNA-injected oocytes, but the magnitude of $I_{H^+\ leak}$ is larger in oocytes expressing SERT [154,155]. Superfusion of 5-HT (3.2 μM) at pH 5.0 potentiates 5-HT-induced current, (Fig. 15, $I_{(5\text{-}HT)\ pH\ 5.0}$). H^+-potentiation of $I_{(5\text{-}HT)}$ confirms rSERT expression ($I_{(5\text{-}HT)}$ in hSERT is insensitive to

extracellular acidification [154]) and allows us to more easily measure $I_{(5\text{-}HT)}$ in oocytes injected with small quantities of cRNA.

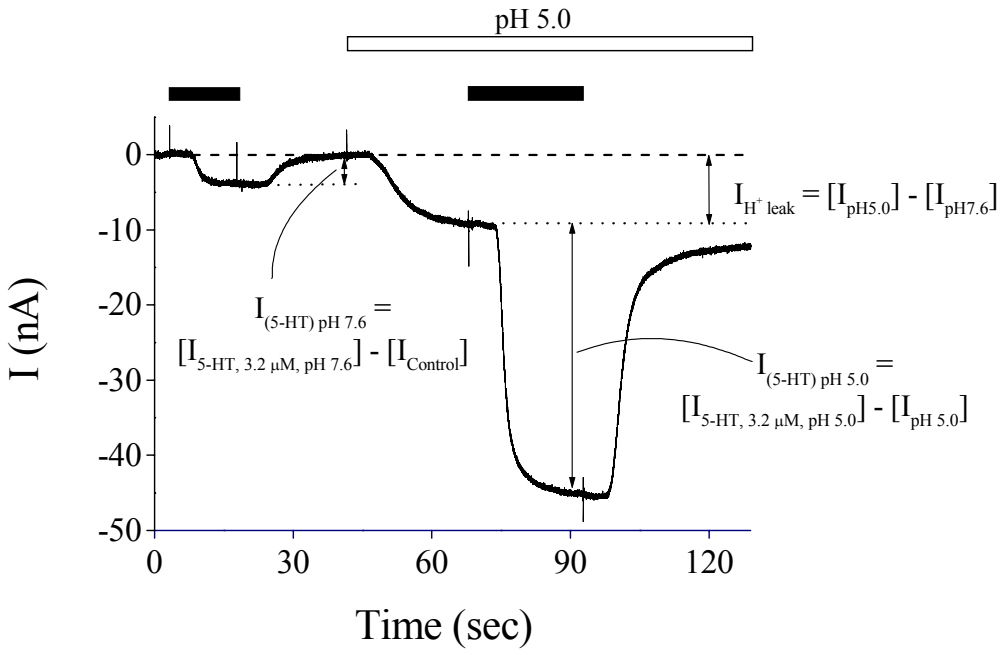

Figure 15. H^+-potentiation of $I_{(5\text{-}HT)}$ in rSERT.
Oocytes are injected with 14 ng rSERT cRNA and cultured for 13 days (18°C). Data represent baseline-subtracted current from a single representative oocyte. Dashed line indicates the zero current level. Filled bars indicate time during which 5-HT (3.2 μM) is superfused and open bar indicates time during which frog Ringer's, pH 5.0 is superfused. Artifact spikes in current recording indicate actual time that superfusion switches are initiated; the delay between switch artifact and change in current represents the combination of a) lag time for superfusion to reach the oocyte in the recording chamber, and b) penetration of 5-HT through the oocyte's protective vitelline layer.

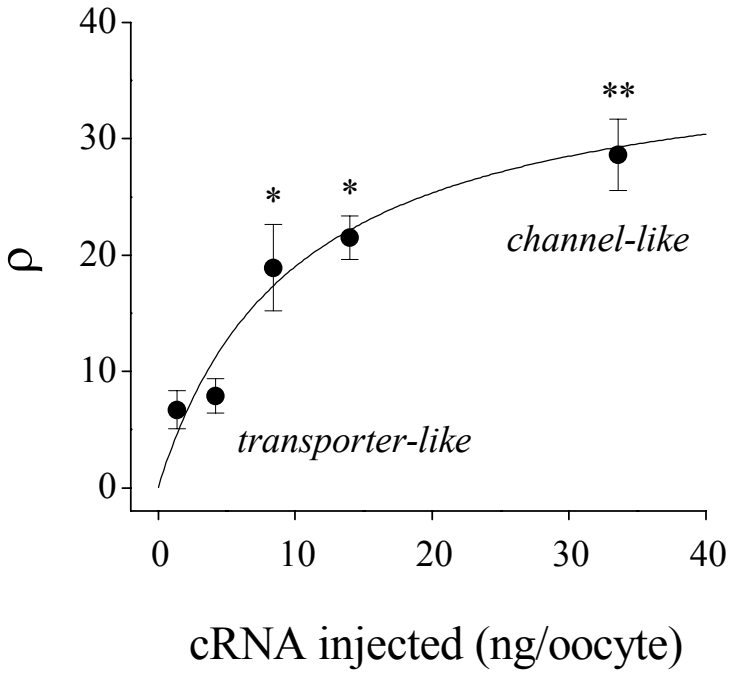

Figure 16. Increasing rSERT expression alters ρ.
Oocytes are injected with increasing amounts of rSERT cRNA and cultured for 14-16 days (18°C). $I_{(5\text{-}HT)}$ is measured at -80 mV, pH 5.0 during a 2 min. superfusion of 5-HT (3.2 μM) + [^{3}H]-5-HT (30 nM). $Q_{5\text{-}HT}$ and $Q_{(5\text{-}HT)}$ are calculated as described to obtain ρ. Data represent means ± SEM from n = 3–6 oocytes/condition in a single representative experiment. Line represents a fit to the Hill equation (ρ_{max} = 37.5 ± 5.6 *e*/5-HT; $EC_{50\ cRNA}$ = 10.2 ± 3.7 ng/oocyte; n_H = 1.0). Statistically significant differences are indicated by *, p , 0.05, **, p < 0.01 versus oocytes injected with 1.4 ng cRNA.

In order to test whether the differential cRNA dependence of $\Phi_{5\text{-}HT}$ and $I_{(5\text{-}HT)}$ is due to voltage differences intrinsic to the respective assay conditions, we measure $\Phi_{5\text{-}HT}$ and $I_{(5\text{-}HT)}$ simultaneously under voltage clamp at –80 mV. Superfusion of 5-HT (3.2 μM) + [^{3}H]-5-HT (30 nM) for 2 min. at 24°C elicits both $\Phi_{5\text{-}HT}$ and $I_{(5\text{-}HT)}$, from which we calculate charge movement associated with 5-HT flux ($Q_{5\text{-}HT}$) and total charge movement ($Q_{(5\text{-}HT)}$) (Eqn. 2). Fig. 16 shows that ρ increases 4.3-fold as the amount of cRNA increases from 1.4 ng to 33.6 ng (ρ = 6.7 ± 1.6 and 28.6 ± 3.1, respectively). In contrast to $I_{(5\text{-}HT)}$, $\Phi_{5\text{-}HT}$ is relatively insensitive to pH change [77,154]. We therefore calculate that under physiological conditions (–80 mV, pH 7.6), ρ varies between ~1 and

~4 over a range of rSERT expression in oocytes. The validity of this calculation is reinforced by the observation that ρ = 4.4 when measured at pH 7.6 in a separate batch of oocytes injected with 8.3 ng/oocyte rSERT cRNA (Fig. 22). The differential cRNA dependence of $I_{(5\text{-}HT)}$ and $\Phi_{5\text{-}HT}$ is therefore not due to differences in membrane potential. We conclude that one or more microscopic properties of SERT function (Eqn. 3) are therefore sensitive to expression level.

Fig. 17 shows the H^+-potentiation ratio of $I_{(5\text{-}HT)}$ in the same batch of oocytes as those shown in Fig. 16. $I_{(5\text{-}HT)\ pH\ 7.6}$ and $I_{(5\text{-}HT)\ pH\ 5.0}$ are highly correlated across the range of cRNA tested (R^2 = 0.99, Fig. 14 and data not shown), indicating that cRNA potency is

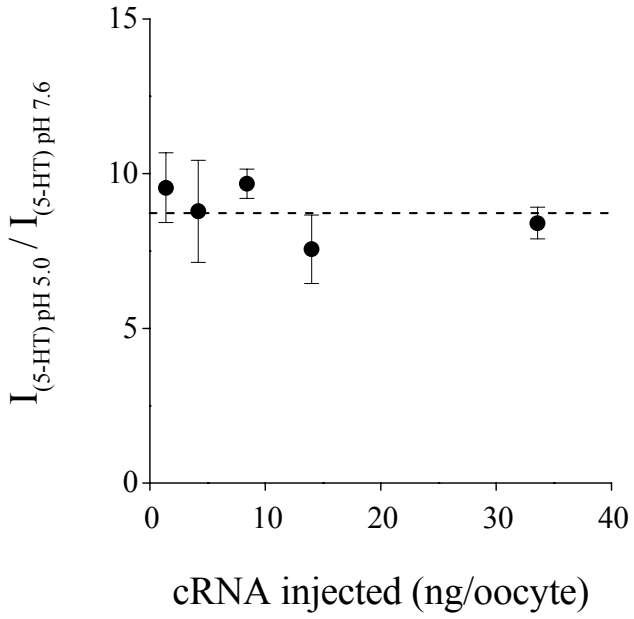

Figure 17. H^+-potentiation of $I_{(5\text{-}HT)}$ is independent of rSERT expression level.
Data is from oocytes shown in Fig. 16. $I_{(5\text{-}HT)}$ is measured at -80 mV, pH 7.6 and pH 5.0. Data represent means ± SEM from n = 4 - 10 oocytes/condition in a single representative experiment. Dashed line indicates average level of H^+ potentiation across all cRNA injections tested.

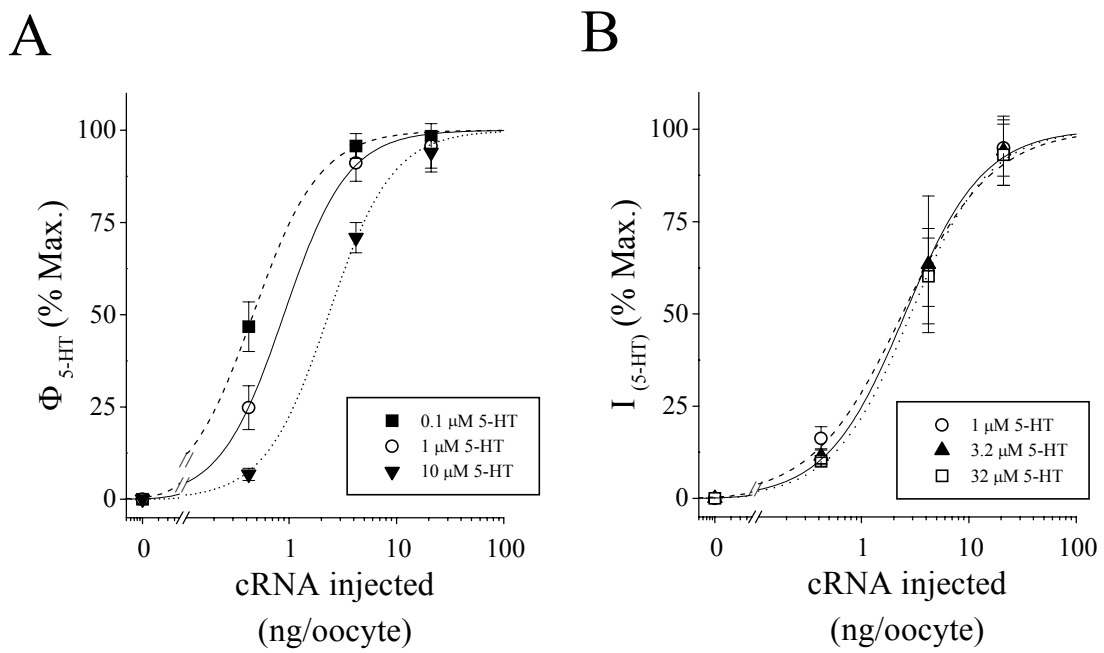

Figure 18. Increasing 5-HT concentration decreases cRNA potency for $\Phi_{5\text{-HT}}$ but not $I_{5\text{-HT}}$. Oocytes are injected with increasing amounts of hSERT cRNA and cultured for 2 days (24°C). $\Phi_{5\text{-HT}}$ is measured in the presence of 0.1 μM 5-HT (filled squares, dotted line), 1.0 μM 5-HT (open circles, sold line), or 10 μM 5-HT (filled triangles, dashed line) and normalized to the respective $\Phi_{5\text{-HTmax}}$. Lines represent fits to the Hill equation (0.1 μM 5-HT, $EC_{50\ cRNA}$ = 0.45 ± 0.01 ng/oocyte; 1.0 μM 5-HT, $EC_{50\ cRNA}$ = 0.84 ± 0.04 ng/oocyte; 10 μM 5-HT, $EC_{50\ cRNA}$ = 2.20 ± 0.12 ng/oocyte; n_H = 1.3). [^{3}H]-5-HT concentration in all experiments is 30 nM and indicated 5-HT concentration is achieved by addition of non-labeled 5-HT. **B,** $I_{5\text{-HT}}$ measured at different 5-HT concentrations (1.0 μM 5-HT (open circles, dashed line), 3.2 μM 5-HT (solid triangles, sold line), or 32 μM 5-HT (open squares, dotted line) and normalized to the respective $I_{5\text{-HTmax}}$. Lines represent fits to the Hill equation (1.0 μM 5-HT, $EC_{50\ cRNA}$ = 3.0 ± 0.4 ng/oocyte; 3.2 μM 5-HT, $EC_{50\ cRNA}$ = 3.1 ± 0.4 ng/oocyte; 32 μM 5-HT, $EC_{50\ cRNA}$ = 3.5 ± 0.5 ng/oocyte; n_H = 1.0 for all fits). Data are expressed as a percentage of the maximal $\Phi_{5\text{-HT}}$ (**A**) or $I_{5\text{-HT}}$ (**B**) measured for each condition. For **A** and **B**, data represent mean ± SEM from n = 4 - 6 oocytes/condition in a single representative experiment.

not altered by extracellular acidification. When measured directly, the ratio of $I_{(5\text{-HT})\ pH\ 7.6}$ to $I_{(5\text{-HT})\ pH\ 5.0}$ is independent of SERT expression level (Fig. 17, dashed line, $I_{(5\text{-HT})\ pH5.0}/I_{(5\text{-HT})\ pH7.6}$ = 8.8 ± 0.4, from 1.4 to 33.6 ng/oocyte). In contrast to the ratio of $I_{(5\text{-HT})}$ to $\Phi_{5\text{-HT}}$ (Figs. 13, 14, 16), H^+-potentiation conforms to the predicted behavior for SERTs operating according to a simple model (Eqn. 3).

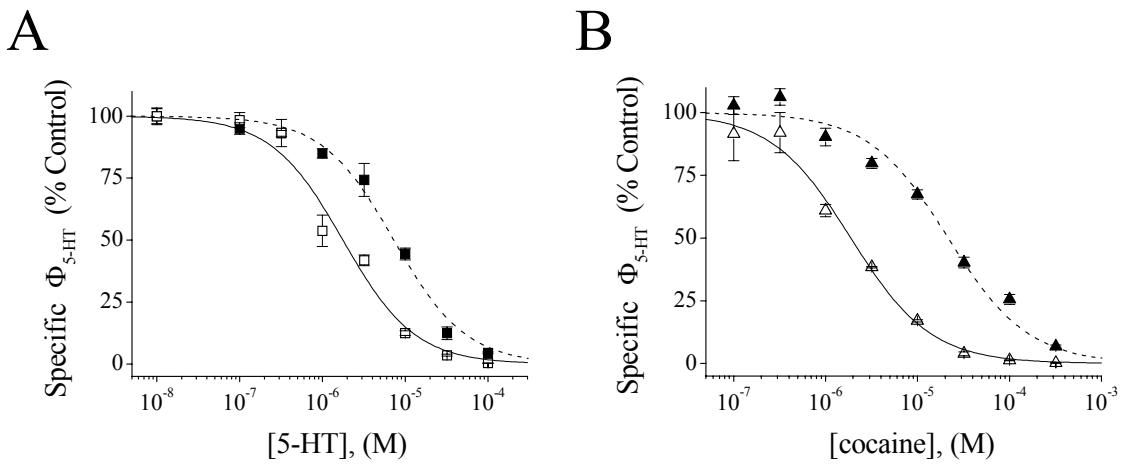

Figure 19. Potency for inhibition of $\Phi_{5\text{-HT}}$ is sensitive to hSERT expression level.
Oocytes are injected with 0.42 ng/oocyte (open symbols, solid lines) or 21 ng/oocyte (filled symbols, dashed lines) hSERT cRNA and cultured for two days (24°C). **A,** $\Phi_{5\text{-HT}}$ is measured in the presence of increasing concentrations of non-labeled 5-HT (squares). Lines represent fits to the Hill equation (0.42 ng/oocyte, solid line, IC_{50} = 1.6 ± 0.3 μM; 21 ng/oocyte, dashed line, IC_{50} = 7.7 ± 0.9 μM; n_H = 1.0). **B,** $\Phi_{5\text{-HT}}$ is measured in the presence of increasing concentrations of cocaine (triangles). Lines represent fits to the Hill equation (0.42 ng/oocyte, solid line, IC_{50} = 1.9 ± 0.42 μM; 21 ng/oocyte, dashed line, IC_{50} = 20 ± 3.2 μM; n_H = 1.0). Data represent means ± SEM from n = 4 - 6 oocytes/condition in a single representative experiment.

In order to investigate whether other SERT properties are sensitive to SERT expression level, we examine hSERT pharmacology in oocytes injected with varying quantities of hSERT cRNA. As expected, $\Phi_{5\text{-HT}}$ increases as 5-HT concentration increases (0.1 μM 5-HT, $\Phi_{5\text{-HTmax}}$ = 0.38 ± 0.07 pmol/min./oocyte; 1.0 μM 5-HT, $\Phi_{5\text{-HTmax}}$ = 3.08 ± 0.08 pmol/min./oocyte; 10 μM 5-HT, $\Phi_{5\text{-HTmax}}$ = 17.39 ± 0.11 pmol/min./oocyte). Fig. 18A shows normalized data in order to emphasize the 5-HT concentration-dependent shift in apparent cRNA potency (0.1 μM 5-HT, $EC_{50\ cRNA}$ = 0.45 ± 0.01 ng/oocyte; 1.0 μM 5-HT, $EC_{50\ cRNA}$ = 0.84 ± 0.04 ng/oocyte; 10 μM 5-HT, $EC_{50\ cRNA}$ = 2.20 ± 0.12 ng/oocyte; n_H = 1.3 for all fits). Over a similar range of 5-HT concentrations, cRNA potency for $I_{(5\text{-HT})}$ is unchanged (Fig. 18B, 1.0 μM 5-HT, $EC_{50\ cRNA}$ = 3.0 ± 0.4 ng/oocyte; 3.2 μM 5-HT, $EC_{50\ cRNA}$ = 3.1 ± 0.4 ng/oocyte; 32 μM 5-HT, $EC_{50\ cRNA}$ = 3.5 ± 0.5 ng/oocyte; n_H = 1.0 for all fits).

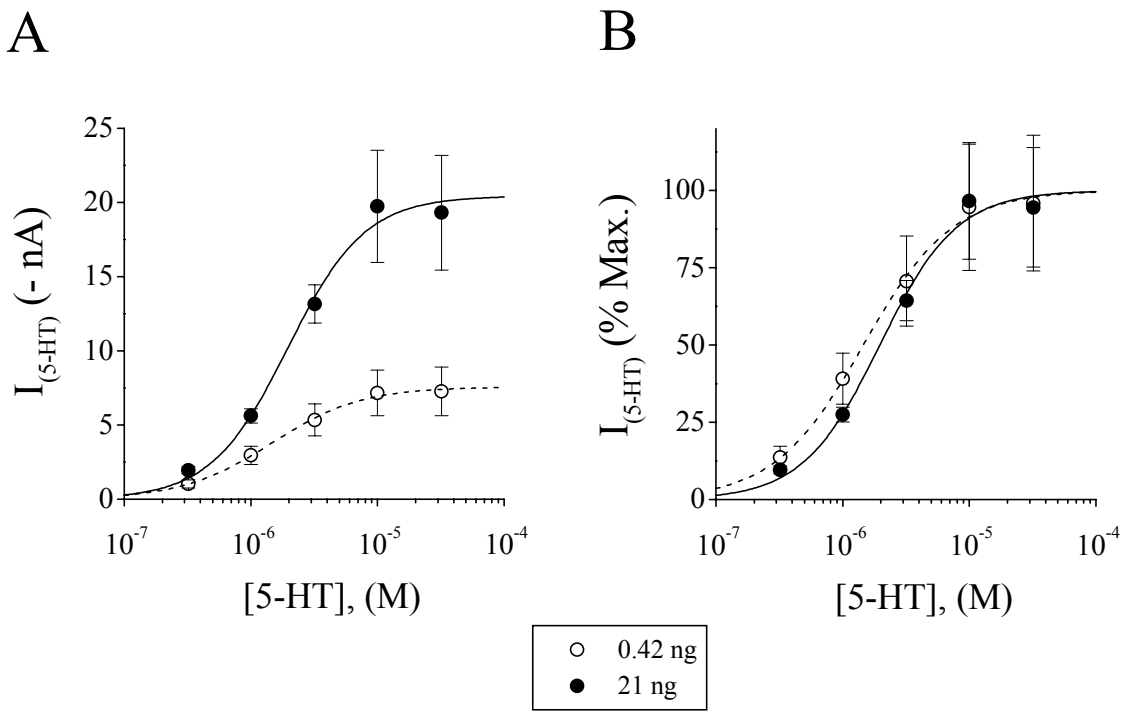

Figure 20. 5-HT potency for $I_{5\text{-}HT}$ is independent of hSERT expression level.
Oocytes are injected with 0.42 ng/oocyte (open circles) or 21 ng/oocyte (filled circles) hSERT cRNA and cultured for 2 days (24°C). **A**, $I_{(5\text{-}HT)}$ measured at -80 mV, pH 7.6. Data are expressed as the inverse of the actual current. Data represent mean ± SEM from n = 5 or 7 oocytes/condition in a single representative experiment. Lines represent fits to the Hill equation (0.42 ng/oocyte, dashed line, $I_{(5\text{-}HT)max}$ = -7.6 ± 0.9 nA, $EC_{50\ 5\text{-}HT}$ = 1.5 ± 0.1 μM, n_H = 1.2; 21 ng/oocyte, solid line, $I_{(5\text{-}HT)max}$ = –20.4 ± 0.9 nA, $EC_{50\ 5\text{-}HT}$ = 2.0 ± 0.2, n_H = 1.4). **B**, data from A expressed as a percentage of the respective maximal current.

We also plot $\Phi_{5\text{-}HT}$ data from the experiment shown in Fig. 18A against [5-HT] to measure changes in 5-HT potency at different levels of cRNA injection (data not shown). We observe that 5-HT exhibits higher potency at lower hSERT expression (0.42 ng/oocyte, $EC_{50\ 5\text{-}HT}$ = 1.7 ± 0.5 μM; 21 ng/oocyte, $EC_{50\ 5\text{-}HT}$ = 8.0 ± 4.0 μM; n_H = 1.0 for all fits, mean ± SEM from n = 3 separate experiments, data not shown). 5-HT potency is therefore inversely correlated with SERT expression and cRNA potency is inversely correlated with 5-HT concentration.

Expression-level-dependent shifts in substrate potency are also observed in competition assays where we measure concentration-dependent inhibition of $\Phi_{5\text{-}HT}$ (Fig.

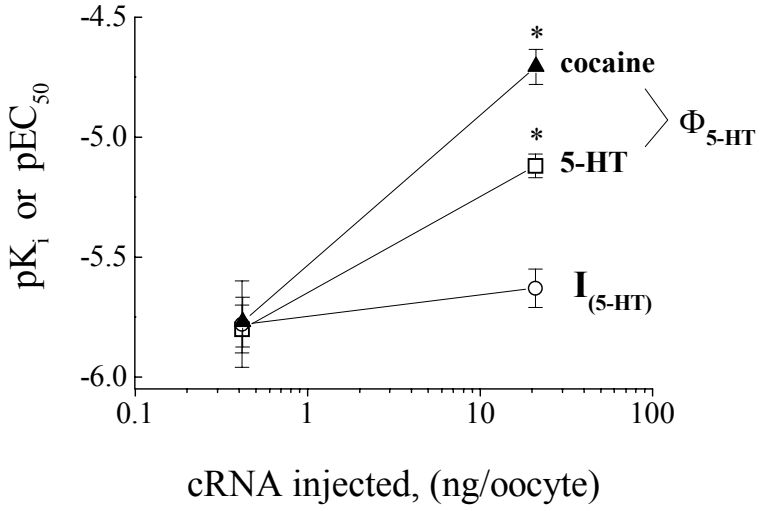

Figure 21. SERT ligands exhibit expression level-sensitive potency shifts for $\Phi_{5\text{-HT}}$ but not $I_{(5\text{-HT})}$.
pK_i for inhibition of $\Phi_{5\text{-HT}}$ by 5-HT (open squares, data from Fig. 19), cocaine (filled triangles, data from Fig. 19), and pEC_{50} for 5-HT (open circles, data from Fig. 20). pK_i values are calculated from Eqn. 4. * $p < 0.05$ vs. $I_{(5\text{-HT})}$.

19). 5-HT potency for inhibition of $\Phi_{5\text{-HT}}$ is higher in oocytes injected with 0.42 ng hSERT cRNA than in oocytes injected with 21 ng hSERT cRNA (Fig. 19A). Inhibitory potency for the non-transported ligand cocaine follows the same trend as 5-HT, only the magnitude of the potency shift is larger (Fig. 19B). The transported substrate D-amphetamine (AMPH) shares expression-level sensitivity with 5-HT (0.42 ng/oocyte, $IC_{50} = 40 \pm 5.7$ μM; 21 ng/oocyte, $IC_{50} = 170 \pm 30$ μM, data not shown), and the non-transported antidepressant paroxetine ($IC_{50} = 7.9 \pm 1.3$ nM; 21 ng/oocyte, $IC_{50} = 55.2 \pm 9.6$ nM, data not shown) shifts similarly to cocaine. pK_i values are estimated for 5-HT and cocaine (Eqn. 4, pK_i = -5.8 and –5.12 for 5-HT and pK_i = –5.73 and –4.7 for cocaine in oocytes injected with 0.42 ng/oocyte and 21ng/oocyte, respectively).

In contrast to $\Phi_{5\text{-HT}}$, the potency for 5-HT to elicit $I_{(5\text{-HT})}$ is insensitive to hSERT expression level (Fig. 20). At low hSERT cRNA (0.42 ng/oocyte), 5-HT potency for $I_{(5\text{-}}$

$_{HT)}$ is similar to that seen for $\Phi_{5\text{-}HT}$ (Fig. 20, $I_{(5\text{-}HT)max}$ = -7.6 ± 0.9 nA, $EC_{50\ 5\text{-}HT}$ = 1.6 ± 0.9 μM, n_H = 1.0, mean ± SEM from n = 5 oocytes). At higher expression level (21 ng/oocyte), 5-HT potency remains essentially unchanged (Fig. 20, $I_{(5\text{-}HT)max}$ = –20.4 ± 0.9 nA, $EC_{50\ 5\text{-}HT}$ = 2.4 ± 0.4, n_H = 1.0, n = 7 oocytes).

Fig. 21 summarizes changes in ligand potency observed at low and high SERT expression. Inhibitory potency decreases 4 to 5 fold for 5-HT and 10 fold for cocaine when cRNA is increased from 0.42 ng/oocyte to 21 ng/oocyte (Fig. 19). Over the same range of cRNA, however, 5-HT potency for $I_{(5\text{-}HT)}$ does not change substantially (Fig. 20). Substrate and inhibitor potency is therefore sensitive to SERT expression level when measured in the functional context of 5-HT transport, but not 5-HT-induced current. The finding that SERT transport and current properties are differentially sensitive to expression level suggests that SERT may interact with a protein or cellular factor that modulates its function. One possibility is that ρ is sensitive to inter-subunit interactions in an oligomeric SERT functional complex [119,132].

In order to determine whether rSERT and D98G exhibit functional interactions, we inject oocytes with rSERT cRNA alone (8.3 ng/oocyte) or mixed with D98G (rSERT, 8.3 ng + D98G, 33.1 ng/oocyte) and measure $\Phi_{5\text{-}HT}$ and $I_{(5\text{-}HT)}$ during 1 min. (24°C) assays at –80 mV to obtain ρ. Fig. 22A shows that co-injection of rSERT + D98G attenuates total charge movement, $Q_{(5\text{-}HT)}$, by 51% compared to rSERT alone. However, the charge movement associated with 5-HT flux, $Q_{5\text{-}HT}$, is unaffected (Fig. 22B). D98G consequently decreases ρ by 35% compared to rSERT (Fig. 22C). D98G alone mediates no detectable $I_{(5\text{-}HT)}$ above that seen in non-injected oocytes (data not shown). D98G therefore selectively attenuates $I_{(5\text{-}HT)}$ when co-expressed with rSERT.

The effect of D98G in oocytes is specific, since when we co-inject rSERT with a *Shaker* K^+ channel (rSERT, 8.3 ng + ZH4IR, 2.3 ng/oocyte), we observe no effect on $\Phi_{5\text{-}HT}$ or $I_{(5\text{-}HT)}$. However, in the same batch of oocytes we do record a large outward current (up to 16 μA at +100 mV, data not shown). Given that under voltage clamp in oocytes, $p_o \approx 0.75$ and $i \approx 1$ pA for this *Shaker* construct [156], we calculate that there are ~1.3×10^6 *Shaker* channels expressed on the plasma membrane of an oocyte generating

10 μA current at +60 mV (Eqn. 3).

In order to determine whether SERT and D98G interact to alter ion permeation properties, we examine the voltage dependence of $I_{(5\text{-}HT)}$ in oocytes injected with rSERT cRNA alone or together with D98G cRNA. Fig. 23A shows representative raw currents from an oocyte injected with rSERT cRNA alone (8.3 ng/oocyte) recorded over the indicated voltage ramp in the absence and presence of 5-HT (10 μM), pH 5.0. $I_{(5\text{-}HT)}$ is defined by subtraction (Fig. 15) and plotted as a function of membrane voltage to generate $I_{(5\text{-}HT)}$ (V) in Fig. 23B. $I_{(5\text{-}HT)}$(V) exhibits the inward rectification and

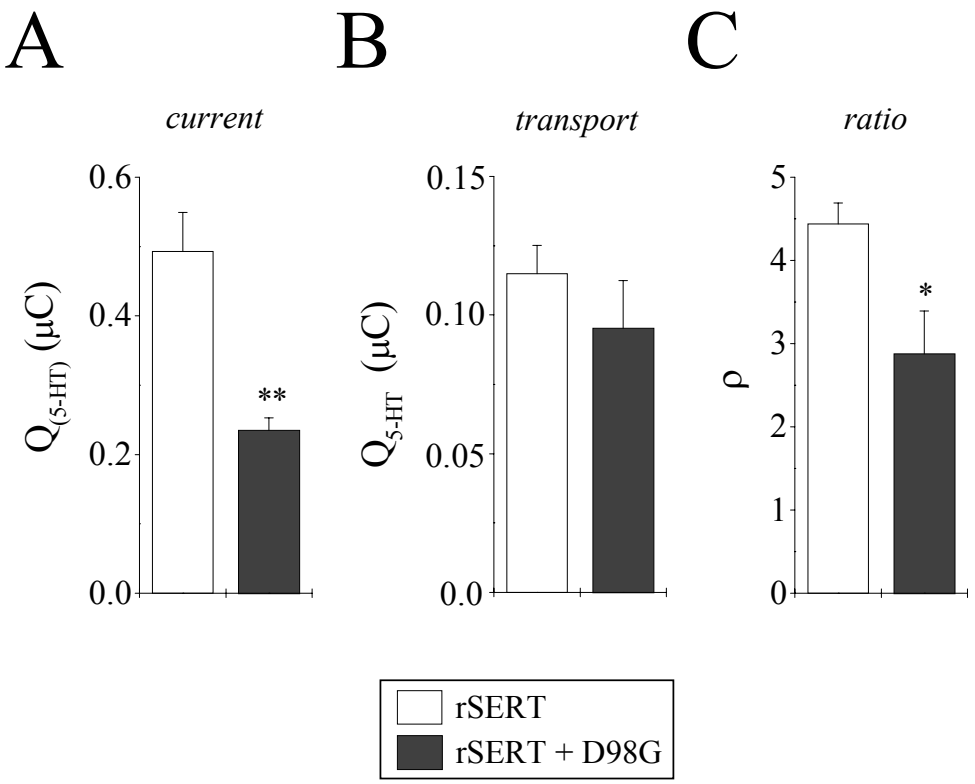

Figure 22. ρ is sensitive to co-expression of rSERT with D98G.
Oocytes are injected with rSERT cRNA (8.3 ng/oocyte, open bars) or rSERT + D98G (8.3 ng/oocyte + 33.1 ng/oocyte, filled bars) and cultured for 8 days (18°C). **A,** total charge movement ($Q_{(5\text{-}HT)}$) obtained from integration of $I_{(5\text{-}HT)}$; **B,** charge movement due to 5-HT itself ($Q_{5\text{-}HT}$) while $I_{(5\text{-}HT)}$ is induced; **C,** ρ, the ratio $Q_{(5\text{-}HT)}/Q_{5\text{-}HT}$. Data represent means ± SEM for n = 6 or n = 5 oocytes/condition in a single representative experiment. * $p < 0.05$, ** $p < 0.001$ vs. rSERT alone.

exponential dependence on membrane potential that is characteristic of SERTs [95,98] (Fig. 23B). Extracellular acidification (from pH 7.6 to pH 5.0) increases the magnitude of $I_{(5\text{-}HT)}$ (V) (see Fig. 15) but does not change the shape of $I_{(5\text{-}HT)}$ (V) (data not shown). In oocytes injected with a mixture of rSERT + D98G (8.3 ng/oocyte + 33.1 ng/oocyte, respectively), $I_{(5\text{-}HT)}$ is attenuated at all membrane potentials tested (Fig. 23B). At –80 mV, $I_{(5\text{-}HT)}$ is inhibited 89% by D98G (Fig. 23B, rSERT, -44.45 ± 9.47 nA; rSERT + D98G, -5.12 ± 2.19 nA). We are unable to detect $I_{(5\text{-}HT)}$ at any membrane potential in oocytes injected with D98G alone (33.1 ng/oocyte, data not shown). Normalizing the data shows that co-expression of rSERT and D98G does not change the shape of the $I_{(5\text{-}HT)}$ (V) despite a marked reduction in current amplitude (Fig. 23C).

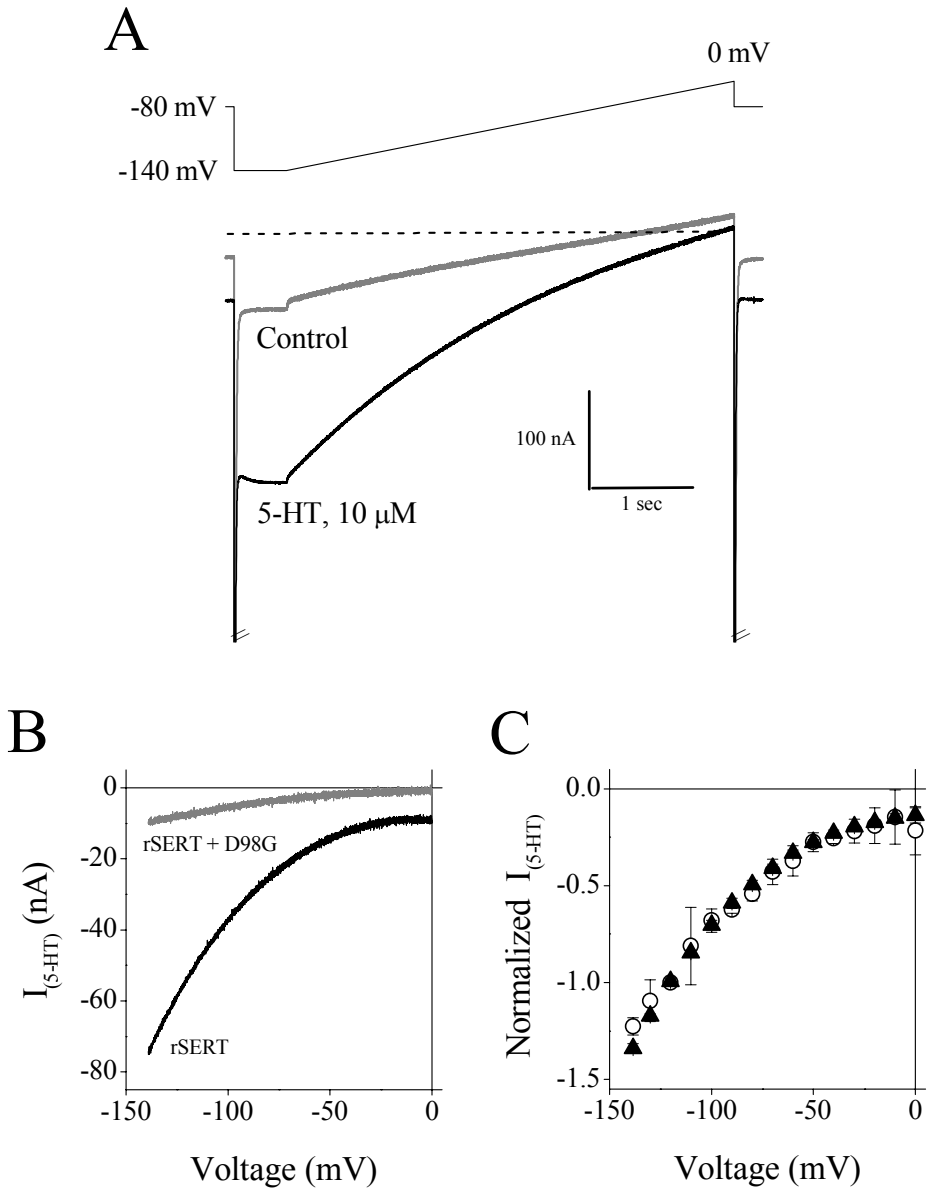

Figure 23. Co-expression of rSERT and D98G decreases $I_{5\text{-}HT}$ without altering its voltage dependence.

Oocytes are injected with indicated cRNA and cultured for 8 days (18°C). **A,** ***upper panel***: voltage ramp command protocol; ***lower panel***: representative raw currents measured at pH 5.0 in the absence (Control, gray line) and presence of 5-HT (10 μM, black line). Data represent current in a single oocyte injected with 8.3 ng rSERT cRNA. The dashed line indicates zero current level. **B,** $I_{(5\text{-}HT)}(V)$ at pH 5.0 in oocytes injected with either rSERT (8.3 ng, black line) or rSERT + D98G (8.3 ng + 33.1 ng, gray line). **C,** $I_{(5\text{-}HT)}(V)$ in oocytes injected with rSERT (8.3 ng, open circles) or rSERT + D98G (8.3 ng + 33.1 ng, filled triangles). Data are expressed as the fraction of at –120 mV, pH 5.0. Data represent means ± SD from n = 3 (rSERT) or n = 4 (rSERT + D98G) oocytes/condition in a single representative experiment.

Chapter IV

Discussion

We express mammalian SERTs in two different heterologous hosts in order to study the function of transporters that are natively expressed in blood platelets and serotonergic neurons of the central and enteric nervous systems [7].

We choose the cell line CHO-K1 to study the 5-HT transport activity and *Xenopus laevis* oocytes to study biophysical properties of mammalian SERTs in heterologous host cells. These expression systems represent the state of the art for heterologous expression of transporters and ion channel proteins for the purposes of studying integral membrane protein physiology. Their use in this study is therefore consistent with established paradigms in our field of study. We demonstrate that CHO-K1 and oocytes cells are appropriate heterologous hosts that, a) lack endogenous 5-HT transport activity and background currents that could interfere with our ability to identify the SERT-specific component of our measurements, and b) are easily made to express SERT protein by transient cDNA transfection or cRNA injection, respectively (Figs. 2, 9).

SERT interactions in transiently transfected CHO-K1 cells

Expression of SERT-mediated 5-HT transport activity ($\Phi_{5\text{-HT}}$) in cells depends on the amount of SERT cDNA transfected and on the total amount of cDNA in the transfection reaction. Our experiments utilize a cationic lipid-mediated transfection reagent to achieve transient expression of SERT for functional studies in the absence and presence of after SERT mutants and other putative interacting proteins. It is therefore important to understand the effects of increasing cDNA on $\Phi_{5\text{-HT}}$. Increasing the amount of empty plasmid vector (pcDNA3) in the presence of a fixed SERT cDNA produces a biphasic $\Phi_{5\text{-HT}}$ response (Fig. 2). $\Phi_{5\text{-HT}}$ is therefore sensitive to changes in the transfection conditions. Since the amount of transfection reagent is constant, we

interpret the results in Fig. 3 to mean that transfection efficiency in CHO-K1 cells is strongly influenced by the overall DNA:Lipofectamine ratio. In order to eliminate this variable from subsequent studies of SERT in CHO-K1 cells, we add pcDNA3 to all transfections so that the total quantity of cDNA remains constant (400 ng/well).

Saturation of $\Phi_{5\text{-HT}}$ signal due to intrinsic limitations in the cell's ability to produce SERT protein is another possible source of experimental artifact in heterologous expression systems. The cDNA-response curve establishes that $\Phi_{5\text{-HT}}$ does saturate (Fig. 3), suggesting that SERT expression may be limited at high cDNA levels. In order to avoid ceiling artifacts associated with saturating $\Phi_{5\text{-HT}}$, we subsequently transfect a half-maximal effective quantity of cDNA ($EC_{50\ cDNA}$, 25-50 ng/well). Similar cDNA-response curves are seen for multiple different batches of both rSERT and C109A cDNA (data not shown).

In order to test for inter-subunit cooperativity in the SERT oligomer, we transfect cells with wild-type rSERT alone or a point mutation (C109A) that is resistant to inhibition by methanethiosulfonate (MTS) reagents. Inhibition of rSERT-mediated $\Phi_{5\text{-HT}}$ by extracellularly applied membrane-impermeant MTS reagents is a results from covalent modification of Cys109 [150]. Consistent with previous observations [119], co-expression of rSERT + C109A alters the timecourse for inhibition of $\Phi_{5\text{-HT}}$ by MTSET and MTSEA, indicating that Cys109 reactivity is sensitive to interactions between rSERT and C109A. Because C109A is non-reactive over our incubation time, MTS inhibition in co-transfected cells should be conferred solely by the reactivity rSERT.

MTSET and MTSEA are cationic at neutral pH, and are largely impermeant to the plasma membrane lipid bilayer [157]. The reactivity rate of MTS reagents with cysteine in aqueous solution is orders of magnitude faster [157] than the inhibition rate we measure for rSERT in intact cells (Fig. 4). Our results are consistent with the time-dependence of SERT inactivation reported by other investigators [150], suggesting that aqueous accessibility of Cys109 is rate limiting for MTS inhibition of rSERT. Thus, allosteric interactions between rSERT and C109A located on the plasma membrane are likely to alter the MTS inhibition rate. Despite its effects in MTS inhibition, co-

expression of rSERT with C109A does not perturb the magnitude of $\Phi_{5\text{-HT}}$ in our experiments. The data suggest that the changes in SERT properties that we see in transfected host cells are not due to interactions that are forced by heterologous overexpression. We therefore conclude that SERT expression in CHO-K1 cells reveals authentic SERT functional properties.

In order to determine whether rSERT interactions occur under more physiologically relevant conditions, we co-transfect the functionally impaired D98G mutant with rSERT and measure the Na^+-dependence of $\Phi_{5\text{-HT}}$. Although D98G generates detectable $\Phi_{5\text{-HT}}$ in our assays (< 10 % of $\Phi_{5\text{-HTmax}}$ for rSERT), the Na^+–dependence of D98G-mediated $\Phi_{5\text{-HT}}$ is right-shifted 6.6-fold relative to rSERT. Like C109A, rSERT also interacts with D98G, resulting in decreased $\Phi_{5\text{-HT}}$ and a loss in Na^+ potency for activation of $\Phi_{5\text{-HT}}$. Assuming that Na^+ kinetics in cells expressing rSERT + D98G are described by the Hill equation, Na^+ potency should be approximated by the sum of the two independent responses if rSERT and D98G function independently. When the data are modeled in this way, $EC_{50\ Na}$ for rSERT + D98G increases only 0.5 mM relative to rSERT alone (data not shown). Experimentally, we observe a 7.8 mM increase in $EC_{50\ Na^+}$ (Fig. 6), indicating that rSERT and D98G do not function independently with respect to Na^+–dependent activation of $\Phi_{5\text{-HT}}$. The D98G-mediated decrease in $\Phi_{5\text{-HT}}$ is not due to addition of excess cDNA (Fig. 3), but we cannot rule out the possibility that D98G attenuates surface expression of rSERT by an unknown mechanism.

However, we rule out the possibility that Na^+ potency depends solely on SERT expression level. Despite a decrease in $\Phi_{5\text{-HT}}$ that is comparable to rSERT + D98G (50 ng/well + 250 ng/well), transfection with less rSERT cDNA (10 ng/well) does not change $EC_{50\ Na}$. Na^+ potency therefore represents an expression level-independent microscopic property of SERT function. The sensitivity of Na^+ potency to D98G co-expression therefore supports the hypothesis that SERT function is mediated by

interdependent SERT proteins that interact to modulate function under physiological conditions.

Structural similarities in GAT/NET proteins may allow for promiscuous hetero-oligomerization between different transporters [132]. We test for interactions between rSERT and rGAT1 (which interact in FRET assays [132]) by co-transfection in CHO-K1 cells. Like D98G, rGAT1 co-expression decreases $\Phi_{5\text{-HT}}$ and Na^+ potency at rSERT. rSERT does not affect rGAT1 function (Fig. 8), suggesting that even if SERT and GAT form mixed oligomers, the functional consequences of their physical association are distinct.

Substrate potency is higher for expressed SERT ($EC_{50\ 5\text{-HT}}$ = 0.3 - 3 μM) than for GAT1 ($EC_{50\ GABA}$ = 5 - 8 μM); Na^+ potency is similarly increased at GAT1 (rSERT, $EC_{50\ Na}$ = 13 mM; rGAT1, $EC_{50\ Na}$ = 55 mM, data not shown) [54,94,100,106,158]. The data suggest a role for oligomerization in maintaining the precise alignment of critical residues that comprise binding sites and gating apparatus required for higher potency interactions with 5-HT and Na^+ seen in SERT. SERT oligomeric structure may help to coordinate inter-subunit interactions for SERT in the same way that the K^+ channel tetrameric structure creates an energetically flat landscape for potassium that simultaneously facilitates K^+ selectivity and a high rate of ion flux [158]. The higher sensitivity of SERT to Na^+ and substrate (compared to rGAT1) may confer increased sensitivity to functional perturbations by co-assembly with integral membrane proteins (Table 1).

Interestingly, the Hill slope for the Na^+-dependence of $\Phi_{5\text{-HT}}$ is insensitive to manipulations that alter the magnitude of and potency (Table 1). Since co-transfection of rSERT with neither D98G nor rGAT1 alters n_H, we surmise that this factor reflects a required step in the 5-HT translocation process. Similar to Q_{10}, the Hill slope may therefore report cooperativity that is required for a high energy conformational transition such as 5-HT permeation itself. We conclude therefore that either a) cooperative interactions between SERT subunits do not affect the mechanism reported by the Hill slope, or b) subunit interactions that do perturb the mechanism underlying Hill slope are non-productive for 5-HT transport.

Co-expression studies in CHO-K1 cells reveal that a) rSERT interacts with C109A to change intrinsic properties of MTS reactivity, b) rSERT interacts with D98G to alter $EC_{50\ Na}$, a microscopic SERT property, c) rSERT interacts with multiple polytopic integral membrane proteins to decrease $\Phi_{5\text{-}HT}$. Decreases in $\Phi_{5\text{-}HT}$ and Na^+ potency shifts are not due to nonspecific effects because co-transfection of transport-capable SERTs (C109A, rSERT itself) mimics the effects of transport-incapable protein co-expression (rGAT1, GluR4, HA-α_{2A}AR). Furthermore, co-expression of single-TM (CD8) and cytosolic (EGFP) proteins do not affect rSERT $\Phi_{5\text{-}HT}$ activity. Our data are consistent with the notion that SERT may form hetero-oligomeric complexes with proteins outside of the GAT/NET transporter family, suggesting that SERT may interact with other integral membrane proteins to alter its function in the native context.

SERT interactions in cRNA-injected oocytes

In oocytes, injection of SERT cRNA leads to expression of $\Phi_{5\text{-}HT}$ and $I_{(5\text{-}HT)}$ that varies considerably depending on species (rSERT vs. hSERT), culture time and temperature, and the quantity of cRNA injected. As for expression in CHO-K1 cells, we establish parameters for SERT expression in oocytes in order to focus our studies on how varying expression level and co-expression affects microscopic properties of SERT function.

cRNA potency for $\Phi_{5\text{-}HT}$ and $I_{(5\text{-}HT)}$ depends on factors (time, temperature) that are not expected to alter intrinsic SERT properties (Eqn. 3). For example, increasing culture time decreases cRNA potency for $\Phi_{5\text{-}HT}$ but not $I_{(5\text{-}HT)}$ (Fig. 11). Simple transporter models also do not predict $\Phi_{5\text{-}HT}$ and $I_{(5\text{-}HT)}$ to vary independently. The differential effect of culture time suggests that elementary properties of SERT function vary with expression level.

In order to test this hypothesis, we measure biotinylated SERT protein in Western blots from oocytes injected with varying amounts of hSERT cRNA. Increasing hSERT cRNA does cause expression of hSERT protein on the plasma membrane to increase (Fig. 12). $\Phi_{5\text{-}HT}$ and $I_{(5\text{-}HT)}$ both increase as expression level rises, but the

amount of cRNA required to elicit half-maximal $\Phi_{5\text{-}HT}$ is 26-fold lower than $I_{(5\text{-}HT)}$ and 49-fold lower than surface SERT protein (Fig. 13). A similar 34-fold potency difference between $\Phi_{5\text{-}HT}$ and $I_{(5\text{-}HT)}$ is seen for rSERT (Fig. 14). Because $\Phi_{5\text{-}HT}$ and $I_{(5\text{-}HT)}$ necessarily result from the activity of functional SERT on the plasma membrane, a simple model of SERT function predicts that $\Phi_{5\text{-}HT}$ and $I_{(5\text{-}HT)}$ will be linearly correlated (Eqn. 3). This is clearly not the case (Figs. 13, 14, 16). We conclude that the balance of channel-like to transporter-like SERT function results from allosteric cooperativity that is revealed by changes in expression level.

The data in Fig. 13 further suggest that counting transporters from $I_{(5\text{-}HT)}$ data (Eqn. 3, denominator) leads to significant overestimates of the number of transporters on the cell surface. Consider an oocyte injected with a half-maximal quantity of hSERT for $I_{(5\text{–}HT)}$ (3.4 ng, Fig. 13). A reasonable value for $I_{(5\text{-}HTmax)}$ at –80 mV, pH 7.6 is -10 nA (Fig. 20). Given literature values for single channel conductance and turnover rate (i = 0.48 pA at –80 mV [82] and ν = 1/sec. [11]), Eqn. 3 predicts 6.25 x 10^{10} SERTs on the oocyte surface, consistent with other measurements [103,106,159]. From Hill fits to the data in Fig. 13 we calculate that at the $EC_{50\ cRNA}$ for $\Phi_{5\text{-}HT}$ (0.13 ng/oocyte), surface SERT represents only 2% of its maximum value. Correcting for this overestimate yields 1.25 x 10^9 transporters, 50-fold fewer than Eqn. 3 predicts.

We rule out several alternative explanations for the differential cRNA-dependence of $\Phi_{5\text{-}HT}$ and $I_{(5\text{-}HT)}$. The expression-level dependence of ρ does not result from an inability to measure steady-state current at low cRNA because even below 1 ng cRNA, $I_{(5\text{-}HT)}$ at pH 7.6 is greater than 5-HT-induced current in non-injected oocytes. Furthermore, $I_{(5\text{-}HT)}$ is 9-fold larger at pH 5.0 (Fig. 15) but exhibits the same cRNA dependence as current at physiological pH.

The results in Figs. 13 and 14 could also be explained by increasing transporter number and activity, which significantly depletes 5-HT concentrations in the reaction well. A decrease in 5-HT concentration would result in apparent saturation of $\Phi_{5\text{-}HT}$ by decreasing the effective 5-HT concentration and limiting substrate availability for $\Phi_{5\text{-}HT}$. However, a) we measure initial transport rates [96] in brief assays (2.5 min.) to minimize

the possibility that extracellular depletion or intracellular accumulation of substrate will alter $\Phi_{5\text{-}HT}$; b) increasing incubation time by 30 fold, which should magnify substrate depletion at all expression levels, does not change $EC_{50\ cRNA}$ (Fig. 14); c) even in long (60 min.) uptake assays in oocytes injected with 33.6 ng rSERT cRNA, less than 5% of the added [^{3}H]-5-HT is accumulated inside the oocyte. Saturation of $\Phi_{5\text{-}HT}$ at high expression is therefore due to a functional limitation in SERT transport activity.

The voltage disparity intrinsic to separate current (V_m = -80 mV) and transport assays ($V_m = V_{rest}$) could also differentially affect $\Phi_{5\text{-}HT}$ and $I_{(5\text{-}HT)}$. However, ρ is sensitive to the amount of cRNA injected even under constant voltage (Fig. 16). Extrinsic chemical and electrical driving forces that are experimentally controlled in Fig. 16 are unlikely to account for the results shown in Figs. 13 and 14. Like ρ, the H^+-potentiation ratio is predicted to be independent of the number of expressed SERTs (Eqn. 3). In contrast to ρ, H^+-potentiation of $I_{(5\text{-}HT)}$ does not vary with expression level (Fig. 17). We therefore conclude that increasing the amount of transporter protein on the plasma membrane alters an intrinsic molecular property of 5-HT transport (Eqn. 3, ν or q) relative to 5-HT-induced current (Eqn. 3, *i* or p_o). Interestingly, expression level-dependent changes in SERT function are seen only in the functional context of $\Phi_{5\text{-}HT}$.

Changing SERT expression level also changes its pharmacology. 5-HT activates $\Phi_{5\text{-}HT}$ with higher potency at low SERT expression. The same data, expressed as a function of cRNA injected Fig. 18, show that cRNA potency is lower when $\Phi_{5\text{-}HT}$ is assayed in the presence of high 5-HT concentrations. Because 5-HT exposure is acute (2.5 min. preincubation plus 2.5 min. assay incubation), we conclude that interactions between 5-HT and SERT alter a dynamic property of SERT-mediated $\Phi_{5\text{-}HT}$. Thus, the data argue that changing expression level alters SERT's sensitivity to 5-HT concentration. 5-HT-dependent shifts in cRNA potency therefore report changes in intrinsic SERT properties that result from varying SERT expression level.

High expression level also decreases potency for inhibition of $\Phi_{5\text{-}HT}$ by both substrates (5-HT and AMPH) and inhibitors (cocaine and paroxetine; Fig. 19, data not shown). For net transport measurements, alterations in 5-HT potency need not

necessarily reflect changes in binding affinity if a rate-limiting transition occurs after initial 5-HT binding. In oocytes expressing dSERT, both $\Phi_{5\text{-HT}}$ and $I_{(5\text{-HT})}$ exhibit temperature sensitivities ($Q_{10} \approx 3$) that are typically associated with relatively large conformational changes [97]. 5-HT potency may therefore be modulated by interactions that affect rate-limiting steps leading to substrate translocation or gating of current. For dSERT, 5-HT concentration modulates ρ in dSERT due to its differential potency for activation of transport versus current [97]. We find that 5-HT potency for $\Phi_{5\text{-HT}}$ and $I_{(5\text{-HT})}$ is similar at high hSERT expression (Figs. 11, 18). However, low hSERT expression reveals differential 5-HT potency for $\Phi_{5\text{-HT}}$ and $I_{(5\text{-HT})}$. 5-HT potency is therefore not a constant, but instead reports cooperative interactions between 5-HT and SERT that vary with expression level only in the functional context of $\Phi_{5\text{-HT}}$.

ρ is also sensitive to co-injection of rSERT with an inactive mutant, D98G, which affects ρ by inhibiting current without affecting transport (Fig. 22). Based on previous data [77,119], we assume that SERT forms oligomers capable of functional interactions in oocytes as well as mammalian cells. D98G might therefore form a mixed oligomeric complex that disrupts interactions that are important for determining ρ. Residues in TMD 1 are implicated in substrate and inhibitor recognition and translocation [72,77,160], suggesting that perturbations of this structure could interfere with substrate and ion conduction if they permeate through a shared pore. However, both $\Phi_{5\text{-HT}}$ and $I_{(5\text{-HT})}(V)$ are unaffected by D98G, suggesting that ion permeation properties (such as selectivity) that would alter $I_{(5\text{-HT})}(V)$ are not perturbed by D98G. One possible explanation is that D98G acts as a dominant-negative subunit such that oligomers containing D98G become functionally silent; D98G expression therefore effectively decreases the number of active SERTs.

The effect of D98G in oocytes to decrease $I_{(5\text{-HT})}$ but not $\Phi_{5\text{-HT}}$ is contrasted with its ability to inhibit $\Phi_{5\text{-HT}}$ in co-transfected CHO-K1 cells (Figs. 5. 6). However, this apparent discrepancy can be explained by differences in the relative expression of $\Phi_{5\text{-HT}}$ and $I_{(5\text{-HT})}$ in oocytes and cells. In oocytes, the amount of rSERT cRNA (Figs. 22, 23; 8.3

ng/oocyte) is saturating for $\Phi_{5\text{-}HT}$ but approximately half-maximal for $I_{(5\text{-}HT)}$ (Figs. 13, 14). We may assume that rSERT + D98G complexes form but are nonfunctional. D98G decreases $I_{(5\text{-}HT)}$ ~60%, suggesting that ~40% of remaining transporters are composed of only rSERT. Since surface SERT expression and $I_{(5\text{-}HT)}$ are highly correlated, it is reasonable to assume that the amount of functional SERT is effectively decreased 60% by D98G co-injection. From Fig. 13, 60% of $I_{(5\text{-}HT)}$ corresponds to $I_{(5\text{-}HT)}$ from oocytes injected with ~ 1 ng cRNA. However, at 1ng/oocyte, $\Phi_{5\text{-}HT}$ is still near saturation (Fig. 13). Thus, the effect of D98G to inhibit in oocytes is masked by the saturation of $\Phi_{5\text{-}HT}$. This analysis suggests the presence of spare transporters for $\Phi_{5\text{-}HT}$ after injection of high levels of cRNA.

The concept of spareness implies the existence of an enabling factor for $\Phi_{5\text{-}HT}$ that can dynamically associate with functional transporters to stimulate $\Phi_{5\text{-}HT}$. The data suggest that if an enabling factor normally associates with rSERT, it does not interact directly with D98G. Expression of D98G might be expected to compete with rSERT for association, which would decrease the effect of the factor (and thereby decrease $\Phi_{5\text{-}HT}$), the opposite of what we observe. The existence of a $\Phi_{5\text{-}HT}$-enabling factor with limited but constitutive cellular expression can also explain the differential sensitivity of $\Phi_{5\text{-}HT}$ and $I_{(5\text{-}HT)}$ to SERT expression level. The factor stimulates $\Phi_{5\text{-}HT}$ at low, but not at high, expression levels, effectively increasing cRNA potency for $\Phi_{5\text{-}HT}$ relative to $I_{(5\text{-}HT)}$. $\Phi_{5\text{-}HT}$ saturates when increasing SERT expression exhausts the supply of the endogenous enabling factor. $I_{(5\text{-}HT)}$ is not affected by the activity of an enabling factor and therefore correlates linearly with surface SERT protein. cRNA potency for $\Phi_{5\text{-}HT}$ therefore reports SERT association with the unknown factor. The effects of an enabling factor may also mediate expression-level dependent changes in SERT pharmacology. At high expression, where $\Phi_{5\text{-}HT}$ is not activated by the enabling factor, ligand potency is decreased. Interaction with the factor is therefore correlated with higher ligand potency for $\Phi_{5\text{-}HT}$. Consistent with this interpretation, high substrate concentrations decrease cRNA potency.

Other explanations for our data are possible. Increasing SERT expression level might favor the formation of oligomeric SERT complexes if multimer formation is mass-dependent. If monomeric SERT supports 5-HT transport but an oligomeric structure is required for current, then altering the relative proportions of these different quaternary structures will perturb ρ. At low expression, monomers generate $\Phi_{5\text{-}HT}$; as expression level increases, so does the relative abundance of oligomers. $I_{(5\text{-}HT)}$ is therefore stimulated at high expression levels. A variable oligomer model is also consistent with the effect of D98G to perturb current but not transport in oocytes. If D98G mediates its effect on $I_{(5\text{-}HT)}$ by forming current-impaired complexes with rSERT, then D98G should selectively decrease $I_{(5\text{-}HT)}$ without affecting $\Phi_{5\text{-}HT}$. mSERT monomers exhibit different pharmacological properties from concatenated oligomers [134], suggesting that expression-level dependent oligomerization may also explain differences in SERT pharmacology that we observe.

However, the variable oligomer model does not explain our results in CHO-K1 cells where D98G inhibits $\Phi_{5\text{-}HT}$ and alters Na^+ potency. We find little precedent for variable oligomerization in the transporter or ion channel literature. On the contrary, K_{ATP} channel expression in oocytes is subject to a strict control mechanism that prevents expression of incomplete assemblies [161]. The application of ultrastructural techniques to visualize oligomer formation in cells where SERT function has been measured should allow for the design of discriminating experiments to test the variable oligomer model. A linear correlation between freeze-fracture particle and pre-steady-state current is reported for EAAT3 glutamate transporters that form a pentameric structure [162]. In light of our findings, it would be interesting to know how transport and steady-state currents correlate with particle density, size and shape for EAAT-3.

Another possibility is that SERTs are physically linked into oligomeric complexes by an accessory protein. GAT/NET transporters are known to associate with syntaxin 1A and the catalytic subunit of PP2A [110,111]. Catecholamine transporters interact with the PDZ-containing protein PICK-1 [112], which is also involved in PKC regulation of AMPA-type glutamate receptors [163]. Our observation that rSERT interacts with GluR4

in CHO-K1 cells could therefore be mediated by common interactions with PICK-1, a PICK-1 homologue, or an associated protein. It is temping to speculate that neurotransmitter transporters might be tethered into complexes by proteins such as PSD-95 family or GRIP proteins that cluster NMDA [164] and AMPA [165,166] glutamate receptors, respectively. However, direct association between channel-clustering proteins and neurotransmitter transporters have not been reported in the literature.

Since association with PKC thus appears to be a common theme for both transporter regulation and transporter-associated proteins [167], PKC itself or an unidentified PKC-associated protein may be reasonably hypothesized to play a role in transporter tethering. Indeed, rGAT1 localization and function are regulated by PKC in oocytes, and high transporter expression abolishes PKC-dependent subcellular trafficking [168]. We suspect that cRNA potency in oocytes reflects SERT interactions with host factors that are required for, or regulate, function on the plasma membrane. In addition to SERT itself [119], candidate factors include molecules that interact with GAT/NET transporters [110-112,118,167,169,170]. Regulators of SERT function may similarly limit uptake as transporter number increases, especially if their abundance or activity is endogenously limited. Induction of $I_{(5\text{-}HT)}$ and saturation of at high SERT expression may therefore reflect disassembly or functional uncoupling of SERT-associated regulatory complexes. As suggested by SERT phosphorylation studies [113], ligand occupancy may modulate functional associations between SERT and associated proteins to alter the balance of transporter-like to channel-like function. However, the identity of proteins or cellular factors that may be responsible for promoting SERT or oligomerization is presently unknown

A model for Cooperative SERT interactions

Although existing transporter models can account for large transporter-mediated ion fluxes [95,98,171-173], they do not predict the expression-level dependence of ρ or the substrate and inhibitor potency reported here. To explain our data, we propose the following model (Fig. 24): functional SERT exists as part of a ternary complex composed

of the SERT oligomer (T), substrate (S), and an endogenous oocyte factor of limited abundance (X). The total number of oligomeric transporters on the plasma membrane is N = T + TS + TX + TSX. In our experiments, we vary N by increasing cRNA injection, and we vary S by addition of 5-HT. X is required for 5-HT transport activity and modulates ρ by promoting $\Phi_{5\text{-HT}}$ in favor of $I_{(5\text{-HT})}$. cRNA potency for therefore reports association of X and T. Factor X also governs ligand recognition: at low N, substrates and inhibitors interact with higher potency at T. Reciprocally, T-X association is sensitive to substrate concentration: high [S] decreases cRNA potency, consistent with a functional uncoupling of X and T.

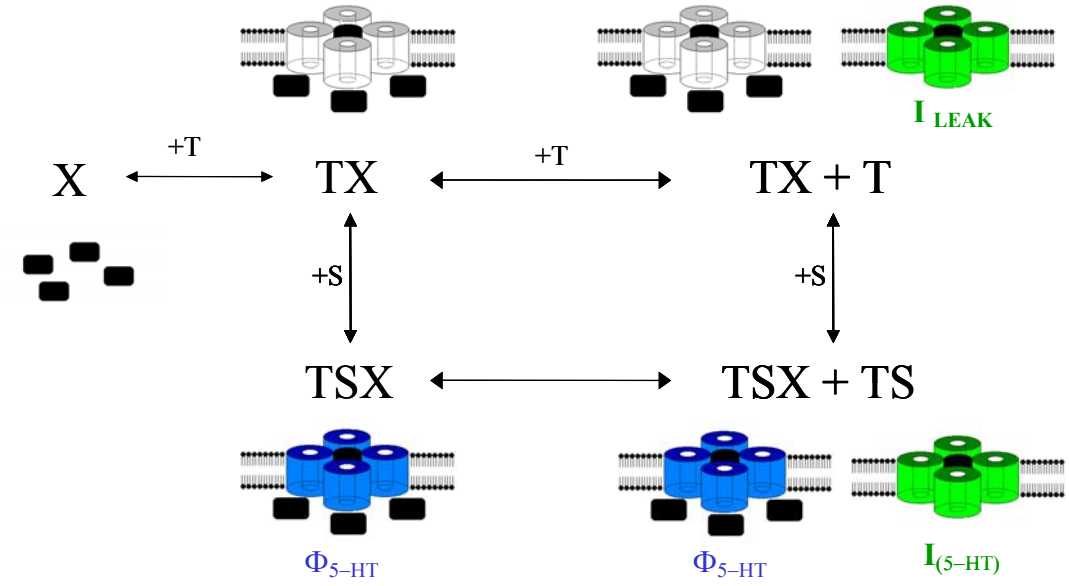

Figure 24. Model for SERT interactions with 5-HT and an endogenous cellular factor of limited abundance.
SERT (T, cylinders) associates with an endogenous factor (X, black rectangles). ***Top row***, in the absence of 5-HT (S), association of X with T decreases the magnitude of SERT-associated leak current (I_{LEAK}). At low SERT expression, T is electrically silent (white cylinders), whereas at higher SERT expression levels, T generates measurable current (green cylinders). ***Bottom row,*** in the presence of S, X stimulates T to produce measurable 5-HT transport (blue cylinders, $\Phi_{5\text{–HT}}$) even at low expression levels. At higher expression, S induces current (green cylinders, $I_{5\text{–HT}}$) when T is not associated with X.

At low N, endogenous levels of X saturate available transporters such that constitutive current is suppressed. TX dominates, generating little constitutive current. In the presence of a fixed, low concentration of S generates TSX, which mediates appreciable $\Phi_{5\text{-}HT}$. $I_{(5\text{-}HT)}$ remains small because X keeps T running in transporter mode and $\rho \approx 1$. As N rises due to increased cRNA injection, X becomes limiting and TSX-mediated $\Phi_{5\text{-}HT}$ plateaus. Both constitutive and substrate-induced currents grow in proportion to N because the measured $I_{(5\text{-}HT)}$ is generated mainly by T. Transporters that exist free of X are therefore spare with respect to $\Phi_{5\text{-}HT}$: they are capable of participating in transport but lack a required interaction with X to become active for $\Phi_{5\text{-}HT}$.

Our data also indicate that X and S interact allosterically through T. TSX generates $\Phi_{5\text{-}HT}$ while TS generates $I_{(5\text{-}HT)}$; thus transport and current both increase dose-dependently with [S]. However, cRNA potency for $\Phi_{5\text{-}HT}$ is higher at low substrate concentrations (Fig. 18A) because S interacts more potently with T than with TX. This is unexpected if S and X are independent. Thus we hypothesize that high concentrations of S cause X to dissociate from T, decreasing cRNA potency for $\Phi_{5\text{-}HT}$. The same result occurs at high N, where T is physically dissociated from X. As a corollary, S-X interactions are independent of X for $I_{(5\text{-}HT)}$: S activates $I_{(5\text{-}HT)}$ with constant potency at either low or high expression (Fig. 20), and cRNA potency is unaffected by S (Fig. 18B)

Although our model appears to make $\Phi_{5\text{-}HT}$ and $I_{(5\text{-}HT)}$ mutually exclusive, (depending on functional association with X), we hypothesize that T and TX represent extremes on a continuum of SERT function. S increases the probability that we measure T alone vs. TX and X changes the probability of finding T in $\Phi_{5\text{-}HT}$ mode versus $I_{(5\text{-}HT)}$ mode. Ligand-dependent modulation of T function suggests that T-X transitions may be dynamically regulated by substrates, regulatory proteins, or post-translational modifications such as those seen for hSERT [111,113] and rGAT1 [174,175]. Dynamic regulation raises the possibility that the behavior of any individual SERT may therefore change from one instant to the next. Amperometric or time-resolved fluorescent methods that measure transport in combination with voltage clamp may be able to overcome the

bandwidth limitations of the present study to measure millisecond fluctuations in ρ at the level of the elementary SERT functional unit.

Finally, our model provides an explanation for apparent discrepancies in the literature. The heterogeneity of currents associated with GABA transporter function [94,102,107,108,176], may be reconciled if different experimental protocols alter the relative abundance of transporters and regulatory factors. We speculate that the balance of 5-HT transport to 5-HT-induced current will depend on the relative expression and localization of transporters and associated factors in the native environment. Indeed, large pre-synaptic 5-HT-induced currents are also observed in native synapses [52]. Furthermore, 5-HT stimulates transport more potently in brain vesicles and synaptosomes (EC_{50} = 50-100 nM) than in heterologous cellular hosts (EC_{50} = 0.5-1 μM), suggesting that SERT expression alone may fail to fully recapitulate the native 5-HT transport system [8,27,33,57,86,88-92,177,177,177].

Summary and Conclusions

Molecular biological techniques such as heterologous expression of recombinant cDNA are powerful because they allow for insightful studies the activity of specific proteins. Ideally, controlled expression isolates the activity of interest from complicating factors that may be present in the native context. Heterologous expression carries an important caveat: factors that modulate the activity of a given protein *in situ* are not necessarily recapitulated in the experimental context of host cells. Thus, heterologous expression may result in the absence of regulatory factors that are required for protein structure or function, thereby altering intrinsic properties of the expressed protein activity.

Expression of transporters and ion channels in host cells is particularly useful for physiological studies, since endogenous (and sometimes redundant) transport pathways and currents can contaminate measurements in native cells. Although pharmacological blockers and ion substitutions can be used to discriminate among otherwise similar activities, selectivity itself must first be defined. However, inhibitor

selectivity may be problematic if it is defined using heterologous expression systems [178]. Nonetheless, *in vitro* expression permits the use of methods (such as simultaneous transport and current measurements) that would otherwise be difficult or impossible *in vivo*.

Channel-like activity in heterologous systems is generally ascribed to expressed GAT/NET transporters because a) large currents are observed concomitant with transport and radioligand binding in transfected or injected cells but not naïve controls and b) transport and current exhibit similar ionic requirements and inhibitor sensitivities [103-105]. Furthermore, channel events correlate with spikes of NE flux in membrane patches containing hNET [179]. For SERT, we observe robust $\Phi_{5\text{-HT}}$ even under conditions when $I_{(5\text{-HT})}$ is negligible, but never the reverse, and expression of $I_{(5\text{-HT})}$ is highly correlated with plasma membrane SERT protein (Fig. 11). It is therefore unlikely that substrate-induced and constitutive ionic currents are simply due to induction of endogenous channels [180].

Non-classical transporter properties are not unique to the GAT/NET family. EAAC1-mediated glutamate transport is biphasic with respect to the amount of injected cRNA [181], and Cl^- flux through NaPi-1 exhibits a different cRNA dependence than P_i transport [182]. Large currents and variable stoichiometry are common for GAT/NET and EAAT transporters [103-105], but are also found in other transporters. Depending on Na^+ concentration, sugar concentration, and membrane voltage, ρ may be either 1 or 2 for the SGLT1 Na^+/glucose co-transporter expressed in *Xenopus* oocytes [183] and hormones modulate glucose transport kinetics and ion stoichiometry in *Tilapia* intestinal brush-border membranes [184]. Stoichiometry of the $Na^+/HCO3^-$ transporter NBC1 depends on the cellular host in which it is expressed [185].

Constitutive (leak) conductances are also found in a wide variety of transport proteins, including SGLT1 [183], NBC1 and NBCn1-B [185,186], the H^+/metal ion transporter DCT1 [187,188], Na^+/L-ascorbic acid transporters SVCT1 and SVCT2 [189], Na^+/PO_4 transporter NaPi-1 [190], vesicular glutamate transporter VGLUT1 [191], the amino acid transporter rBAT [192], the yeast iron transporter SMF1 [193], and an insect amino acid

transporter, CAATCH1 [194]. The existence of such functional parallels across disparate structures suggests that channel-like properties represent a conserved theme in transporter function.

Classical transporter models predict ρ to be between zero and two for GAT/NET transporters [33,91,103,105]. Experimentally, however, ρ is as high as 7 for hDAT [99] and rSERT [98] and 50 for dSERT [95,97] expressed in oocytes. In our experiments, low SERT expression results in a functional unit that moves ~7*e* per 5-HT at pH 5.0; ρ increases 4.3-fold as expression level rises (Fig. 16). Our results are thus consistent with other studies where large SERT currents are measured in oocytes injected with relatively large quantities of cRNA [95-99]. However, the present data do not allow us to discriminate whether the ρ we measure reflects a property of each transporter, or the average behavior of a heterogeneous SERT population operating with intrinsically different ρ values. On average, SERT behaves as expected for a classical transporter at low expression level but becomes increasingly channel-like as the surface density of SERT protein increases.

We present evidence from two different expression systems that SERT functions as part of a heteromeric complex possessing inter-subunit cooperativity. The data fail to conform to the expected behavior for classical transporter models which postulate a SERT protein that possessively catalyzes the transmembrane flux of 5-HT, Na^+ and Cl^- in 1:1:1 stoichiometry, generating +1*e* per transport cycle [17]. We conclude that allosteric interactions between individual SERT gene products and between SERT and an as yet unidentified cellular factor alter intrinsic properties of serotonin transporter function and pharmacology.

The model that we propose provides a unifying framework for understanding the complexity of SERT function. Depending on expression level, SERT function ranges from transporter-like (zero or small net change movement accompanying 5-HT transport) to channel-like (large net charge movement in synchrony with 5-HT flux). The model also accounts for the expression level-dependent changes in SERT

pharmacology that we observe. Furthermore, we model SERTs as functional oligomers that are sensitive to inter-subunit interactions in heteromeric complexes.

Our representation for neurotransmitter transporters is reminiscent of the ternary complex model for G-protein coupled receptors (GPCRs) [195], where ligand affinity is regulated by association with an interacting factor that acts as a molecular switch (G-protein). The presence of spareness in our model further strengthens the functional parallel with classical GPCR models of GPCR function. Although the identity of transporter-modulating factors remains unknown, our results suggest strong functional parallels between channels, receptors, and transporters.

Future Directions

1) Identification of factors responsible for the differential cRNA-dependence of $\Phi_{5\text{-}HT}$ and $I_{(5\text{-}HT)}$.

Our experiments reveal a method for identifying novel factors that could be responsible for enabling 5-HT transport in Xenopus oocytes. We observe that the quantity of cRNA required to achieve half-maximal $\Phi_{5\text{-}HT}$ is lower than that required for $I_{(5\text{-}HT)}$. If the novel factor responsible for this difference is a protein whose endogenous abundance is limited, we imagine that it could be identified through expression cloning in oocytes. Increasing expression of the limiting factor above the endogenous level should increase $\Phi_{5\text{-}HT}$ at high SERT expression, where it is normally in saturation.

mRNA isolated from cells that natively express SERT, such as placenta or serotonergic neurons, could be used as a source for genetic sequences encoding a putative $\Phi_{5\text{-}HT}$-enabling factor. Alternatively, mRNA may be identified by *a priori* determination of candidate factors (i.e. PICK-1 or Syntaxin 1A) . In either case, mRNA is co-injected into oocytes with or without with varying quantities of SERT cRNA. The cRNA potency for and are then assayed for $\Phi_{5\text{-}HT}$ and $I_{(5\text{-}HT)}$. Expression of the enabling factor should shift the cRNA dependence of $\Phi_{5\text{-}HT}$ leftward, increase maximal $\Phi_{5\text{-}HT}$, and shift the cRNA dependence of $I_{(5\text{-}HT)}$ rightward.

An alternative approach that could allow for more rapid screening might involbe measurement of $\Phi_{5\text{-}HT}$ in single SERT-transfected mammalian cells. Methodologies such as amperometry, that can detect loss of oxidizable substrate from a localized space or fluorimitry, which may report intracellular accumulation of fluorescent 5-HT congeners caould be useful in this regard. Expression of a $\Phi_{5\text{-}HT}$-enabling protein should increase $\Phi_{5\text{-}HT}$ even at high SERT expression where is otherwise limited by functional saturation.

2) Test for transporter spareness.

High SERT expression functionally uncouples SERT from a putative transport-enabling factor, resulting in transporters that are spare with respect to $\Phi_{5\text{-}HT}$. The existence of spare G-protein coupled receptors (GPCRs) in physiological systems has long been appreciated, and reliable tests for receptor reserve have been devised [196]. This classical methodology is applicable to testing for the existence of spare transporters as well. Irreversible inacitvators of SERT have been reported [197-199]. Other covalent inhibitors such as MTSEA or MTSET may also be sufficient for this in heterologous systems where SERT responses can be easily discriminated from background responses.

For GPCRs, receptor activity is measured in agonist concentration-response curves. If spare receptors are present, increasing concentrations of an irreversible antagonist will first shift the agonist EC_{50} rightward without decreasing the maximal response [196]. As receptor spareness is exhausted by inactivation, further increases in irreversible inhibitor concentration will decrease the maximal agonist-elicited effect. For SERT, we envision utilizing the cRNA-$\Phi_{5\text{-}HT}$ response curve as a functional readout of transporter spareness. If SERTs are able to dynamically interact with a factor that stimulates $\Phi_{5\text{-}HT}$, addition of an irreversible inhibitor should decrease $EC_{50\ cRNA}$ without affecting $\Phi_{5\text{-}HT}$. Since spare transporters in our model primarily generate $I_{(5\text{-}HT)}$, irreversible inhibitors should decrease $I_{(5\text{-}HT)}$ even though $\Phi_{5\text{-}HT}$ may not change.

3) Screen for compounds that discriminate $\Phi_{5\text{-}HT}$ mode from $I_{(5\text{-}HT)}$ mode.

SERT ligands more potently inhibit $\Phi_{5\text{-}HT}$ at low expression in oocytes, when SERT is functionally associated with an $\Phi_{5\text{-}HT}$-enabling factor. In the present study, all

tested ligands exhibit expression level-dependent shifts in inhibitory potency, although the magnitude of the shift is greater for non-transported inhibitors (cocaine, paroxetine) than for transportable substrates (5-HT, AMPH). A reasonable hypothesis that we have not yet tested directly is that there exists a spectrum of intrinsic activity for inhibition of $\Phi_{5\text{-}HT}$ at low vs. high expression. Alternatively, compounds may selectively inhibit $\Phi_{5\text{-}HT}$ or $I_{(5\text{-}HT)}$. We anticipate that there exist ligands which will exhibit K_i values for inhibition of $\Phi_{5\text{-}HT}$ at low SERT expression that are several orders of magnitude smaller than for the K_i for inhibition of $I_{(5\text{-}HT)}$ or inhibition of $\Phi_{5\text{-}HT}$ at high SERT expression.

Since we speculate that interconversion of SERT function may be dynamically regulated by interactions with the putative enabling factor, and since dysregulation of SERT is implicated in human disease phenotypes, there exists a possibility that selective inhibition of SERT in different functional modes will be therapeutically advantageous. We therefore suggest designing a pharmacological screen to identify compounds that selectively inhibit of $\Phi_{5\text{-}HT}$ at low vs. high expression, and for compounds that exhibit selectively inhibit $\Phi_{5\text{-}HT}$ relative to $I_{(5\text{-}HT)}$.

APPENDIX A. DEFINITIONS AND ABBREVIATIONS

5-HT, 5-hydroxytryptamine, serotonin; MDMA, 3,4-methylene-deoxymethamphetamine, ecstasy; AMPH, d-amphetamine; MTS, methanethiosulfonate; MTSEA, (2-aminoethyl)methanethiosulfonate; MTSET, [2-(Trimethylammonium)ethyl] methanethiosulfonate; TMD, transmembrane-spanning segment; Asp98, aspartate 98 in the primary sequence of rSERT; D98G, Asp98 mutation to glycine in rSERT; Cys109, cysteine 109 in rSERT; C109A, Cys109 mutation to alanine in rSERT; CHO-K1, Chinese hamster ovary cell line; HEK-293, human embryonic kidney cell line; *e*, elementary charge (1.602×10^{-19} Coulombs, C); *F*, Faraday's constant, 9.548×10^4 C/mol; $\Phi_{5\text{-HT}}$, 5-HT transport rate (mol 5HT/unit time); $\Phi_{5\text{HTmax}}$, maximal $\Phi_{5\text{-HT}}$; $I_{5\text{-HT}}$, current carried by 5-HT, equal to $F \cdot \Phi_{5\text{-HT}}$ (Amps, A); $Q_{5\text{HT}}$, time integral of $I_{5\text{-HT}}$, charge movement due to the 5-HT^+ itself (C); $I_{(5\text{-HT})}$, 5-HT-induced current (A); $I_{(5\text{-HT})\ pH\ 5.0}$, $I_{(5\text{-HT})}$ at indicated pH; I_{H^+leak}, constitutive current induced by extracellular acidification; I_{max}, maximal $I_{(5\text{-HT})}$; $Q_{(5\text{-HT})}$, time integral of $I_{(5\text{-HT})}$, total 5-HT-induced charge movement (C); ρ, charge/transport ratio, $Q_{(5\text{-HT})}/Q_{5\text{HT}}$ (unitless); Φ_{GABA}, GABA transport rate (mol GABA/unit time);V_m, membrane potential; V_{rest}, resting membrane potential; $EC_{50\ cRNA}$, half-maximal quantity of injected cRNA (ng/oocyte); $EC_{50\ Na}$, half-maximal concentration of Na^+ (mM); IC_{50}, half-maximal inhibitory concentration; n_H, Hill slope (unitless); PKC, protein kinase C; PP2A, protein phosphatase 2A catalytic subunit; PICK-1, protein interacting with C-kinase 1; GRIP, glutamate receptor interacting protein.

APPENDIX B. STATISTICS AND CURVE FITTING

Reported values represent mean ± SEM from replicate determination in a single experiment unless otherwise indicated. Statistical significance is determined using Student's non-paired t-test (Origin). Significant differences are indicated by *, $p < 0.05$ or **, $p < 0.001$.

For curve fits, parameter values represent mean ± 95% C.I. from at least 10 iterative fits using the Levenberg-Marquardt nonlinear least squares algorithm (Origin) unless otherwise indicated.

APPENDIX C. EQUATIONS

The Hill equation. A generic form of the equation is shown. Variables are indicated in Results. E, effect (e.g. $\Phi_{5\text{-HT}}$ or $I_{(5\text{-HT})}$); x, independent variable (e.g. quantity of cRNA, Na^+, 5-HT or drug concentration); EC_{50}, half-maximal value of x; n_H, Hill slope.

$$E = \frac{E_{max} \cdot x^{n_H}}{EC_{50}^{\ n_H} + x^{n_H}} \qquad \textbf{Eqn 1.}$$

Mathematical definition of ρ. Terms are defined in APPENDIX A.

$$\rho = \frac{\int I_{(5\text{-HT})} dt}{F \int \Phi_{5\text{-HT}} dt} = \frac{Q_{(5\text{-HT})}}{Q_{5\text{-HT}}} \qquad \textbf{Eqn. 2}$$

Predicted relationship between current generated by a transporter or channel. N, number of functional units, *i*, single channel conductance, p_o, open probability, ν, turnover rate, q charge transfer per cycle.

$$\frac{I_{CHANNEL}}{I_{TRANSPORTER}} = \frac{N i p_o}{N \nu q} \qquad \textbf{Eqn. 3}$$

Calculation of K_i values by the method of Cheng-Prusoff. The form of the equation is adapted from [200].

$$K_i = \frac{IC_{50}}{1 + \frac{[5\text{-HT}]}{EC_{50}}} \qquad \textbf{Eqn. 4}$$

REFERENCES

1. Sjoerdsma, A. and Palfreyman, M. G. (1990). History of serotonin and serotonin disorders. *Annals of the New York Academy of Sciences* **600:** 1-7.

2. Roberts, M. H. (1984). 5-Hydroxytryptamine and antinociception. *Neuropharmacology* **23:** 1529-1536.

3. Murphy, D. L., Andrews, A. M., Wichems, C. H., Li, Q., Tohda, M., and Greenberg, B. (1998). Brain serotonin neurotransmission: an overview and update with an emphasis on serotonin subsystem heterogeneity, multiple receptors, interactions with other neurotransmitter systems, and consequent implications for understanding the actions of serotonergic drugs. *Journal of Clinical Psychiatry* **59 Suppl 15:** 4-12.

4. Tork, I. (1990). Anatomy of the serotonergic system. *Annals of the New York Academy of Sciences* **600:** 9-34.

5. Azmitia, E. C. (1999). Serotonin neurons, neuroplasticity, and homeostasis of neural tissue. *Neuropsychopharmacology* **21:** 33S-45S.

6. Stahl, S. M. (1998). Mechanism of action of serotonin selective reuptake inhibitors. Serotonin receptors and pathways mediate therapeutic effects and side effects. *Journal of Affective Disorders* **51:** 215-235.

7. Ross, S. B. (1982) The characteristics of serotonin uptake systems. In Osborne, N. N., editor. *Biology of Serotonerigic Transmisssion*, John Wiley & Sons Ltd., New York. pp. 159-195.

8. Iversen, L. L. (1971). Role of transmitter uptake mechanisms in synaptic neurotransmission. *British Journal of Pharmacology* **41:** 571-591.

9. Mann, J. J. (1999). Role of the serotonergic system in the pathogenesis of major depression and suicidal behavior. [Review] [65 refs]. *Neuropsychopharmacology* **21:** 99S-105S.

10. de Montigny, C. and Blier, P. (1984). Effects of antidepressant treatments on 5-HT neurotransmission: electrophysiological and clinical studies. *Advances in Biochemistry & Psychopharmacology* **39:** 223-239.

11. Blakely, R. D., DeFelice, L. J., and Hartzell, H. C. (1994). Molecular physiology of norepinephrine and serotonin transporters. *Journal of Experimental Biology* **196:** 263-281.

12. Bunin, M. A. and Wightman, R. M. (1999). Paracrine neurotransmission in the CNS: involvement of 5-HT. *Trends in Neurosciences* **22:** 377-382.

13. Falkenburger, B. H., Barstow, K. L., and Mintz, I. M. (2001). Dendrodendritic inhibition through reversal of dopamine transport. *Science* **293:** 2465-2470.

14. Bunin, M. A. and Wightman, R. M. (1998). Quantitative evaluation of 5-hydroxytryptamine (serotonin) neuronal release and uptake: an investigation of extrasynaptic transmission. *Journal of Neuroscience* **18:** 4854-4860.

15. Nelson, N. (1998). The family of Na+/Cl- neurotransmitter transporters. *Journal of Neurochemistry* **71:** 1785-1803.

16. Fuller, R. W. and Wong, D. T. (1990). Serotonin uptake and serotonin uptake inhibition. *Annals of the New York Academy of Sciences* **600:** 68-78.

17. Rudnick, G. and Clark, J. (1993). From synapse to vesicle: the reuptake and storage of biogenic amine neurotransmitters. *Biochimica et Biophysica Acta* **1144:** 249-263.

18. Blier, P. and de Montigny, C. (1999). Serotonin and drug-induced therapeutic responses in major depression, obsessive-compulsive and panic disorders. *Neuropsychopharmacology* 91S-98S.

19. Parry, B. L. (2001). The role of central serotonergic dysfunction in the aetiology of premenstrual dysphoric disorder: therapeutic implications. *CNS Drugs* **15:** 277-285.

20. Tamiz, A. P., Bandyopadhyay, B. C., Zhang, J., Flippen-Anderson, J. L., Zhang, M., Wang, C. Z., Johnson, K. M., Tella, S., and Kozikowski, A. P. (2001). Pharmacological and behavioral analysis of the effects of some bivalent ligand-based monoamine reuptake inhibitors. *Journal of Medicinal Chemistry* **44:** 1615-1622.

21. Feighner, J. P. (1999). Overview of antidepressants currently used to treat anxiety disorders. *Journal of Clinical Psychiatry* **60 Suppl 22:** 18-22.

22. Gorman, J. M. and Kent, J. M. (1999). SSRIs and SMRIs: broad spectrum of efficacy beyond major depression. *Journal of Clinical Psychiatry* **60 Suppl 4:** 33-38.

23. Blier, P. (2001). Pharmacology of rapid-onset antidepressant treatment strategies. *Journal of Clinical Psychiatry* **62 Suppl 15:** 12-17.

24. Tatsumi, M., Groshan, K., Blakely, R. D., and Richelson, E. (1997). Pharmacological profile of antidepressants and related compounds at human monoamine transporters. *European Journal of Pharmacology* **340:** 249-258.

25. Owens, M. J., Morgan, W. N., Plott, S. J., and Nemeroff, C. B. (1997). Neurotransmitter receptor and transporter binding profile of antidepressants and their metabolites. *Journal of Pharmacology & Experimental Therapeutics* **283:** 1305-1322.

26. Rudnick, G. and Wall, S. C. (1991). Binding of the cocaine analog 2 beta-[3H] carboxymethoxy-3 beta-(4-fluorophenyl)tropane to the serotonin transporter. *Molecular Pharmacology* **40:** 421-426.

27. Blakely, R. D., Berson, H. E., Fremeau, R. T., Jr., Caron, M. G., Peek, M. M., Prince, H. K., and Bradley, C. C. (1991). Cloning and expression of a functional serotonin transporter from rat brain. *Nature* **354:** 66-70.

28. Rudnick, G. and Wall, S. C. (1992). The molecular mechanism of "ecstasy" [3,4-methylenedioxy-methamphetamine (MDMA)]: serotonin transporters are targets for MDMA-induced serotonin release. *Proceedings of the National Academy of Sciences of the United States of America* **89:** 1817-1821.

29. Ramamoorthy, S., Prasad, P. D., Kulanthaivel, P., Leibach, F. H., Blakely, R. D., and Ganapathy, V. (1993). Expression of a cocaine-sensitive norepinephrine transporter in the human placental syncytiotrophoblast. *Biochemistry* **32:** 1346-1353.

30. Rudnick, G. and Wall, S. C. (1992). The platelet plasma membrane serotonin transporter catalyzes exchange between neurotoxic amphetamines and serotonin. *Annals of the New York Academy of Sciences* **648:** 345-347.

31. Rudnick, G. and Wall, S. C. (1993). Non-neurotoxic amphetamine derivatives release serotonin through serotonin transporters. *Molecular Pharmacology* **43:** 271-276.

32. Ramamoorthy, J. D., Ramamoorthy, S., Leibach, F. H., and Ganapathy, V. (1995). Human placental monoamine transporters as targets for amphetamines. *American Journal of Obstetrics & Gynecology* **173:** 1782-1787.

33. Wall, S. C., Gu, H., and Rudnick, G. (1995). Biogenic amine flux mediated by cloned transporters stably expressed in cultured cell lines: amphetamine specificity for inhibition and efflux. *Molecular Pharmacology* **47:** 544-550.

34. Cinquanta, M., Ratovitski, T., Crespi, D., Gobbi, M., Mennini, T., and Simantov, R. (1997). Carrier-mediated serotonin release induced by d-fenfluramine: studies

with human neuroblastoma cells transfected with a rat serotonin transporter. *Neuropharmacology* **36:** 803-809.

35. Johnson, R. A., Eshleman, A. J., Meyers, T., Neve, K. A., and Janowsky, A. (1998). [3H]substrate- and cell-specific effects of uptake inhibitors on human dopamine and serotonin transporter-mediated efflux. *Synapse* **30:** 97-106.

36. Sitte, H. H., Scholze, P., Schloss, P., Pifl, C., and Singer, E. A. (2000). Characterization of carrier-mediated efflux in human embryonic kidney 293 cells stably expressing the rat serotonin transporter: a superfusion study. *Journal of Neurochemistry* **74:** 1317-1324.

37. Kuhar, M. J., Ritz, M. C., and Boja, J. W. (1991). The dopamine hypothesis of the reinforcing properties of cocaine. *Trends in Neurosciences* **14:** 299-302.

38. Rothman, R. B., Baumann, M. H., Dersch, C. M., Romero, D. V., Rice, K. C., Carroll, F. I., and Partilla, J. S. (2001). Amphetamine-type central nervous system stimulants release norepinephrine more potently than they release dopamine and serotonin. *Synapse* **39:** 32-41.

39. Giros, B., Jaber, M., Jones, S. R., Wightman, R. M., and Caron, M. G. (1996). Hyperlocomotion and indifference to cocaine and amphetamine in mice lacking the dopamine transporter. *Nature* 606-612.

40. Sora, I., Hall, F. S., Andrews, A. M., Itokawa, M., Li, X. F., Wei, H. B., Wichems, C., Lesch, K. P., Murphy, D. L., and Uhl, G. R. (2001). Molecular mechanisms of cocaine reward: combined dopamine and serotonin transporter knockouts eliminate cocaine place preference. *Proceedings of the National Academy of Sciences of the United States of America* **98:** 5300-5305.

41. Cunningham, K. A., Paris, J. M., and Goeders, N. E. (1992) Serotonin neurotransmision in cocaine sensitization. In Kalivas, P. W. and Samson, H. H., editors. *Neurobiology of Drug and Alcohol Addiction*, New York Academy of Science, New York. pp. 117-127.

42. Schroeter, S. and Blakely, R. D. (1996). Drug targets in the embryo. Studies on the cocaine- and antidepressant-sensitive serotonin transporter. *Annals of the New York Academy of Sciences* **801:** 239-255.

43. Jones, S. R., Gainetdinov, R. R., Jaber, M., Giros, B., Wightman, R. M., and Caron, M. G. (1995). Profound neuronal plasticity in response to inactivation of the dopamine transporter. *Proceedings of the National Academy of Sciences of the United States of America* 4029-4034.

44. Sneddon, J. M. (1969). Sodium-dependent accumulation of 5-hydroxytryptamine by rat blood platelets. *British Journal of Pharmacology* **37:** 680-688.

45. Rudnick, G. (1977). Active transport of 5-hydroxytryptamine by plasma membrane vesicles isolated from human blood platelets. *Journal of Biological Chemistry* **252:** 2170-2174.

46. Rudnick, G., Fishkes, H., Nelson, P. J., and Schuldiner, S. (1980). Evidence for two distinct serotonin transport systems in platelets. *Journal of Biological Chemistry* **255:** 3638-3641.

47. Keyes, S. R. and Rudnick, G. (1982). Coupling of transmembrane proton gradients to platelet serotonin transport. *Journal of Biological Chemistry* **257:** 1172-1176.

48. Reith, M. E., Zimanyi, I., and O'Reilly, C. A. (1989). Role of ions and membrane potential in uptake of serotonin into plasma membrane vesicles from mouse brain. *Biochemical Pharmacology* **38:** 2091-2097.

49. Cool, D. R., Leibach, F. H., and Ganapathy, V. (1990). Modulation of serotonin uptake kinetics by ions and ion gradients in human placental brush-border membrane vesicles. *Biochemistry* **29:** 1818-1822.

50. Sneddon, J. M. (1971). Relationship between internal Na^+-K^+ and the accumulation of [^{14} C]-5-hydroxytryptamine by rat platelets. *British Journal of Pharmacology* **43:** 834-844.

51. Ramamoorthy, S., Cool, D. R., Leibach, F. H., Mahesh, V. B., and Ganapathy, V. (1992). Reconstitution of the human placental 5-hydroxytryptamine transporter in a catalytically active form after detergent solubilization. *Biochemical Journal* **286:** 89-95.

52. Bruns, D., Engert, F., and Lux, H. D. (1993). A fast activating presynaptic reuptake current during serotonergic transmission in identified neurons of Hirudo. *Neuron* **10:** 559-572.

53. Pacholczyk, T., Blakely, R. D., and Amara, S. G. (1991). Expression cloning of a cocaine- and antidepressant-sensitive human noradrenaline transporter. *Nature* **350:** 350-354.

54. Guastella, J., Nelson, N., Nelson, H., Czyzyk, L., Keynan, S., Miedel, M. C., Davidson, N., Lester, H. A., and Kanner, B. I. (1990). Cloning and expression of a rat brain GABA transporter. *Science* **249:** 1303-1306.

55. Ramamoorthy, S., Bauman, A. L., Moore, K. R., Han, H., Yang-Feng, T., Chang, A. S., Ganapathy, V., and Blakely, R. D. (1993). Antidepressant- and cocaine-sensitive human serotonin transporter: molecular cloning, expression, and chromosomal localization. *Proceedings of the National Academy of Sciences of the United States of America* **90:** 2542-2546.

56. Lesch, K. P., Wolozin, B. L., Estler, H. C., Murphy, D. L., and Riederer, P. (1993). Isolation of a cDNA encoding the human brain serotonin transporter. *Journal of Neural Transmission - General Section* **91:** 67-72.

57. Hoffman, B. J., Mezey, E., and Brownstein, M. J. (1991). Cloning of a serotonin transporter affected by antidepressants. *Science* **254:** 579-580.

58. Ramamoorthy, S., Leibach, F. H., Mahesh, V. B., Han, H., Yang-Feng, T., Blakely, R. D., and Ganapathy, V. (1994). Functional characterization and chromosomal localization of a cloned taurine transporter from human placenta. *Biochemical Journal* **300 (Pt 3):** 893-900.

59. Saltarelli, M. D., Bauman, A. L., Moore, K. R., Bradley, C. C., and Blakely, R. D. (1996). Expression of the rat brain creatine transporter in situ and in transfected HeLa cells. *Developmental Neuroscience* **18:** 524-534.

60. Giros, B., el Mestikawy, S., Bertrand, L., and Caron, M. G. (1991). Cloning and functional characterization of a cocaine-sensitive dopamine transporter. *FEBS Letters* 149-154.

61. Kilty, J. E., Lorang, D., and Amara, S. G. (1991). Cloning and expression of a cocaine-sensitive rat dopamine transporter. *Science* **254:** 578-579.

62. Fremeau, R. T., Jr., Caron, M. G., and Blakely, R. D. (1992). Molecular cloning and expression of a high affinity L-proline transporter expressed in putative glutamatergic pathways of rat brain. *Neuron* **8:** 915-926.

63. Corey, J. L., Quick, M. W., Davidson, N., Lester, H. A., and Guastella, J. (1994). A cocaine-sensitive Drosophila serotonin transporter: cloning, expression, and electrophysiological characterization. *Proceedings of the National Academy of Sciences of the United States of America* **91:** 1188-1192.

64. Demchyshyn, L. L., Pristupa, Z. B., Sugamori, K. S., Barker, E. L., Blakely, R. D., Wolfgang, W. J., Forte, M. A., and Niznik, H. B. (1994). Cloning, expression, and localization of a chloride-facilitated, cocaine-sensitive serotonin transporter from Drosophila melanogaster. *Proceedings of the National Academy of Sciences of the United States of America* **91:** 5158-5162.

65. Blakely, R. D. and Apparsundaram, S. (1998). Structural diversity in the catecholamine transporter gene family: molecular cloning and characterization of an L-epinephrine transporter from bullfrog sympathetic ganglia. *Advances in Pharmacology* **42:** 206-210.

66. Apparsundaram, S., Moore, K. R., Malone, M. D., Hartzell, H. C., and Blakely, R. D. (1997). Molecular cloning and characterization of an L-epinephrine transporter from sympathetic ganglia of the bullfrog, Rana catesbiana. *Journal of Neuroscience* **17:** 2691-2702.

67. Lopez-Corcuera, B., Liu, Q. R., Mandiyan, S., Nelson, H., and Nelson, N. (1992). Expression of a mouse brain cDNA encoding novel gamma-aminobutyric acid transporter. *Journal of Biological Chemistry* **267:** 17491-17493.

68. Amara, S. G. and Kuhar, M. J. (1993). Neurotransmitter transporters: recent progress. *Annual Review of Neuroscience* **16:** 73-93.

69. Kilty, J. E. and Amara, S. G. (1992). Families of twelve transmembrane domain transporters. **3:** 675-682.

70. Barker, E. L. and Blakely, R. D. (1996). Identification of a single amino acid, phenylalanine 586, that is responsible for high affinity interactions of tricyclic antidepressants with the human serotonin transporter. *Molecular Pharmacology* **50:** 957-965.

71. Barker, E. L. and Blakely, R. D. (1998). Structural determinants of neurotransmitter transport using cross- species chimeras: studies on serotonin transporter. *Methods in Enzymology* **296:** 475-498.

72. Barker, E. L., Perlman, M. A., Adkins, E. M., Houlihan, W. J., Pristupa, Z. B., Niznik, H. B., and Blakely, R. D. (1998). High affinity recognition of serotonin transporter antagonists defined by species-scanning mutagenesis. An aromatic residue in transmembrane domain I dictates species-selective recognition of citalopram and mazindol. *Journal of Biological Chemistry* **273:** 19459-19468.

73. Barker, E. L., Kimmel, H. L., and Blakely, R. D. (1994). Chimeric human and rat serotonin transporters reveal domains involved in recognition of transporter ligands. *Molecular Pharmacology* **46:** 799-807.

74. Buck, K. J. and Amara, S. G. (1994). Chimeric dopamine-norepinephrine transporters delineate structural domains influencing selectivity for catecholamines and 1-methyl-4- phenylpyridinium. *Proceedings of the National Academy of Sciences of the United States of America* **91:** 12584-12588.

75. Buck, K. J. and Amara, S. G. (1995). Structural domains of catecholamine transporter chimeras involved in selective inhibition by antidepressants and psychomotor stimulants. *Molecular Pharmacology* **48:** 1030-1037.

76. Giros, B., Wang, Y. M., Suter, S., McLeskey, S. B., Pifl, C., and Caron, M. G. (1994). Delineation of discrete domains for substrate, cocaine, and tricyclic antidepressant interactions using chimeric dopamine-norepinephrine transporters. *Journal of Biological Chemistry* 15985-15988.

77. Barker, E. L., Moore, K. R., Rakhshan, F., and Blakely, R. D. (1999). Transmembrane domain I contributes to the permeation pathway for serotonin and ions in the serotonin transporter. *Journal of Neuroscience* **19:** 4705-4717.

78. Adkins, E. M. and Blakely, R. D. (2001). Serotonin and cocaine-sensitive inactivation of human serotonin transporters by methanethiosulfonates targeted to transmembrane domain 1. *Journal of Biological Chemistry* **submitted**.

79. Chen, J. G., Sachpatzidis, A., and Rudnick, G. (1997). The third transmembrane domain of the serotonin transporter contains residues associated with substrate and cocaine binding. *Journal of Biological Chemistry* **272:** 28321-28327.

80. Penado, K. M., Rudnick, G., and Stephan, M. M. (1998). Critical amino acid residues in transmembrane span 7 of the serotonin transporter identified by random mutagenesis. *Journal of Biological Chemistry* **273:** 28098-28106.

81. Chen, J. G. and Rudnick, G. (2000). Permeation and gating residues in serotonin transporter. *Proceedings of the National Academy of Sciences of the United States of America* **97:** 1044-1049.

82. Lin, F., Lester, H. A., and Mager, S. (1996). Single-channel currents produced by the serotonin transporter and analysis of a mutation affecting ion permeation. *Biophysical Journal* **71:** 3126-3135.

83. Gu, H. H., Wall, S., and Rudnick, G. (1996). Ion coupling stoichiometry for the norepinephrine transporter in membrane vesicles from stably transfected cells. *Journal of Biological Chemistry* **271:** 6911-6916.

84. Gu, H., Wall, S. C., and Rudnick, G. (1994). Stable expression of biogenic amine transporters reveals differences in inhibitor sensitivity, kinetics, and ion dependence. *Journal of Biological Chemistry* **269:** 7124-7130.

85. Gu, H., Caplan, M. J., and Rudnick, G. (1998). Cloned catecholamine transporters expressed in polarized epithelial cells: sorting, drug sensitivity, and ion-coupling stoichiometry. *Advances in Pharmacology* **42:** 175-179.

86. Elkins, R. L., Orr, T. E., Li, J. Q., Walters, P. A., Whitford, J. L., Carl, G. F., and Rausch, J. L. (2000). Serotonin reuptake is less efficient in taste aversion resistant than in taste aversion-prone rats. *Pharmacology Biochemistry & Behavior* **66:** 609-614.

87. Qian, Y., Galli, A., Ramamoorthy, S., Risso, S., DeFelice, L. J., and Blakely, R. D. (1997). Protein kinase C activation regulates human serotonin transporters in HEK-293 cells via altered cell surface expression. *Journal of Neuroscience* **17:** 45-57.

88. Ross, S. B. and Renyi, A. L. (1975). Tricyclic antidepressant agents. I. Comparison of the inhibition of the uptake of 3-H-noradrenaline and 14-C-5-hydroxytryptamine in slices and crude synaptosome preparations of the midbrain-hypothalamus region of the rat brain. *Acta Pharmacolgy & Toxicology (Copenhagen)* **36:** 382-394.

89. Angel, I. and Paul, S. M. (1984). Inhibition of synaptosomal 5-[3H]hydroxytryptamine uptake by endogenous factor(s) in human blood. *FEBS Letters* **171:** 280-284.

90. Wood, M. D., Broadhurst, A. M., and Wyllie, M. G. (1986). Examination of the relationship between the uptake system for 5- hydroxytryptamine and the high-affinity [3H]imipramine binding site--I. Inhibition by drugs. *Neuropharmacology* **25:** 519-525.

91. Rudnick, G. and Nelson, P. J. (1978). Reconstitution of 5-hydroxytryptamine transport from cholate-disrupted platelet plasma membrane vesicles. *Biochemistry* **17:** 5300-5303.

92. O'Reilly, C. A. and Reith, M. E. (1988). Uptake of [3H]serotonin into plasma membrane vesicles from mouse cerebral cortex. *Journal of Biological Chemistry* **263:** 6115-6121.

93. Galli, A., DeFelice, L. J., Duke, B. J., Moore, K. R., and Blakely, R. D. (1995). Sodium-dependent norepinephrine-induced currents in norepinephrine-transporter-transfected HEK-293 cells blocked by cocaine and antidepressants. *Journal of Experimental Biology* **198 (Pt 10):** 2197-2212.

94. Risso, S., DeFelice, L. J., and Blakely, R. D. (1996). Sodium-dependent GABA-induced currents in GAT1-transfected HeLa cells. *Journal of Physiology* **490 (Pt 3):** 691-702.

95. Galli, A., Petersen, C. I., deBlaquiere, M., Blakely, R. D., and DeFelice, L. J. (1997). Drosophila serotonin transporters have voltage-dependent uptake coupled to a serotonin-gated ion channel. *Journal of Neuroscience* **17:** 3401-3411.

96. Petersen, C. I. and DeFelice, L. J. (1999). Ionic interactions in the Drosophila serotonin transporter identify it as a serotonin channel. *Nature Neuroscience* **2:** 605-610.

97. Beckman, M. L. and Quick, M. W. (2001). Substrates and temperature differentiate ion flux from serotonin flux in a serotonin transporter. *Neuropharmacology* **40:** 526-535.

98. Mager, S., Min, C., Henry, D. J., Chavkin, C., Hoffman, B. J., Davidson, N., and Lester, H. A. (1994). Conducting states of a mammalian serotonin transporter. *Neuron* **12:** 845-859.

99. Sonders, M. S., Zhu, S. J., Zahniser, N. R., Kavanaugh, M. P., and Amara, S. G. (1997). Multiple ionic conductances of the human dopamine transporter: the actions of dopamine and psychostimulants. *Journal of Neuroscience* **17:** 960-974.

100. Mager, S., Kleinberger-Doron, N., Keshet, G. I., Davidson, N., Kanner, B. I., and Lester, H. A. (1996). Ion binding and permeation at the GABA transporter GAT1. *Journal of Neuroscience* **16:** 5405-5414.

101. Galli, A., Blakely, R. D., and DeFelice, L. J. (1996). Norepinephrine transporters have channel modes of conduction. *Proceedings of the National Academy of Sciences of the United States of America* **93:** 8671-8676.

102. Cammack, J. N. and Schwartz, E. A. (1996). Channel behavior in a gamma-aminobutyrate transporter. *Proceedings of the National Academy of Sciences of the United States of America* **93:** 723-727.

103. DeFelice, L. J. and Blakely, R. D. (1996). Pore models for transporters? *Biophysical Journal* **70:** 579-580.

104. Lester, H. A., Cao, Y., and Mager, S. (1996). Listening to neurotransmitter transporters. *Neuron* **17:** 807-810.

105. Sonders, M. S. and Amara, S. G. (1996). Channels in transporters. *Current Opinion in Neurobiology* **6:** 294-302.

106. Kavanaugh, M. P., Arriza, J. L., North, R. A., and Amara, S. G. (1992). Electrogenic uptake of gamma-aminobutyric acid by a cloned transporter expressed in Xenopus oocytes. *Journal of Biological Chemistry* **267:** 22007-22009.

107. Lu, C. C. and Hilgemann, D. W. (1999). GAT1 (GABA:Na+:Cl-) cotransport function. Kinetic studies in giant Xenopus oocyte membrane patches. *Journal of General Physiology* **114:** 445-457.

108. Lu, C. C. and Hilgemann, D. W. (1999). GAT1 (GABA:Na+:Cl-) cotransport function. Steady state studies in giant Xenopus oocyte membrane patches. *Journal of General Physiology* **114:** 429-444.

109. Galli, A., Jayanthi, L. D., Ramsey, I. S., Miller, J. W., Fremeau, R. T., Jr., and DeFelice, L. J. (1999). L-proline and L-pipecolate induce enkephalin-sensitive currents in human embryonic kidney 293 cells transfected with the high-affinity mammalian brain L-proline transporter. *Journal of Neuroscience* **19:** 6290-6297.

110. Beckman, M. L., Bernstein, E. M., and Quick, M. W. (1998). Protein kinase C regulates the interaction between a GABA transporter and syntaxin 1A. *Journal of Neuroscience* **18:** 6103-6112.

111. Bauman, A. L., Apparsundaram, S., Ramamoorthy, S., Wadzinski, B. E., Vaughan, R. A., and Blakely, R. D. (2000). Cocaine and antidepressant-sensitive biogenic amine transporters exist in regulated complexes with protein phosphatase 2A. *Journal of Neuroscience* **20:** 7571-7578.

112. Torres, G. E., Yao, W. D., Mohn, A. R., Quan, H., Kim, K. M., Levey, A. I., Staudinger, J., and Caron, M. G. (2001). Functional interaction between monoamine plasma membrane transporters and the synaptic PDZ domain-containing protein PICK1. *Neuron* **30:** 121-134.

113. Ramamoorthy, S. and Blakely, R. D. (1999). Phosphorylation and sequestration of serotonin transporters differentially modulated by psychostimulants. *Science* **285:** 763-766.

114. Ramamoorthy, S., Giovanetti, E., Qian, Y., and Blakely, R. D. (1998). Phosphorylation and regulation of antidepressant-sensitive serotonin transporters. *Journal of Biological Chemistry* **273:** 2458-2466.

115. Sakai, N., Sasaki, K., Nakashita, M., Honda, S., Ikegaki, N., and Saito, N. (1997). Modulation of serotonin transporter activity by a protein kinase C activator and an inhibitor of type 1 and 2A serine/threonine phosphatases. *Journal of Neurochemistry* **68:** 2618-2624.

116. Marazziti, D., Rossi, A., Masala, I., Rotondo, A., Palego, L., Mazzoni, M., Giannaccini, G., Lucacchini, A., and Cassano, G. B. (1999). Regulation of the platelet serotonin transporter by protein kinase C in the young and elderly. *Biological Psychiatry* **45:** 443-447.

117. Corey, J. L., Davidson, N., Lester, H. A., Brecha, N., and Quick, M. W. (1994). Protein kinase C modulates the activity of a cloned gamma-aminobutyric acid transporter expressed in Xenopus oocytes via regulated subcellular redistribution of the transporter. *Journal of Biological Chemistry* **269:** 14759-14767.

118. Deken, S. L., Beckman, M. L., Boos, L., and Quick, M. W. (2000). Transport rates of GABA transporters: regulation by the N-terminal domain and syntaxin 1A. *Nature Neuroscience* **3:** 998-1003.

119. Kilic, F. and Rudnick, G. (2000). Oligomerization of serotonin transporter and its functional consequences. *Proceedings of the National Academy of Sciences of the United States of America* **97:** 3106-3111.

120. O'Riordan, C., Phillips, O. M., and Williams, D. C. (1990). Two affinity states for [3H]imipramine binding to the human platelet 5- hydroxytryptamine carrier: an explanation for the allosteric interaction between 5-hydroxytryptamine and imipramine. *Journal of Neurochemistry* **54:** 1275-1280.

121. Plenge, P., Mellerup, E. T., and Laursen, H. (1991). Affinity modulation of [3H]imipramine, [3H]paroxetine and [3H]citalopram binding to the 5-HT transporter from brain and platelets. *European Journal of Pharmacology* **206:** 243-250.

122. Sur, C., Betz, H., and Schloss, P. (1998). Distinct effects of imipramine on 5-hydroxytryptamine uptake mediated by the recombinant rat serotonin transporter SERT1. *Journal of Neurochemistry* **70:** 2545-2553.

123. Plenge, P. and Mellerup, E. T. (1997). An affinity-modulating site on neuronal monoamine transport proteins. *Pharmacology & Toxicology* **80:** 197-201.

124. Unwin, N. (1989). The structure of ion channels in membranes of excitable cells. *Neuron* **3:** 665-676.

125. Rosenmund, C., Stern-Bach, Y., and Stevens, C. F. (1998). The tetrameric structure of a glutamate receptor channel. *Science* **280:** 1596-1599.

126. Green, W. N. and Millar, N. S. (1995). Ion-channel assembly. *Trends in Neurosciences* **18:** 280-287.

127. MacKinnon, R. (1991). Determination of the subunit stoichiometry of a voltage-activated potassium channel. *Nature* **350:** 232-235.

128. Yang, J., Jan, Y. N., and Jan, L. Y. (1995). Determination of the subunit stoichiometry of an inwardly rectifying potassium channel. *Neuron* **15:** 1441-1447.

129. Chang, G., Spencer, R. H., Lee, A. T., Barclay, M. T., and Rees, D. C. (1998). Structure of the MscL homolog from Mycobacterium tuberculosis: a gated mechanosensitive ion channel. *Science* **282:** 2220-2226.

130. Miyazawa, A., Fujiyoshi, Y., Stowell, M., and Unwin, N. (1999). Nicotinic acetylcholine receptor at 4.6 A resolution: transverse tunnels in the channel wall. *Journal of Molecular Biology* **288:** 765-786.

131. Doyle, D. A., Morais, C. J., Pfuetzner, R. A., Kuo, A., Gulbis, J. M., Cohen, S. L., Chait, B. T., and MacKinnon, R. (1998). The structure of the potassium channel: molecular basis of K+ conduction and selectivity. *Science* **280:** 69-77.

132. Schmid, J. A., Scholze, P., Kudlacek, O., Freissmuth, M., Singer, E. A., and Sitte, H. H. (2001). Oligomerization of the human serotonin transporter and of the rat GABA transporter 1 visualized by fluorescence resonance energy transfer microscopy in living cells. *Journal of Biological Chemistry* **276:** 3805-3810.

133. Jess, U., Betz, H., and Schloss, P. (1996). The membrane-bound rat serotonin transporter, SERT1, is an oligomeric protein. *FEBS Letters* **394:** 44-46.

134. Chang, A. S., Starnes, D. M., and Chang, S. M. (1998). Possible existence of quaternary structure in the high-affinity serotonin transport complex. *Biochemical & Biophysical Research Communications* **249:** 416-421.

135. Ramamoorthy, S., Leibach, F. H., Mahesh, V. B., and Ganapathy, V. (1993). Partial purification and characterization of the human placental serotonin transporter. *Placenta* **14:** 449-461.

136. Cesura, A. M., Muller, K., Peyer, M., and Pletscher, A. (1983). Solubilization of imipramine-binding protein from human blood platelets. *European Journal of Pharmacology* **96:** 235-242.

137. Habert, E., Graham, D., and Langer, S. Z. (1986). Solubilization and characterization of the 5-hydroxytryptamine transporter complex from rat cerebral cortical membranes. *European Journal of Pharmacology* **122:** 197-204.

138. Talvenheimo, J. and Rudnick, G. (1980). Solubilization of the platelet plasma membrane serotonin transporter in an active form. *Journal of Biological Chemistry* **255:** 8606-8611.

139. Launay, J. M., Geoffroy, C., Mutel, V., Buckle, M., Cesura, A., Alouf, J. E., and Da Prada, M. (1992). One-step purification of the serotonin transporter located at the human platelet plasma membrane. *Journal of Biological Chemistry* **267:** 11344-11351.

140. Berger, S. P., Farrell, K., Conant, D., Kempner, E. S., and Paul, S. M. (1994). Radiation inactivation studies of the dopamine reuptake transporter protein. *Molecular Pharmacology* **46:** 726-731.

141. Milner, H. E., Beliveau, R., and Jarvis, S. M. (1994). The in situ size of the dopamine transporter is a tetramer as estimated by radiation inactivation. *Biochimica et Biophysica Acta* **1190:** 185-187.

142. Qian, Y., Melikian, H. E., Rye, D. B., Levey, A. I., and Blakely, R. D. (1995). Identification and characterization of antidepressant-sensitive serotonin transporter proteins using site-specific antibodies. *Journal of Neuroscience* **15:** 1261-1274.

143. Wennogle, L. P. and Meyerson, L. R. (1985). Serotonin uptake inhibitors differentially modulate high affinity imipramine dissociation in human platelet membranes. *Life Sciences* **36:** 1541-1550.

144. Meyerson, L. R., Ieni, J. R., and Wennogle, L. P. (1987). Allosteric interaction between the site labeled by [3H]imipramine and the serotonin transporter in human platelets. *Journal of Neurochemistry* **48:** 560-565.

145. Kim, S. S. and Reith, M. E. (1986). Effect of serotonin on the dissociation of high-affinity binding of [3H]imipramine in mouse cerebral cortex. *Neuroscience Letters* **67:** 123-128.

146. Plenge, P., Mellerup, E. T., and Laursen, H. (1991). Affinity modulation of [3H]imipramine, [3H]paroxetine and [3H]citalopram binding to the 5-HT transporter from brain and platelets. *European Journal of Pharmacology* **206:** 243-250.

147. Humphreys, C. J., Levin, J., and Rudnick, G. (1988). Antidepressant binding to the porcine and human platelet serotonin transporters. *Molecular Pharmacology* **33:** 657-663.

148. D'Amato, R. J., Largent, B. L., Snowman, A. M., and Snyder, S. H. (1987). Selective labeling of serotonin uptake sites in rat brain by [3H]citalopram contrasted to labeling of multiple sites by [3H]imipramine. *Journal of Pharmacology & Experimental Therapeutics* **242:** 364-371.

149. Ni, Y. G., Chen, J. G., Androutsellis-Theotokis, A., Huang, C. J., Moczydlowski, E., and Rudnick, G. (2001). A lithium-induced conformational change in serotonin transporter alters cocaine binding, ion conductance, and reactivity of Cys-109. *Journal of Biological Chemistry* **276:** 30942-30947.

150. Chen, J. G., Liu-Chen, S., and Rudnick, G. (1997). External cysteine residues in the serotonin transporter. *Biochemistry* **36:** 1479-1486.

151. Chen, J. G., Liu-Chen, S., and Rudnick, G. (1998). Determination of external loop topology in the serotonin transporter by site-directed chemical labeling. *Journal of Biological Chemistry* **273:** 12675-12681.

152. Talvenheimo, J., Fishkes, H., Nelson, P. J., and Rudnick, G. (1983). The serotonin transporter-imipramine "receptor". *Journal of Biological Chemistry* **258:** 6115-6119.

153. Talvenheimo, J., Nelson, P. J., and Rudnick, G. (1979). Mechanism of imipramine inhibition of platelet 5-hydroxytryptamine transport. *Journal of Biological Chemistry* **254:** 4631-4635.

154. Cao, Y., Mager, S., and Lester, H. A. (1997). H+ permeation and pH regulation at a mammalian serotonin transporter. *Journal of Neuroscience* **17:** 2257-2266.

155. Cao, Y., Li, M., Mager, S., and Lester, H. A. (1998). Amino acid residues that control pH modulation of transport-associated current in mammalian serotonin transporters. *Journal of Neuroscience* **18:** 7739-7749.

156. Rodriguez, B. M., Sigg, D., and Bezanilla, F. (1998). Voltage gating of Shaker K+ channels. The effect of temperature on ionic and gating currents. *Journal of General Physiology* **112:** 223-242.

157. Karlin, A. and Akabas, M. H. (1998). Substituted-cysteine accessibility method. *Methods in Enzymology* **293:** 123-145.

158. Morais-Cabral, J. H., Zhou, Y., and MacKinnon, R. (2001). Energetic optimization of ion conduction rate by the K+ selectivity filter. *Nature* **414:** 37-42.

159. Zampighi, G. A., Kreman, M., Boorer, K. J., Loo, D. D., Bezanilla, F., Chandy, G., Hall, J. E., and Wright, E. M. (1995). A method for determining the unitary functional capacity of cloned channels and transporters expressed in Xenopus laevis oocytes. *Journal of Membrane Biology* 65-78.

160. Adkins, E. M., Barker, E. L., and Blakely, R. D. (2001). Interactions of tryptamine derivatives with serotonin transporter species variants implicate transmembrane domain I in substrate recognition. *Molecular Pharmacology* **59:** 514-523.

161. Zerangue, N., Schwappach, B., Jan, Y. N., and Jan, L. Y. (1999). A new ER trafficking signal regulates the subunit stoichiometry of plasma membrane K(ATP) channels. *Neuron* **22:** 537-548.

162. Eskandari, S., Kreman, M., Kavanaugh, M. P., Wright, E. M., and Zampighi, G. A. (2000). Pentameric assembly of a neuronal glutamate transporter. *Proceedings of the National Academy of Sciences of the United States of America* **97:** 8641-8646.

163. Perez, J. L., Khatri, L., Chang, C., Srivastava, S., Osten, P., and Ziff, E. B. (2001). PICK1 targets activated protein kinase Calpha to AMPA receptor clusters in spines of hippocampal neurons and reduces surface levels of the AMPA- type glutamate receptor subunit 2. *Journal of Neuroscience* **21:** 5417-5428.

164. Niethammer, M., Kim, E., and Sheng, M. (1996). Interaction between the C terminus of NMDA receptor subunits and multiple members of the PSD-95 family of membrane-associated guanylate kinases. *Journal of Neuroscience* **16:** 2157-2163.

165. Osten, P., Khatri, L., Perez, J. L., Kohr, G., Giese, G., Daly, C., Schulz, T. W., Wensky, A., Lee, L. M., and Ziff, E. B. (2000). Mutagenesis reveals a role for ABP/GRIP binding to GluR2 in synaptic surface accumulation of the AMPA receptor. *Neuron* **27:** 313-325.

166. Dong, H., O'Brien, R. J., Fung, E. T., Lanahan, A. A., Worley, P. F., and Huganir, R. L. (1997). GRIP: a synaptic PDZ domain-containing protein that interacts with AMPA receptors. *Nature* **386:** 279-284.

167. Blakely, R. D. and Bauman, A. L. (2000). Biogenic amine transporters: regulation in flux. *Current Opinion in Neurobiology* **10:** 328-336.

168. Quick, M. W., Corey, J. L., Davidson, N., and Lester, H. A. (1997). Second messengers, trafficking-related proteins, and amino acid residues that contribute to the functional regulation of the rat brain GABA transporter GAT1. *Journal of Neuroscience* **17:** 2967-2979.

169. Ingram, S. L. and Amara, S. G. (2000). Arachidonic acid stimulates a novel cocaine-sensitive cation conductance associated with the human dopamine transporter. *Journal of Neuroscience* **20:** 550-557.

170. Beckman, M. L. and Quick, M. W. (1998). Neurotransmitter transporters: regulators of function and functional regulation. *Journal of Membrane Biology* **164:** 1-10.

171. Cammack, J. N. and Schwartz, E. A. (1993). Ions required for the electrogenic transport of GABA by horizontal cells of the catfish retina. *Journal of Physiology* 81-102.

172. Wadiche, J. I., Amara, S. G., and Kavanaugh, M. P. (1995). Ion fluxes associated with excitatory amino acid transport. *Neuron* **15:** 721-728.

173. Su, A., Mager, S., Mayo, S. L., and Lester, H. A. (1996). A multi-substrate single-file model for ion-coupled transporters. *Biophysical Journal* **70:** 762-777.

174. Whitworth, T. L. and Quick, M. W. (2001). Substrate-induced regulation of {gamma}-aminobutyric acid (GABA) transporter trafficking requires tyrosine phosphorylation. *Journal of Biological Chemistry*.

175. Bernstein, E. M. and Quick, M. W. (1999). Regulation of gamma-aminobutyric acid (GABA) transporters by extracellular GABA. *Journal of Biological Chemistry* **274:** 889-895.

176. Cammack, J. N., Rakhilin, S. V., and Schwartz, E. A. (1994). A GABA transporter operates asymmetrically and with variable stoichiometry. *Neuron* 949-960.

177. Inserte, J., Najib, A., Pelliccioni, P., Gil, C., and Aguilera, J. (1999). Inhibition by tetanus toxin of sodium-dependent, high-affinity [3H]5- hydroxytryptamine uptake in rat synaptosomes. *Biochemical Pharmacology* **57:** 111-120.

178. Hoffman, B. J. (1994). Expression cloning of a serotonin transporter: a new way to study antidepressant drugs. *Pharmacopsychiatry* **27:** 16-22.

179. Galli, A., Blakely, R. D., and DeFelice, L. J. (1998). Patch-clamp and amperometric recordings from norepinephrine transporters: channel activity and voltage-dependent uptake. *Proceedings of the National Academy of Sciences of the United States of America* **95:** 13260-13265.

180. Tzounopoulos, T., Maylie, J., and Adelman, J. P. (1995). Induction of endogenous channels by high levels of heterologous membrane proteins in Xenopus oocytes. *Biophysical Journal* **69:** 904-908.

181. Dowd, L. A., Coyle, A. J., Rothstein, J. D., Pritchett, D. B., and Robinson, M. B. (1996). Comparison of Na+-dependent glutamate transport activity in synaptosomes, C6 glioma, and Xenopus oocytes expressing excitatory amino acid carrier 1 (EAAC1). *Molecular Pharmacology* **49:** 465-473.

182. Broer, S., Schuster, A., Wagner, C. A., Broer, A., Forster, I., Biber, J., Murer, H., Werner, A., Lang, F., and Busch, A. E. (1998). Chloride conductance and Pi transport are separate functions induced by the expression of NaPi-1 in Xenopus oocytes. *Journal of Membrane Biology* **164:** 71-77.

183. Mackenzie, B., Loo, D. D., and Wright, E. M. (1998). Relationships between Na+/glucose cotransporter (SGLT1) currents and fluxes. *Journal of Membrane Biology* **162:** 101-106.

184. Reshkin, S. J., Grover, M. L., Howerton, R. D., Grau, E. G., and Ahearn, G. A. (1989). Dietary hormonal modification of growth, intestinal ATPase, and glucose transport in tilapia. *American Journal of Physiology* **256:** E610-E618.

185. Gross, E., Hawkins, K., Abuladze, N., Pushkin, A., Cotton, C. U., Hopfer, U., and Kurtz, I. (2001). The stoichiometry of the electrogenic sodium bicarbonate cotransporter NBC1 is cell-type dependent. *Journal of Physiology* **531:** 597-603.

186. Choi, I., Romero, M. F., Khandoudi, N., Bril, A., and Boron, W. F. (1999). Cloning and characterization of a human electrogenic Na+-HCO-3 cotransporter isoform (hhNBC). *American Journal of Physiology* **276:** C576-C584.

187. Sacher, A., Cohen, A., and Nelson, N. (2001). Properties of the mammalian and yeast metal-ion transporters DCT1 and Smf1p expressed in Xenopus laevis oocytes. *Journal of Experimental Biology* **204:** 1053-1061.

188. Gunshin, H., Mackenzie, B., Berger, U. V., Gunshin, Y., Romero, M. F., Boron, W. F., Nussberger, S., Gollan, J. L., and Hediger, M. A. (1997). Cloning and characterization of a mammalian proton-coupled metal-ion transporter. *Nature* **388:** 482-488.

189. Tsukaguchi, H., Tokui, T., Mackenzie, B., Berger, U. V., Chen, X. Z., Wang, Y., Brubaker, R. F., and Hediger, M. A. (1999). A family of mammalian Na+-dependent L-ascorbic acid transporters. *Nature* **399:** 70-75.

190. Busch, A. E., Biber, J., Murer, H., and Lang, F. (1996). Electrophysiological insights of type I and II Na/Pi transporters. *Kidney International* **49:** 986-987.

191. Bellocchio, E. E., Reimer, R. J., Fremeau, R. T., Jr., and Edwards, R. H. (2000). Uptake of glutamate into synaptic vesicles by an inorganic phosphate transporter. *Science* **289:** 957-960.

192. Coady, M. J., Chen, X. Z., and Lapointe, J. Y. (1996). rBAT is an amino acid exchanger with variable stoichiometry. *Journal of Membrane Biology* **149:** 1-8.

193. Chen, X. Z., Peng, J. B., Cohen, A., Nelson, H., Nelson, N., and Hediger, M. A. (1999). Yeast SMF1 mediates H(+)-coupled iron uptake with concomitant uncoupled cation currents. *Journal of Biological Chemistry* **274:** 35089-35094.

194. Quick, M. and Stevens, B. R. (2001). Amino Acid Transporter CAATCH1 Is Also an Amino Acid-gated Cation Channel. *Journal of Biological Chemistry* **276:** 33413-33418.

195. De Lean, A., Stadel, J. M., and Lefkowitz, R. J. (1980). A ternary complex model explains the agonist-specific binding properties of the adenylate cyclase-coupled beta-adrenergic receptor. *Journal of Biological Chemistry* **255:** 7108-7117.

196. Limbird, L. E. (1996) *Cell Surface Receptors: A Short Course on Theory and Methods*, Second Edition Ed., Kluwer Academic Publishers, Norwell, Massachussetts

197. Rego, J. C., Syringas, M., Leblond, B., Costentin, J., and Bonnet, J. J. (1999). Recovery of dopamine neuronal transporter but lack of change of its mRNA in substantia nigra after inactivation by a new irreversible inhibitor characterized in vitro and ex vivo in the rat. *British Journal of Pharmacology* **128:** 51-60.

198. Ransom, R. W., Lee, J. D., Bolger, M. B., and Shih, J. C. (1985). Photoinactivation of serotonin uptake by an arylazido derivative of 5-hydroxytryptamine. *Molecular Pharmacology* **28:** 185-190.

199. Rehavi, M., Ittah, Y., Skolnick, P., Rice, K. C., and Paul, S. M. (1982). Nitroimipramines - synthesis and pharmacological effects of potent long-acting inhibitors of [3H] serotonin uptake and [3H] imipramine binding. *Naunyn-Schmiedebergs Archives of Pharmacology* **320:** 45-49.

200. Cheng, Y. and Prusoff, W. H. (1973). Relationship between the inhibition constant (K1) and the concentration of inhibitor which causes 50 per cent inhibition (I50) of an enzymatic reaction. *Biochemical Pharmacology* **22:** 3099-3108.